
# Role of Purinergic Ligands to Enhance Cisplatin Sensitivity in Ovarian Cancer Cells

Inaugural-Dissertation

for the attainment of the title of doctor
in the Faculty of Mathematics and Natural Sciences
at the Heinrich Heine University Düsseldorf

presented by

**Parichat Sureechatchaiyan**
From Chiang Rai, Thailand

Düsseldorf, October 2017

from the Institute of Pharmaceutical and Medicinal Chemistry
at the Heinrich Heine University Düsseldorf

Published by permission of the
Faculty of Mathematics and Natural Sciences at
Heinrich Heine University Düsseldorf

Supervisor: Prof. Dr. Matthias U. Kassack
Co-supervisor: Prof. Dr. Peter Proksch

Date of the oral examination:

# Declaration

I declare under oath that I have compiled my dissertation independently and without any undue assistance by third parties under consideration of the 'Principles for the Safeguarding of Good Scientific Practice at Heinrich Heine University Düsseldorf. This dissertation has not been submitted, in whole or in part, in any previous application for a degree. The work presented is entirely my own.

Düsseldorf, October 2017

Parichat Sureechatchaiyan

# Acknowledgements

It is a pleasure to thank those who made this thesis possible.

First of all, I would like to thank you Professor Matthias Kassack for giving me a great opportunity for doctoral study in Germany. Thank you very much all the precious suggestion, knowledge and support during my time here.

Thank you very much for the kindness and helpful suggestion from Dr. Alexandra Hamacher. Many thanks for helping me in everything from the beginning of my study. Your help always make me go through all the tough times.

Besonderen Dank an Magda, du machst immer meinen Tag mit deiner freundlichen und herzlichen Umarmung.

Thank you to all my colleagues, Christian Urban., Ana, Kati, Laura, Nicole and David. Thank you for your warm welcome, kindness and helpful support. Chenyin, it is so nice that you are here. Thank you for your kindness, great support and care as well as your joyful laughing.

Thank you for Christian Schrenk and Jan J. Bandolik for revising the summary of my dissertation to be a nice Germen version.

I would like to show my gratitude to Dr. Busaban Sirithunyalug and Dr. Darunee Hongwiset for all the support and giving me a great chance to come to Germany. Without you, I will never be here.

Thank you to Payap University for the financial support during the time of my study.

Words are powerless to express my gratitude to my parents and my beloved sister. All your support and the greatest, endless love make all the best of me.

(ขอบพระคุณพ่อแม่และพี่บุ๋ม ปลามีวันนี้ได้ก็เพราะความรักยิ่งใหญ่)

Finally, Rafat…thanks for everything. Thank you for your patient and always by my side.

# Table of contents


| | Page |
|---|---|
| **Declaration** | I |
| **Acknowledgement** | II |
| **Table of contents** | III |
| **List of tables** | VII |
| **List of figures** | IX |
| **Publications** | XIII |
| **Abbreviations** | XIV |
| **1. Summary** | 1 |
| **2. Zusammenfassung** | 2 |
| **3. Introduction** | 5 |
| 3.1 Ovarian cancer | 5 |
| 3.1.1 Etiology and epidemiology | 5 |
| 3.1.2 Pathology and classification | 6 |
| 3.1.3 Diagnosis | 7 |
| 3.1.4 Staging | 8 |
| 3.1.5 Treatment | 8 |
| 3.1.6 Treatment of recurrent disease | 10 |
| 3.2 Drug resistance | 13 |
| 3.2.1 Mechanisms of drug resistance | 13 |
| 3.2.2 Cisplatin resistance development | 15 |
| 3.3 Purinergic receptors and ligands | 17 |

Page

3.3.1 P2 receptors 18

3.3.2 P1 receptors 20

3.3.3 Purinergic ligands: adenosine triphosphate (ATP) and adenosine 21

3.4 Adenosine uptake inhibitors 23

3.5 AMP-activated protein kinase (AMPK) and mechanistic target of rapamycin (mTOR) 24

3.5.1 AMPK subunit structure 24

3.5.2 AMPK regulation and function 25

3.5.3 Role of AMPK in cancer 26

3.5.4 Mechanistic target of rapamycin (mTOR) 27

**4. Objective** 30

**5. Materials and Methods** 31

5.1 Materials 31

Chemical reagents 31

Cell lines 34

Selective agonists and antagonists of purinergic receptors 34

Antibodies for western blot analysis 35

Equipment 36

Instrument 36

Software 38

5.2 Buffers and solutions 39

5.2.1 Cell culture 39

5.2.2 RT-PCR 39

5.2.3 Western blot analysis 40

Page

5.2.4 Calcium assay 43

5.2.5 cAMP reporter gene assay 44

5.2.6 MTT assay 45

5.2.7 Cell cycle analysis 45

5.2.8 Apoptosis assay 46

5.3 Methods 47

5.3.1 Cell culture 47

5.3.2 Reverse Transcriptase – Polymerase Chain Reaction (RT-PCR) 48

5.3.3 Western blot analysis 51

5.3.4 Calcium assay 54

5.3.5 cAMP reporter gene assay 57

5.3.6 MTT assay 61

5.3.7 Cell cycle analysis 63

5.3.8 Apoptosis assay 64

5.4 Statistics 65

**6. Results**

**Effect of purinergic ligands on chemosensitivity of cisplatin**

6.1 Characterization of ovarian cancer cells for purinergic receptor expression 66

6.1.1 P2 receptor expression 66

6.1.2 P1 receptor expression 68

6.2 Functional activity of purinergic P2 and P1 receptors 69

6.2.1 Evaluation of P2 receptor functional activity by calcium assay 69

6.2.2 Evaluation of the functional activity of P1 receptors by cAMP assay 75

Page

6.3 ATP enhances cisplatin-induced cytotoxicity 79

6.4 Adenosine enhances cisplatin-induced cytotoxicity 84

6.4.1 Cytotoxicity of adenosine and adenosine effects in combination treatment with cisplatin 84

6.4.2 Synergistic effects of adenosine and cisplatin in combination treatments 87

6.5 Adenosine signaling in ovarian cancer cells 88

6.5.1 Role of adenosine receptors and nucleoside transporters in adenosine treatment 88

6.5.2 Role of adenosine receptors and nucleoside transporters in the combination treatment of adenosine and cisplatin 89

6.6 Effect of ATP and adenosine on cell cycle and apoptosis induction in ovarian cancer cell lines 93

6.6.1 ATP and adenosine effects on cell cycle 93

6.6.2 ATP and adenosine effects on the induction of apoptosis 95

6.7 Adenosine uptake is essential for adenosine-induced apoptosis via caspase pathway 95

6.8 Intracellular adenosine activates the AMP-activated protein kinase (AMPK) pathway 101

6.9 Effect of adenosine on the HEK293 cell line 104

**7. Discussion** 106

**8. Conclusion** 112

**References** 113

# List of Tables


| **Introduction** | | **Page** |
|---|---|---|
| **Table 3.1** | The International Federation of Gynecology and Obstertric (FIGO) staging of ovarian cancer, 2014 | 8 |
| **Materials and Methods** | | 31 |
| **Table 5.1** | List of general chemical reagents | 31 |
| **Table 5.2** | List of cell lines | 34 |
| **Table 5.3** | List of selective agonists and antagonists of purinergic receptors | 34 |
| **Table 5.4** | List of antibodies for western blot | 35 |
| **Table 5.5** | List of equipment | 36 |
| **Table 5.6** | List of instrument | 36 |
| **Table 5.7** | List of software | 38 |
| **Table 5.8** | Components for reverse transcription | 49 |
| **Table 5.9** | Sequences of forward and reverse primer for PCR | 50 |
| **Table 5.10** | Components for PCR | 51 |
| **Table 5.11** | Gel components for one gel preparation | 53 |
| **Table 5.12** | NOVOstar instrument setting for calcium assay | 56 |
| **Table 5.13** | LUMIstar instrument setting for cAMP assay | 60 |
| **Results** | | |
| **Table 6.1** | Summary of $EC_{50}$ and $pEC_{50}$ ± SEM values of UTP, ATP, ADP and UDP in A2780 cells obtained from calcium assay | 71 |
| **Table 6.2** | Summary of $EC_{50}$ and $pEC_{50}$ ± SEM values of adenosine in A2780, A2780CisR and HEY cells obtained from cAMP reporter gene assay | 78 |
| **Table 6.3** | Summary of $IC_{50}$, $pIC_{50}$ ± SEM values of cisplatin and shift factors (Sf) obtained from combination treatments of ATP and cisplatin in A2780 and A2780CisR cells | 81 |
| **Table 6.4** | Summary of $IC_{50}$, $pIC_{50}$ ± SEM values of cisplatin and shift factors (Sf) obtained from combination treatment of ATP and cisplatin in the presence or absence of AR-C118925 in A2780 cells | 82 |

| | | Page |
|---|---|---|
| **Table 6.5** | Summary of $IC_{50}$ and $pIC_{50}$ ± SEM values of cisplatin obtained from combination treatments of ATP and cisplatin in the presence or absence of dipyridamole | 83 |
| **Table 6.6** | Summary of $IC_{50}$, $pIC_{50}$ ± SEM values of cisplatin and shift factors (Sf) derived from combination treatment of adenosine and cisplatin | 86 |
| **Table 6.7** | Combination index (CI) values derived from combination treatments of adenosine and cisplatin in A2780, A2780CisR and HEY cell lines | 88 |
| **Table 6.8** | Summary of $IC_{50}$, $pIC_{50}$ ± SEM values of cisplatin and shift factors achieved from combination treatments of adenosine and cisplatin in the presence or absence of dipyridamole (MTT assay) | 91 |

# List of Figures


| | | Page |
|---|---|---|
| **Introduction** | | |
| **Figure 3.1** | Classification of purinergic receptors | 18 |
| **Figure 3.2** | Chemical structure of adenosine triphosphate (ATP) | 21 |
| **Figure 3.3** | Chemical structure of adenosine | 21 |
| **Figure 3.4** | Chemical structure of dipyridamole | 23 |
| **Figure 3.5** | Functional and regulation of AMPK leading to tumor suppression | 28 |
| **Materials and Methods** | | |
| **Figure 5.1** | Hemocytometer | 48 |
| **Figure 5.2** | Monitoring of GPCR-induced calcium releases | 54 |
| **Figure 5.3** | Fluorescence-time curves obtained from calcium assay after treatment with agonist in a presence or absence of antagonist compared with untreated control | 56 |
| **Figure 5.4** | Theory of cAMP reporter gene assay | 58 |
| **Figure 5.5** | Luminescence-time curves obtained from cAMP reporter gene assay after treatment with non-selective agonist (adenosine) alone or in combination with antagonists compared to untreated control | 60 |
| **Figure 5.6** | Histogram of PI staining cells in FL2 channel obtained from cell cycle analysis | 64 |
| **Figure 5.7** | Histogram of PI staining cells in FL2 channel obtained from apoptosis assay | 65 |
| **Results** | | |
| **Figure 6.1** | Gene expression of P2Y (A) and P2X (B) receptors in A2780 and A2780CisR cells obtained from RT-PCR | 67 |
| **Figure 6.2** | Protein expression of P2Y receptors ($P2Y_1$, $P2Y_2$, $P2Y_6$, $P2Y_{11}$ and $P2Y_{13}$) and P2X receptors ($P2X_4$ and $P2X_7$) in A2780 and A2780CisR cells obtained from western blot analysis | 67 |
| **Figure 6.3** | Gene expression profile of adenosine receptors A1, A2A, A2B and A3 subtypes in A2780, A2780CisR and HEY cell lines obtained from RT-PCR | 68 |

| | | Page |
|---|---|---|
| **Figure 6.4** | Protein expression of A1, A2A, A2B and A3 adenosine receptors in A2780, A2780CisR and HEY cells obtained from western blot analysis | 69 |
| **Figure 6.5** | Concentration-effect curves of UTP, ATP, ADP or UDP in A2780 cells monitored by calcium assay | 70 |
| **Figure 6.6** | Inhibitory effect of suramin on UTP- or ATP-induced increase in fluorescence in A2780 cells | 71 |
| **Figure 6.7** | Effects of the selective $P2Y_1$, $P2Y_{11}$, $P2X_4$ and $P2X_7$ receptor antagonists MRS 2179, NF340, 5-BDBD and A 740003 on ADP or ATP-induced P2 receptor activation in A2780 cells | 72 |
| **Figure 6.8** | Inhibitory effect of AR-C118925 on ATP-mediated fluorescence increase in A2780 cells | 73 |
| **Figure 6.9** | Functional activity of P2 receptors in HEY cells measured by calcium assay | 74 |
| **Figure 6.10** | Stimulation by ATP or ADP of P2 receptors in A2780CisR cells measured by calcium assay | 75 |
| **Figure 6.11** | Effect of adenosine on cAMP-dependent luminescence-related cAMP levels in A2780 cells | 76 |
| **Figure 6.12** | Effects of the selective adenosine receptor antagonists SLV320, PSB603 and SCH442416 on adenosine-induced increase in luminescence in A2780 cells | 77 |
| **Figure 6.13** | Concentration-dependent effect of adenosine in cAMP reporter gene assay in A2780CisR and HEY cells | 78 |
| **Figure 6.14** | Cytotoxicity of ATP in A2780 and A2780CisR cells (MTT assay) | 79 |
| **Figure 6.15** | Effect of ATP on cisplatin-induced cytotoxicity in A2780 and A2780CisR cells | 80 |
| **Figure 6.16** | Effect of AR-C118925 on ATP-enhanced cisplatin cytotoxicity in A2780 cells | 82 |
| **Figure 6.17** | Effect of dipyridamole (DPM) on ATP-enhanced cisplatin cytotoxicity in A2780 and A2780CisR cells | 83 |
| **Figure 6.18** | Cytotoxicity of adenosine in A2780, A2780CisR, and HEY cells after 48 h treatment | 85 |

| | | Page |
|---|---|---|
| **Figure 6.19** | Concentration-effect curves (MTT assay) of cisplatin in the absence and presence of adenosine and resulting shift factors in A2780, A2780CisR and HEY cells | 86 |
| **Figure 6.20** | Effect of SLV320, PSB603 and dipyridamole on adenosine cytotoxicity in A2780, A2780CisR and HEY cell lines | 89 |
| **Figure 6.21** | Effect of dipyridmole on adenosine-enhanced cisplatin cytotoxicity in the combination treatment of adenosine and cisplatin (MTT assay) | 90 |
| **Figure 6.22** | Effect of the selective A1 receptor antagonist SLV320 on adenosine-enhanced cisplatin cytotoxicity in A2780, A2780CisR and HEY cell lines (MTT assay) | 92 |
| **Figure 6.23** | Effect of the selective A2B receptor antagonist PSB603 on adenosine-enhanced cisplatin cytotoxicity in A2780, A2780CisR and HEY cell lines (MTT assay) | 93 |
| **Figure 6.24** | Effect of ATP and adenosine treatment on cell cycle | 94 |
| **Figure 6.25** | Induction of apoptosis by ATP and adenosine | 95 |
| **Figure 6.26** | Effect of dipyridamole, SLV320 and PSB603 on adenosine-induced apoptosis in A2780, A2780CisR and HEY cell lines | 96 |
| **Figure 6.27** | Effect of the caspase inhibitor QVD-OPh on adenosine-induced apoptosis | 97 |
| **Figure 6.28** | Effect of adenosine on PARP cleavage in A2780, A2780CisR and HEY cell lines | 98 |
| **Figure 6.29** | Induction of apoptosis by a combination of adenosine and cisplatin in the presence or absence of dipyridamole | 99 |
| **Figure 6.30** | Effect of adenosine in combination with cisplatin on PARP cleavage in A2780, A2780CisR, and HEY cell lines | 100 |
| **Figure 6.31** | Effect of adenosine on AMP-activated protein kinase (AMPK) activation | 102 |
| **Figure 6.32** | Phosphorylation of S6K at Thr389 after treatment with adenosine alone or in combination with cisplatin in A2780, A2780CisR and HEY cell lines | 103 |

| | | Page |
|---|---|---|
| **Figure 6.33** | Concentration-effect curves of cisplatin in the absence or presence of adenosine in HEK293 cells and resulting shift factors | 104 |
| **Figure 6.34** | Induction of apoptosis by adenosine in HEK293 cells | 105 |
| **Conclusions** | | |
| **Figure 8.1** | Summary results of the study | 112 |

# Publications

## Co-author

- Catalina F. Pérez Hemphill1, **Parichat Sureechatchaiyan**, Matthias U. Kassack, Raha S. Orfali, Wenhan Lin,Georgios Daletos and Peter Proksch. OSMAC approach leads to new fusarielin metabolitesfrom *Fusarium tricinctum*. J Antibiot. 2017; 70(6):726-732.

- Leandro A. Alves Avelar, Jana Held, Jessica A. Engel, **Parichat Sureechatchaiyan**, Finn K. Hansen, Alexandra Hamacher, Matthias U. Kassack, Benjamin Mordmueller, Katherine T. Andrews, and Thomas Kurz. Design and Synthesis of Novel Anti-Plasmodial Histone Deacetylase Inhibitors Containing an Alkoxyamide Connecting Unit. Arch Pharm. 2017; 350:3-4.

- Amin Mokhlesi, Fabian Stuhldreier, Katharina W. Wex, Anne Berscheid, Rudolf Hartmann, Nidja Rehberg, Parichat Sureechatchaiyan, Chaidir Chaidir, Matthias U. Kassack, Rainer Kalscheuer, Heike Brötz-Oesterhelt, Sebastian Wesselborg, Björn Stork, Georgios Daletos and Peter Proksch. Cyclic Cystine-Bridged Peptides from the Marine Sponge Clathria basilana Induce Apoptosis in Tumor Cells and Depolarize the Bacterial Cytoplasmic Membrane. J. Nat. Prod. DOI: 10.1021/acs.jnatprod.7b00477

## Poster Presentation

**Sureechatchaiyan P**, Hamacher A and Kassack M. Adenosine enhances cisplatin sensitivity in ovarian cancer cell lines. 8$^{th}$ Mildred Scheel Cancer Conference.14 – 16 June 2017. Bonn.

## Submitted

**Parichat Sureechatchaiyan**, Alexandra Hamacher and Matthias U. Kassack. Adenosine enhances cisplatin sensitivity in ovarian cancer cells. Purinergic signaling Journal. October, 2017.

# Abbreviations

| | |
|---|---|
| **AC** | Adenylyl cyclase |
| **ACC** | Acetyl-CoA carboxylase |
| **ADP** | Adenosine Diphosphate |
| **AICAR** | 5-Aminoimidazole-4-carboxamide ribonucleotide |
| **ALL** | Acute Lymphoblastic leukemia |
| **AMP** | Adenosine Monophosphate |
| **AMPK** | AMP-activated protein kinase |
| **ATP** | Adenosine Triphosphate |
| **AUC** | Area Under Curve |
| **BAK** | BCL2 antagonist |
| **BAX** | BCL2 associated X |
| ***BRCA-1*** | Breast Cancer Gene 1 |
| ***BRCA-2*** | Breast Cancer Gene 2 |
| **CA-125** | Carcinoembryonic antigen-125 |
| **CA-19** | Carcinoembryonic antigen-19 |
| **Calcein AM** | Calceine acetoxymethyl ester group |
| **CaMKKβ** | Calcium/calmodulin-dependent kinase kinase |
| **cAMP** | Cyclic adenosine monophosphate |
| **CD39** | Ecto-nucleoside triphosphate diphosphohydrolase (E-NTPDase) |
| **CD73** | Ecto-5'-nucleotidase |
| **CNTs** | Concentrative nucleoside inhibitors |
| **CREB** | cAMP response element binding protein |
| **CRE-luc plasmid** | cAMP reponse element-luciferase plasmid |

| | |
|---|---|
| **ENTs** | Equilibrative nucleoside inhibitors |
| **FIGO** | The International Federation of Gynecology and Obstetrics |
| **HER** | Human epidermal receptor |
| **HMG-CoA** | 3-hydroxy-3-methylglutaryl CoA |
| **HRP-coupled secondary antibody** | Horseradish peroxidase-coupled secondary antibody |
| **LKB1** | Liver Kinase B1 |
| **MMR** | Mismatch Repair |
| **MRP** | Multidrug-resistance protein |
| **mTOR** | Mechanistic target of rapamycin |
| **NER** | Nucleotide Excision Repair |
| **NSCLC** | Non-Small Cell Lung Cancer |
| **Oregon green BAPTA-1 AM** | Oregon green BAPTA-1 acetoxymethyl ester group |
| **PARP** | Poly ADP-ribose polymerase |
| **P-gp** | P-glycoprotein |
| **PLC** | Phospholipase C |
| **PVDF membrane** | Polyvinylidene difluoride membrane |
| **STK** | Serine/threonine kinase |
| **TAK1** | (TGFβ)-activated kinase |
| **TGFβ** | Transforming growth factor β |
| **TNF** | Tumor Necrosis Factor |
| **UDP** | Uridine Diphosphate |
| **UTP** | Uridine Triphosphate |

# 1. Abstract

Resistance development against platinum-based chemotherapy is one of the major burdens in the treatment of ovarian cancer patients. The purinergic ligands ATP and adenosine are found at a much higher concentration in the tumor microenvironment than in normal tissue. This thesis aimed to investigate the roles of ATP and adenosine on the efficacy of platinum-based chemotherapy in ovarian cancer cells. Ovarian cancer cells with different sensitivity against cisplatin were used as cellular model, including cisplatin-sensitive A2780, moderate-sensitive HEY, and resistant, A2780CisR. $P2Y_2$, A1 and A2B receptors were expressed and functionally active in these cell lines. In the first part of the thesis, effects of ATP on the ovarian cancer cell lines were studied. ATP displayed low cytotoxicity with $IC_{50}$ values of 2 to 5 mM in cell viability assays. However, pre-incubation with 500 µM ATP for 48 h prior to 72 h co-incubation with cisplatin resulted in a significant decrease of cisplatin $IC_{50}$ values compared to cisplatin treatment alone. A shift factor of up to 3 was found. Presence of the selective $P2Y_2$ receptor antagonist AR-C118925 had no effect on ATP-enhanced cisplatin cytotoxicity, whereas the nucleoside transporter inhibitor dipyridamole completely abrogated the enhancing effect of ATP on cisplatin cytotoxicity, suggesting an ecto-nucleotidase-dependent generation and subsequent uptake of adenosine.

Therefore, effects of extracellular adenosine were studied in the second part of this thesis. Extracellular adenosine showed moderate cytotoxicity with $IC_{50}$ values of 700 to 900 µM after 48 h treatment in A2780, A2780CisR and HEY cells. Adenosine induced cell cycle arrest in S-phase and significantly induced apoptosis in a concentration-dependent manner. Pre-incubation with adenosine for 48 h followed by 72 h co-incubation with cisplatin resulted in a significant decrease of the cisplatin $IC_{50}$ values and achieved a shift factor up to 4. Synergism between adenosine and cisplatin was confirmed by combination index values of less than 0.9. Interestingly, the effect of adenosine to enhance cisplatin cytotoxicity was higher in cisplatin-sensitive cells than in cisplatin-resistant cells, suggesting an early use of adenosine in ovarian cancer patients obtaining platinum-based chemotherapy. The nucleoside transporter inhibitor dipyridamole completely abrogated adenosine-induced cytotoxicity and apoptosis as well as adenosine-enhanced cisplatin cytotoxicity whereas adenosine receptor antagonists had no effect. Moreover, the increase in phosphorylated AMP-activated protein kinase (pAMPK) and decrease of phosphorylated S6K after treatment with adenosine indicated that intracellular adenosine activates AMPK and leads to an inhibition of mTOR.

In conclusion, this thesis demonstrates that the combination of adenosine and cisplatin enhances cisplatin sensitivity in a synergistic manner. Adenosine increases the induction of apoptosis and inhibits mTOR via AMPK activation after intracellular uptake. The effects of adenosine are independent of adenosine GPCRs, thus allowing circumventing unfavorable adenosine receptor-mediated cancer immune escape. Therefore, application of adenosine prior to administration of platinum-based chemotherapy may be a new therapeutic option to increase the sensitivity towards platinum drugs and prevent or delay the development of platinum resistance in ovarian cancer patients.

# 2. Zusammenfassung

Die Resistenzentwicklung gegen platinbasierte Chemotherapeutika ist eines der Hauptprobleme bei der Behandlung von Patientinnen mit Ovarialkarzinomen. Die purinergen Liganden ATP und Adenosin liegen in der Tumor-Mikroumgebung in einer viel höheren Konzentration vor als in normalem Gewebe. Diese Arbeit hatte zum Ziel, den Einfluss von ATP und Adenosin auf die Wirksamkeit von platinbasierten Chemotherapeutika in Ovarialkarzinomzellen zu untersuchen. Als zelluläre Modelle wurden Ovarialkarzinomzellen verschiedener Sensitivität gegenüber Cisplatin eingesetzt: sensitive A2780-Zellen, mäßig sensitive HEY-Zellen und die resistente Ziellinie A2780CisR. $P2Y_2$-, A1- und A2B-Rezeptoren wurden in allen drei Zelllinien exprimiert und waren funktionell aktiv. Im ersten Teil der Arbeit wurden die Auswirkungen von ATP auf diese Ovarialkarzinomzelllinien untersucht. ATP zeigte –in MTT Assays eine geringe Zytotoxizität mit $IC_{50}$-Werten von 2 bis 5 mM. Eine Präinkubation der Zellen mit 500 µM ATP für 48 Stunden vor der 72-stündigen Inkubation mit Cisplatin führte zu einer signifikanten Abnahme der Cisplatin-$IC_{50}$-Werte im Vergleich zur alleinigen Cisplatin-Behandlung. Es wurden Shift-Faktoren von bis zu 3 festgestellt. Die Anwesenheit des selektiven $P2Y_2$-Rezeptor-Antagonisten AR-C118925 hatte keine Auswirkungen auf die durch ATP verstärkte Zytotoxizität von Cisplatin. Der Nucleosidtransporter-Inhibitor Dipyridamol hob hingegen die verstärkende Wirkung von ATP auf die Cisplatin-Toxizität vollständig auf, was auf eine Ektonukleotidase-abhängige Erzeugung und anschließende intrazelluläre Aufnahme von Adenosin hindeutet.

Aufgrund dessen wurden im zweiten Teil dieser Arbeit die Effekte von extrazellulärem Adenosin untersucht. Extrazelluläres Adenosin zeigte nach 48-stündiger Behandlung von A2780-, A2780CisR- und HEY-Zellen eine mäßige Zytotoxizität mit $IC_{50}$-Werten von 700 bis 900 µM. Adenosin bewirkte einen Zellzyklusarrest in der S-Phase und induzierte signifikant Apoptose in konzentrationsabhängiger Weise. Die 48-stündige Präinkubation von Adenosin gefolgt von einer 72-stündigen Koinkubation mit Cisplatin führte zu einer signifikanten Abnahme der $IC_{50}$-Werte von Cisplatin und erreichte einen Shift-Faktor von bis zu 4. Kombinationsindex-Werte (CI values) von $< 0,9$ bestätigten einen synergistischen Effekt der Kombination von Adenosin und Cisplatin. Interessanterweise war die steigernde Wirkung auf die Cisplatin-Sensitivität in Cisplatin-sensitiven A2780-Zellen höher als in entsprechend resistenten A2780CisR-Zellen, was eine frühzeitige Anwendung von Adenosin bei Ovarialkarzinom-Patientinnen, welche mit platinbasierten Chemotherapeutika behandelt

werden, sinnvoll erscheinen lässt. Der Nukleosidtransporter-Inhibitor Dipyridamol hob die Adenosin-abhängige Zytotoxizität und Apoptose sowie die durch Adenosin verstärkte Cisplatin-Sensitivität vollständig auf, während Adenosinrezeptor-Antagonisten keine Wirkung zeigten. Darüber hinaus zeigte der Anstieg der phosphorylierten AMP-aktivierten Proteinkinase (pAMPK) und die Abnahme von phosphoryliertem S6K nach Behandlung mit Adenosin, dass intrazelluläres Adenosin AMPK aktiviert und zu einer Hemmung von mTOR führt.

Zusammenfassend zeigt diese Arbeit, dass die Kombination von Adenosin mit Cisplatin die Cisplatin-Sensitivität synergistisch erhöht. Adenosin verstärkt weiterhin die Induktion der Apoptose und hemmt mTOR durch AMPK-Aktivierung nach intrazellulärer Aufnahme. Die Wirkung von Adenosin ist unabhängig von Adenosin-GPCRs, was es erlaubt den ungünstigen, Adenosinrezeptor-vermittelten Entzug der Krebszellen vor dem Immunsystem zu umgehen. Daher kann die Applikation von Adenosin vor einer platinbasierten Chemotherapie eine neue therapeutische Option sein, um die Sensitivität gegenüber Platin-Therapeutika zu erhöhen und die Entwicklung einer Platin-Resistenz bei Patientinnen mit Ovarialkarzinomen zu verhindern oder zu verzögern.

# 3. Introduction

## 3.1 Ovarian cancer

### 3.1.1 Etiology and epidemiology

Ovarian cancer is the most lethal cancer among the gynecologic cancers and is the fifth leading cause of cancer-related deaths in women [Coward et al., 2015]. The high mortality rate is related to the onset of nonspecific symptoms and the lack of adequate screening tools which allows the disease to go undiagnosed until it has progressed beyond the pelvic cavity [Smith et al., 2008 and Coward et al., 2015]. Risk of ovarian cancers increases with increasing age. A woman's risk increases from 15.7 to 54 per 100,000 as her age advances from 40 to 79 years. The median age at diagnosis is 59 [Jemal et al., 2007]. Most cases of ovarian cancer present during peri and postmenopausal phase of women's reproductive life span [Colombo et al., 2006 and Ledermann et al., 2013].

Family history is an important risk factor in the development of ovarian cancer. If one family member has a diagnosis of ovarian cancer, the associated lifetime risk is 9% but this risk increases to greater that 50% if there are two or more first-degree relatives (e.g., her mother and sister) with a diagnosis of ovarian cancer or multiple cases of ovarian and breast cancer within the same family [Shepherd, 2000 and Cannistra et al., 2004]. It is well known that about 5% to 10% of ovarian cancers result from an inherited predisposition [Kotsopoulos et al., 2014]. Mutation in the *BRCA-1* and *BRCA-2* tumor suppressor genes is the most common cause of hereditary ovarian carcinomas [Smith et al., 2008]. An inherited *BRCA-1* mutation confers a 15% to 45 % lifetime risk of developing ovarian cancer whereas *BRCA-2* mutation increases the lifetime risk of ovarian cancer to 10% to 20 % [Ledermann et al., 2013]. The hereditary non-polyposis colorectal cancer or Lynch's syndrome is a familial syndrome with germ-line mutations causing defects in enzymes involved in DNA mismatch repair which is associated with up to 12% of hereditary ovarian cancer cases [Lux et al., 2006].

Hormone exposure, specifically estrogen and reproductive history are also associated with the risk of developing ovarian cancer. Conditions that increase the total number of ovulations in women's reproductive history such as nulliparity, early menarche or late menopause are associated with an increasing risk for epithelial ovarian cancers [Martin et al., 2002 and Pecorelli et al., 1998]. Conversely, those conditions that limit ovulations are associated with a protective effect. Each time ovulation occurs, the ovarian epithelium is broken, followed by

cellular repair. According to the incessant ovulation hypothesis, the risk of mutations and ultimately cancer increase each time the ovarian epithelium undergoes cell repair [Smith et al., 2008]. Finally, ovarian cancer is associated with certain dietary and environmental factors. A diet that is high in galactose, animal fat and meat may increase the risk of ovarian cancer whereas a vegetable-rich diet may decrease the risk of ovarian cancer. Although controversial, exogenous factors such as asbestos and talcum powder use in the perineal area are associated with an increased risk of ovarian cancers [Runnebaum et al., 2001 and Edmondson et al., 2001].

### 3.1.2 Pathology and classification

Ovarian cancer is gynecologic cancers mainly originating from the ovary. It usually arises from disruption or mutations in the epithelium of the ovary. Ovarian carcinomas can be classified into three major types according to originated cells: epithelial carcinomas, germ cell tumors and stromal tumors. 85% to 90% of ovarian cancers are derived from the epithelial surface of the ovary [Holschneider et al., 2000]. The World Health Organization histological typing of epithelial ovarian tumors recognizes the following subtypes: serous, endometrioid, clear-cell, mucinous, transition cell, mixed epithelial tumors, undifferentiated and unclassified [Ledermann et al., 2013]. Papillary serous adenocarcinoma is the most common type of epithelial ovarian cancer and accounts for approximately 46% of cases. The peak age of diagnosis ranges from 45 to 65 years with 63 years as the median age of diagnosis [Seidman et al., 2003]. Mucinous carcinomas occur in women between 40 and 70 years of age and account for approximately 36% of all ovarian cancers. The overall prognosis for mucinous carcinoma is better than for serous carcinoma because most patients present with stage I disease. Clear cell carcinoma comprises approximately 3% of ovarian cancers in women with a mean age of 57 years [Smith et al., 2008]. Germ cell tumors of the ovary comprise approximately 2% to 3% of all ovarian cancers in western countries with increasing incidences in black and Asian women [Cherry et al., 2002 and Patterson et al., 2006]. These tumors are highly curable and affect primarily young women. In contrast to epithelial tumors, approximately 60% to 70% of germ cell tumors are stage I at diagnosis which is related to earlier detection and response to symptoms in this younger patient population [Patterson et al., 2006]. Finally, ovarian sex cord-stromal tumors account for 7% of all ovarian cancers and tend to be diagnosed at stage I [Ozols, 2001]. They are associated with hormonal effects such as precocious puberty, amenorrhea and postmenopausal bleeding. Because they are rare, the

optimal treatment is not clear. The current recommended standard of care is surgery followed by treatment with a platinum-based chemotherapy [Smith et al., 2008].

Ovarian cancer is normally spread in the abdominal cavity but can also be found in the lung, liver but less common to the bone and brain. Disease is spread by direct extension, peritoneal seeding, and lymphatic dissemination or by blood-borne metastasis. Lymphatic seeding is the most common pathway and frequently causes ascites [Smith et al., 2008].

### 3.1.3 Diagnosis

Unfortunately, ovarian cancer has no specific symptoms, making clinical diagnosis of early ovarian cancer more difficult. Symptoms are most commonly seen with advanced disease. General symptoms which can be found in any stage of ovarian cancer are abdominal or pelvic pain, constipation, diarrhea, urinary frequency, vaginal bleeding, abdominal distension and fatigue. In advance stage, ascites and abdominal masses lead to an increase in abdominal girth, bloating, nausea, anorexia, dyspepsia and early satiety [Ledermann et al., 2013].

The diagnostic workup for suspected ovarian cancer includes a careful physical examination including a Papanicolaou (Pap) smear, pelvic and rectovaginal examination [Runnebaum et al., 2001]. Transvaginal ultrasonography has improved the visualization of ovarian structures by distinguishing between malignant versus benign condition [Lerner et al., 1994]. The presence of a pelvic mass that is unilateral or bilateral, solid, irregular, fixed or nodular is highly suggestive of ovarian cancer. Unfortunately, by the time pelvic mass can be palpitated on physical exam, the disease is already advanced beyond pelvic cavity.

A complete blood count, chemistry profile (including liver and renal function tests) and CA 125; carcinoembryonic antigen and CA 19 levels should be performed. Although CA 125 is a nonspecific antigen, it is the best current tumor marker for epithelial ovarian carcinoma. A normal CA 125 value is less than 35 units per milliliter. Rising CA 125 titers are often associated with disease progression but this antigen can be elevated in various conditions such as different phases of menstrual cycle, diverticulitis, endometriosis as well as non-gynecologic cancers. In advanced disease, CA 125 is elevated in about 85% of patients [Ledermann et al., 2013]. CA 19 value is used to rule out that ovarian cancer results from other gastrointestinal cancers. Other diagnosis tests should include a transvaginal or abdominal ultrasonography, chest radiography, computer-tomography, magnetic resonance imaging or positron emission tomography scan [Smith et al., 2008 and Ledermann et al., 2013].

### 3.1.4 Staging

In order to classify the progression of tumors and indicate patient prognosis, the International Federation of Gynecology and Obstetrics (FIGO) has proposed criteria for staging of ovarian cancers shown in Table 3.1.

**Table 3.1. The International Federation of Gynecology and Obstetrics (FIGO) staging of ovarian cancers, 2014** [Prat, 2015 and Doubeni et al., 2016]

| Stage | Definition |
|---|---|
| **I** | **Tumor confined to ovaries or fallopian tubes**<br>Sub classified into IA to IC as based on findings if tumor is found in one or both ovaries, if capsules are intact or if there are malignant cells on ovarian surface or in peritoneal washing or ascites. |
| **II** | **Tumor involves one or both ovaries or fallopian tubes with pelvic extension or primary peritoneal cancer**<br>Sub classified into IIA and IIB as based on the extension only on uterus and/or fallopian tubes and/or ovaries, and extension to other pelvic intraperitoneal tissue. |
| **III** | **Tumor involves one or both ovaries or fallopian tubes, or primary peritoneal cancer with cytologically or histologically confirmed spread to peritoneum outside the pelvic and/or metastasis to retroperitoneal lymph nodes**<br>Sub classified into IIIA to IIIC as based on whether affected nodes are retroperitoneal, the extent of peritoneal metastases and involvement of spleen or liver. |
| **IV** | **Distant metastasis excluding peritoneal metastases**<br>Sub classified into IVA and IVB as based on presence of pleural effusion and/or involvement of liver, spleen and lymp nodes outside the abdominal cavity. |

### 3.1.5 Treatment

*Surgery*

Surgery is a primary treatment intervention for ovarian cancer. It may be curative for selected patients with limited stage IA disease. Primary surgical treatment includes a total abdominal hysterectomy with bilateral sapingo-oophorectomy, omentectomy and lymph node dissection [Stratton et al., 2001]. The primary objective of the surgery is to optimally debulk the tumor

to less than 1 cm of residual disease [Bhoola et al., 2006]. Long-term follow up studies confirm that residual disease smaller than 1 cm correlates with higher complete response rates to chemotherapy and longer overall survival as compared to patients with bulky residual disease (larger than 1 cm) [Bristow et al., 2002 and Hoffman et al., 2005]. The skill of the surgeon has a significant impact on prognosis with definitive benefit of trained gynecologic oncologists performing surgery as compared to a gynecologist or general surgeon. The reasons for recommendation of gynecologic oncologists to perform surgery include (a) pelvic tumors cannot be readily biopsied without risk of tumor seeding which can increase the risk of recurrence and (b) surgical staging takes into account the presence of microscopic disease in samples obtained by pelvic washing and lymph node dissection and analysis by a pathologist during the surgical procedure. It is recommended that the initial surgical staging and tumor debulking surgery of ovarian cancer is performed by a trained gynecologic oncology surgeon to prevent under-staging and to optimize overall outcome [Mayer et al., 1992 and Nguyen et al., 1993].

*Chemotherapy*

Systemic chemotherapy with a taxane-platinum regimen following optimal surgical debulking is the standard of care for treatment of epithelial ovarian cancer [Lebermann et al., 2013]. Historically, single-agent alkylating agents such as melphalan and cyclophosphamide were used for treatment of advanced ovarian cancer until the introduction of cisplatin in the 1970s. Combination chemotherapy regimens containing cisplatin and cyclophosphamide achieved higher response rates and overall survival than regimens without cisplatin in patients with advanced ovarian cancer [Ozols et al., 2006]. Based on the results of these trials, the combination of cisplatin plus cyclophosphamide remained the standard of treatment in ovarian cancer until the early 1990s [Smith et al., 2008]. With the introduction of paclitaxel into chemotherapy, McGuire et al. reported the results of Gynecologic Oncology Group (GOG)-111 study that found the combination of paclitaxel 135 mg/m$^2$ over 24 hours and cisplatin 75 mg/m$^2$ achieved higher response rates and longer survival than cyclophosphamide 750 mg/m$^2$ and cisplatin 75 mg/m$^2$ in patients with newly diagnosed, suboptimally debulked, stage III and IV ovarian cancer [McGuire et al., 1996]. Survival improved significantly in the paclitaxel arm with increase in median progression-free survival (18 months vs. 13 months) and overall survival (38 months vs. 24 months). Neutropenia, alopecia and peripheral neuropathy were more severe in paclitaxel/cisplatin group. A large European-Canadian Intergroup Phase III randomized trial (OV10) also confirmed superior

response rates with paclitaxel/cisplatin over cyclophosphamide/cisplatin regimen [Piccart et al., 2003]. Based on these studies, paclitaxel plus cisplatin was widely accepted and became the standard of ovarian cancer treatment [Smith et al., 2008]. The availability of carboplatin led to clinical trials to evaluate whether carboplatin could be substituted for cisplatin which would spare patients from significant neurotoxicity and nephrotoxicity associated with cisplatin. Several prospective randomized comparisons of carboplatin plus paclitaxel versus cisplatin plus paclitaxel in patients with advanced ovarian cancer have been conducted [Bookman et al., 2003, Ozols et al., 2003, du Bois et al., 2003 and Neijt et al., 2000]. The results of these trials showed that carboplatin plus paclitaxel is equally efficacious and better tolerated than cisplatin and paclitaxel. In the GOG-158 study, 840 previously untreated patients with optimally resected stage III disease (no residual tumor nodule > 1 cm) were randomized to carboplatin (AUC = 7.5) plus paclitaxel 175 mg/m$^2$ over 3 hours or cisplatin 75 mg/m$^2$ plus paclitaxel 135 mg/m$^2$ over 24 hours administered every 21 days for six cycles [Bookman et al., 2003 and du Bois et al., 2003]. The results of these trials showed no difference in progression-free survival between the two treatment arms with a median time to progression of 19.4 months in the paclitaxel plus cisplatin versus 20.7 months in the paclitaxel plus carboplatin arm. As expected, the incidence of leukopenia, fever, gastrointestinal toxicity and metabolic toxicity was higher in patients in the cisplatin arm whereas patients in the carboplatin arm experienced more thrombocytopenia and pain. Although the incidence of neurotoxicity was similar in the two treatment arms, it was more severe in the paclitaxel plus cisplatin arm. Thus, the carboplatin-paclitaxel regimen is now first-line chemotherapy for ovarian cancer [Coward et al., 2015]. Chemotherapy is recommended for all patients with FIGO stage II-V disease post-surgery [Ledermann et al., 2013]. A combination of paclitaxel 175 mg/m$^2$ and carboplatin (AUC 5-6), both administered intravenously every 3 weeks is the standard treatment [Ozols et al., 2003, du Bois et al., 2003 Neijt et al., 2000 and Ledermann et al., 2013]. For those patients who develop an allergy to or do not tolerate paclitaxel, the combination of docetaxel-carboplatin or pegylated liposomal doxorubicin-carboplatin can be considered as alternative with similar efficacy [Pignata et al., 2011 and Vasey et al., 2004].

### 3.1.6 Treatment of recurrent disease

Although most patients will achieve a complete response to initial treatment, most patients will eventually have recurrence of their disease. Patients who experience recurrences later than 6 months following a response of platinum-based therapy are characterized as having

platinum-sensitive disease whereas patients who experience recurrences within 6 months following an initial response to platinum-based therapy are defined as having platinum-resistant ovarian cancers [Mantia-Smaldone et al., 2011]. Patients with platinum-sensitive disease generally have a better prognosis than platinum-resistant patients. Topotecan is active in patients with metastatic ovarian cancer and non-cross resistant with platinum-based chemotherapy [Swisher et al., 1997]. Pegylated liposomal doxorubicin is used for second-line therapy of recurrent ovarian cancer. The drug tends to be better tolerated than topotecan which is important for heavily pretreated patients with advanced disease [Muggia et al., 1997]. Gemcitabine is also a widely used agent in the treatment of recurrent platinum-resistant ovarian cancer with an overall response rate of only approximately 13% to 22% with single-agent gemcitabine. The combination of gemcitabine with taxanes has demonstrated response rates from 36% to 90% [Poveda, 2005 and Smith et al., 2008].

There are novel cytotoxic agents introduced into the management of platinum-resistant ovarian cancer such as ixabepilone belonging to a new class of agents, epithilones acting as stabilizers of microtubules [Mantia-Smaldone et al., 2011]. Results from Phase II trial showed that ixabepilone produced objective response rates (ORR) of 14.3% in 49 women with platinum- and taxane-resistant epithelial ovarian cancer (EOC) [De Geest et al., 2010]. Trabectedin binds to DNA and interferes with DNA repair, thereby blocking cell cycle progression [Mantia-Smaldone et al., 2011]. Results from a multicenter phase II trial demonstrated that trabectedin monotherapy was active in platinum-resistant epithelial ovarian cancer with an ORR of 6.3% [Krasner et al., 2007]. Pemetrexed is a folate antimetabolite inhibiting a number of enzymes critical to nucleotide synthesis [Shih et al., 1997]. In phase II GOG trial, pemetrexed monotherapy was administered to 48 women with platinum-resistant EOC , reporting an ORR of 21% with median progression-free and overall survivals of 2.9 months and 11.4 months, respectively [Miller et al., 2009]. Phenoxodiol promotes Fas-mediated apoptosis by activating mitochondrial caspase system, inhibiting X-linked inhibitor of apoptosis and disrupting FLICE inhibitory protein (FLIP) expression [Kamsteeg et al., 2003]. In vitro and preclinical animal studies indicated that phenoxodiol can sensitize EOC cells to carboplatin, paclitaxel and gemcitabine [Alvero et al., 2006]. In a phase II clinical trial aimed to determine the safety and efficacy of intravenous phenoxodiol in combination with cisplatin or paclitaxel in women with platinum/taxane-refractory/resistant ovarian cancers. The 32 patients were randomized to 1 of 2 treatment arms according to their previous responses: (1) platinum refractory/resistant, cisplatin (40 $mg/m^2$ intravenous) weekly on day 2 and phenoxodiol (3 mg/kg) weekly on days 1 and 2 and (2) taxane

refractory/resistant, paclitaxel (80 mg/m$^2$ IV) weekly on day 2 and phenoxodiol (3 mg/kg) weekly on days 1 and 2. Patients continued on treatment until complete response, disease progression, unacceptable toxicity, or voluntary withdrawal. In the cisplatin arm, there were 3 partial responses, 9 patients (56%) achieved stable disease, 4 (25%) progressed, and the overall best response rate was 19%. In the paclitaxel arm, there was one complete response and 2 partial responses, 8 patients (53%) achieved stable disease, 4 patients (27%) progressed, and the overall best response rate was 20%. The cisplatin-phenoxodiol was particularly active and warrants further study in patients with platinum-resistant ovarian cancer [Kelly et al., 2011].

Considering the limitation of traditional chemotherapy, the focus of therapies based on signaling pathway, also known as targeted therapy and emerging agents targeting host-tumor immune response seem to be promising [Kotsopoulos et al., 2014 and Mantia-Smaldone et al., 2011]. Vaccines based on tumor-associated antigen are one of the emerging approaches. Tumor antigens are proteins abnormally expressed in cancer cells and can be used as targets for immunotherapy [Mantia-Smaldone et al., 2011]. In ovarian cancer, MUC1 is a transmembrane mucin overexpressed in more than 90% of epithelial ovarian cancers, including platinum-resistant tumors [Hird et al., 1993 and Nicholson et al., 2004]. In a phase I/II trial, 52 women received an intraperitoneal (IP) radioactively-labeled murine anti-MUC1 antibody (yttrium-90-muHMFG1), following traditional surgery and platinum-based chemotherapy. This regime improved median survival rates in a range of 2 to 31 months compared with control [Hird et al., 1993]. CA 125 (MUC16) is another mucin family member used as marker to monitor response to chemotherapy and to survey for disease recurrence in ovarian cancers [Mantia-Smaldone et al., 2011]. In a phase III trial, 20 patients with advanced recurrent ovarian cancer and a history of platinum exposure received oregovomab, a monoclonal antibody against CA 125, followed by optional chemotherapy [Gordon et al., 2004]. Significant increases in T-cell responses were measured in 7/18 (39%) patients in response to CA125, and in 9/18 (50%) patients in response to oregovomab. Immune responses appeared by week 12 (four doses) and were generally maintained or augmented in patients continuing combined treatment with oregovomab and chemotherapy. Overall median survival and progression-free survival was 70.4 weeks and 11 weeks, respectively [Gordon et al., 2004 and Mantia-Smaldone et al., 2011]. Cytokine therapy is treatment with proinflammatory cytokines, including interleukins (IL) 2, 4, 7, 12 and 18, interferon gamma (IFN-γ), tumor necrosis factor alpha (TNF-α) and granulocyte-macrophage colony-stimulating factor (GM-CSF) [Mantia-Smaldone et al., 2011]. In a phase II trial in

patients with platinum-resistant and refractory epithelial ovarian cancers (EOC), IL-2 was administered intraperitoneal (IP), resulting in an overall response rate of 25% with median survival time of 2.1 years [Vlad et al., 2009]. Tyrosine kinase receptor and intracellular signaling pathways are underevaluated for ovarian cancer targeted therapy [Mantia-Smaldone et al., 2011]. Vascular endothelial growth factor receptors (VEGF-R) has been the most commonly studied tyrosine kinase receptors because of the abundantly of VEGF in the serum of patients with epithelial ovarian cancers [Abu-Jawdeh et al., 1996 and Cooper et al., 2002]. Bevacizumab is a monoclonal antibody binding to VEGF receptors, resulting in anti-angiogenic effects. In a phase II trial, a single treatment of 15 mg/kg every 21 days bevacizumab was administered intravenously to 62 patients with recurrent EOC (41.9% with platinum-resistant disease) [Burger et al., 2007]. Clinical responses were observed in 21% of patients, and median progression-free and overall survivals were 4.7 and 17 months, respectively [Mantia-Smaldone et al., 2011 and Coward et al., 2015]. In a study in relapsed platinum-resistant ovarian cancer patients, median progression-free survival (PFS) was 3.4 months with chemotherapy alone versus 6.7 months with additional bevacizumab. The median overall survival was 13.3 months with chemotherapy alone versus 16.6 months with bevacizumab plus chemotherapy [Pujade-Lauraine et al., 2014 and Coward et al., 2015]. These targeted therapies for recurrent platinum-resistant ovarian cancer are some of current examples. Agents targeting folate metabolism, cell adhesion molecules, hormonal therapy, and PARP inhibitors are under investigated and may offer new strategies for treatment of recurrent ovarian cancers [Mantia-Smaldone et al., 2011].

## 3.2 Drug resistance

### 3.2.1 Mechanisms of drug resistance

Drug resistance is the most important reason for treatment failure. Most chemotherapeutic agents have a low therapeutic index. Therefore, small changes in the sensitivity of tumor cells can lead to clinically relevant resistance [Agarwal et al., 2003]. There are many relevant mechanisms for drug resistance, including

1. Inadequate intra-tumor drug concentrations might explain some cases of drug resistance. Alterations of drug influx and efflux due to cell-membrane transport proteins such as P-glycoprotein (Pgp), multidrug-resistance proteins (MRP) and

further ABC transporters can affect intracellular drug concentrations [Agarwal et al., 2003].

2. The tumor microenvironment can also alter drug sensitivity in tumor cells. There is evidence that hypoxia is related to a reduction in cell cycling, resulting in more G0 arrest [Tomida et al., 1999].
3. Drug inactivation via conjugation to glutathione can also diminish the amount of free intracellular drugs available for their targets [Godwin et al., 1992].
4. Enhanced nucleotide excision repair (NER) and altered mismatch repair (MMR) pathway are also associated to drug resistance [Galluzzi et al., 2012].
5. Mutation of p53 leads to transcriptional down-regulation of pro-apoptotic protein such as BAX, BAK, TNF-related apoptosis-inducing ligand and up-regulation of anti-apoptotic proteins such as BCL2 and BCL-$X_{L,}$ resulting in reduced apoptosis and the development of drug resistance [Agarwal et al., 2003].

Hanahan and Weinberg have summarized molecular mechanisms influencing cancer cell survival and thus leading to chemoresistance, so called "Hallmarks of cancer" including therapeutic targeting relevant to particular hallmarks of cancer [Hanahan et al., 2011]. Three very important hallmarks are:

1. Sustaining proliferative signaling: cancer cells have the ability to sustain chronic proliferation whereas normal tissues carefully control the production and release of growth-promoting signals that instruct entry into and progression through the cell growth and division cycle, thereby ensuring a homeostasis of cells. E.g. epidermal growth factor receptor (EGFR) inhibitors evolved as a therapeutic strategy to fight sustaining proliferative signaling.
2. Evading growth suppressors: in addition to the capability of inducing and sustaining positively acting growth-stimulatory signals, cancer cells also circumvent powerful programs negatively regulating cell proliferation. Many of these programs depend on the actions of tumor suppressor genes. A number of tumor suppressors operating in various ways to limit cell growth and proliferation have been discovered. Cyclin-dependent kinase inhibitors may be one answer to fight this hallmark.
3. Resisting cell death: this mechanism occurs due to an imbalance in apoptosis-induced cell death signaling such as loss of TP53 tumor suppressor, an increase in expression of antiapoptotic regulators like Bcl-2, Bcl-xL or a downregulation of proapoptotic factors such as Bax, Bim, Puma.

### 3.2.2 Cisplatin resistance development

*Cisplatin :Mode of action*

Cisplatin (cDDP) is inactive until one or both chloro groups are replaced by water molecules [Kelland, 2000]. Mono- and bi-aquated forms of cDDP are highly electrophilic and hence prone to form coordinative bonds with methionine as well as with a large panel of cysteine-containing peptides and polypeptides, including reduced glutathione (GSH) and metallo-thioneins [Timerbaev et al., 2006]. The interaction between aquated cDDP and endogenous nucleophiles has dual effects. On one hand, it depletes the cytosol of reducing equivalents, promoting the production of oxidative stress, which may have direct cytotoxic effects or stimulates DNA damage. On the other hand, it results in the inactivation of (at least a fraction of) chemically reactive cDDP, hence functioning as a cytoprotective buffer [Koberle et al., 2010 and Jordan et al., 2000].

Upon aquation, cDDP also binds with high affinity to mitochondrial and nuclear DNA, in particular to nucleophilic N7 sites on purines, thus favoring the generation of heterotypic protein–DNA complexes as well as inter- and intra-strand DNA adducts. If limited in amount, DNA lesions generate by cDDP can be recognized and safely removed by several repair systems normally operating in the context of a temporary cell cycle arrest [Kazak et al., 2012]. In contrast, if the cDDP-induced DNA damage is irreparable, the cell cycle arrest becomes permanent, known as cellular senescence [Muñoz-Espín et al., 2013] cells will then die, often via an excess of DNA lesions promoting widespread mitochondrial outer membrane permeabilization (MOMP) [Tait et al., 2010]. Importantly, there is evidence indicating that cDDP cytotoxic effects originate from both nuclear and cytoplasmic signaling pathways [Gulluzzi et al., 2012], (i) only 1% of intracellular cDDP forms bonds with nuclear DNA [Gonzalez et al., 2001] and (ii) cDDP (as well as oxaliplatin) exerts prominent cytotoxic effects in non-nucleated cells [Mandic et al., 2003]. The molecular mechanisms involved in the cytotoxic potential of cytoplasmic cDDP are poorly understood. These following mechanisms are thought to be involved, (i) the accumulation of reactive oxygen species (ROS) and nitric oxide (NO), which not only exacerbate cDDP toxicity but also exert direct cytotoxic effects by favoring the opening of the permeability transition pore complex (PTPC), (ii) the transduction of a MOMP-stimulatory signal via the pro-apoptotic BCL-2 family member BAK1, the PTPC component voltage-dependent anion channel 1 (VDAC1) and the BAK1 homolog BAX, (iii) the activation of a cytoplasmic pool of p53 that is capable of promoting MOMP via various mechanisms and (iv) in specific cellular models, the establishment of an endoplasmic reticulum (ER) stress response [Galluzzi et al., 2014].

*Mechanism of cisplatin resistance*

Several mechanisms are proposed for cisplatin resistance and can be classified into four categories based on functional and hierarchical parameters [Galluzzi et al., 2014].

1. Pre-target resistance is associated to processes retarding the binding of cDDP to its actual targets. It has been known that cDDP is transported mainly via copper transporters. In particular, copper transporter 1 (CTR1) is significantly associated to cDDP uptake [More et al., 2010] whereas ATPase, $Cu^{2+}$ transporting, β polypeptide (ATP7B), a $Cu^{2+}$ -extruding P-type ATPase plays a significant role in cDDP efflux [Galluzzi et al., 2014]. Alterations in the expression level, subcellular localization and/or functionality of CTR1 and ATP7B have been associated with cDDP resistance, both in preclinical models and in cancer patients [Galluzzi et al., 2014]. In addition, increased concentrations of thiol-containing molecules such as glutathione following chronic cDDP exposure can induce resistance by decreasing the level of antitumor agents available for interaction with target DNA [Siddik, 2003].
2. On-target resistance is the mechanism that is directly related to the molecular damage induced by cDDP [Gallazzi et al., 2014]. Formation and persistence of DNA adducts of cDDP are vital in inducing apoptosis. Therefore, enhanced DNA adduct repair will attenuate the apoptotic process [Siddik, 2003]. Nucleotide excision repair (NER) is a major pathway for repairing of DNA damage. An increased NER proficiency has been associated with cDDP resistance [Siddik, 2003 and Gallazzi et al., 2014]. The MMR system is also believed to detect DNA adducts caused by cDDP, engages to repair but ultimately fails to repair, thus transmitting a pro-apoptotic signal [Vaisman et al., 1998]. Accordingly, genes encoding MMR components such as mutS homolog 2 (MSH2) and mutL homolog 1 (MLH1) are frequently mutated or down-regulated in the context of acquired cDDP resistance [Aebi et al., 1996 and Fink et al., 1998]. Cisplatin- DNA adducts also lead to double-strand breaks (DSBs), which are normally repaired via homologous recombination (HR). Cells with a loss-of-function or mutations in the genes encoding breast cancer 1 (*BRCA1*) or breast cancer 2 (*BRCA2*) are generally more susceptible to the cytotoxic effects of cDDP than HR-proficient cancers of the same cell types [Venkitaraman, 2002 and Farmer et al., 2005]. Moreover, the appearance of compensatory mutations in *BRCA1* and *BRCA2* restoring the functionality of HR has been shown to enhance cDDP resistance in breast cancer cells [Sakai et al., 2008].

3. Post-target resistance may develop in the cellular sensing systems detecting the molecular damage caused by cDDP and convert it into a lethal signal. Post-target cDDP resistance is not only associated to impair p53 signaling but also defects in several other pro-apoptotic signal transducers, including mitogen-activated protein kinase 14 (MAPK14, best known as p38MAPK) and c-Jun N-terminal kinase 1 (JNK1) [Brozovic et al., 2004 and Mansouri et al., 2003]. Further changes in the expression and functional status of BCL-2 family members and caspases have been correlated with cDDP resistance in clinical studies [Sakamoto et al., 2001], including BCL-2-like proteins such as BCL-XL and MCL-1, and survivin, a caspase 9 inhibitor often upregulated in response to cDDP [Galluzzi et al., 2014].
4. Off-target resistance refers to molecular mechanisms delivering compensatory survival signals even though they are not directly activated by cDDP [Galluzzi et al., 2012]. For example, the overexpression of v-erb-b2 (ERBB2), which is commonly upregulated in breast and ovarian carcinomas [Hengstler et al., 1999] has been suggested to promote cDDP resistance not only by delivering robust pro-survival signals via the AKT1 signaling axis, but also by regulating the transitory cell cycle arrest that is required for the repair of cDDP-induced DNA lesions [Galluzzi et al., 2014].

## 3.3 Purinergic receptors and ligands

Since 1972, the idea of purinergic neurotransmission was proposed by Burnstock [Stagg et al., 2010]. The concept was controversially discussed for several years because it was thought that ATP was unlikely to be involved in selective extracellular signaling. However, the purinergic concept is now accepted. Purinergic receptors are classified on the basis of pharmacology and function into P2 receptors, with ATP/UTP and ADP/UDP as the main ligands, and P1 receptors, with adenosine as the main ligand [White et al., 2006]. The classification of purinergic receptors is shown in Figure 3.1.

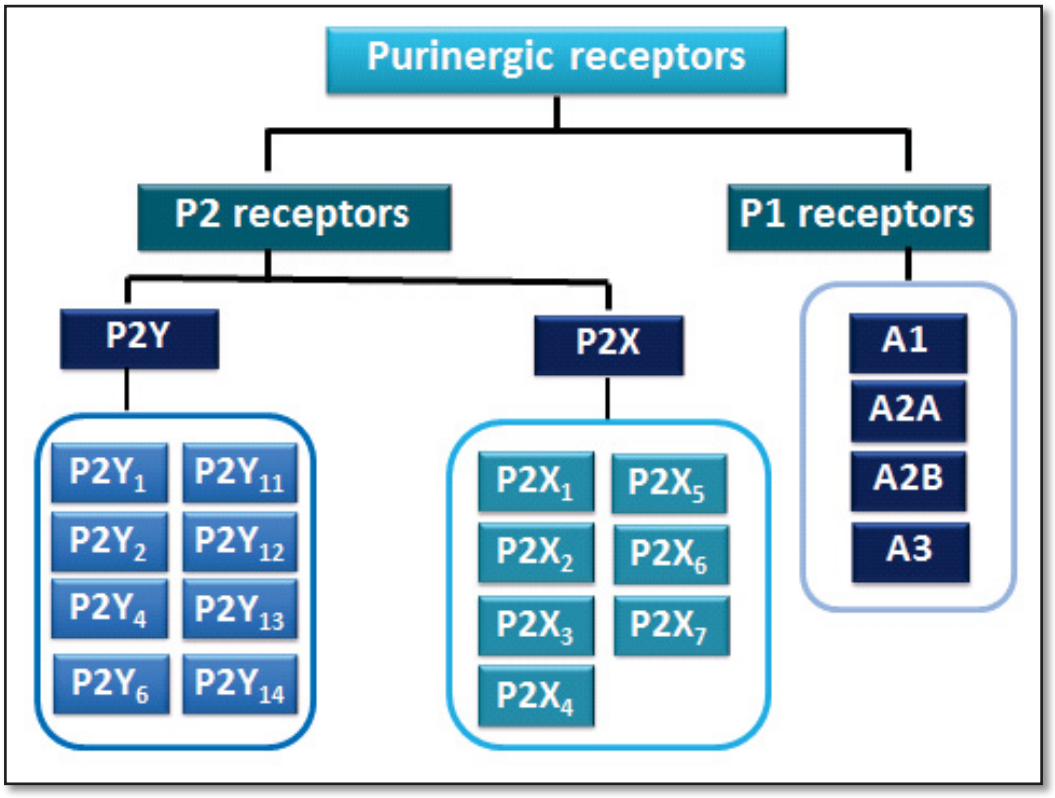


**Figure 3.1. Classification of purinergic receptors**

### 3.3.1 P2 receptors

P2 receptors are subdivided into ionotropic P2X and metabotropic P2Y subtypes. Currently, seven P2X ($P2X_1$, $P2X_2$, $P2X_3$, $P2X_4$, $P2X_5$, $P2X_6$ and $P2X_7$) and eight P2Y ($P2Y_1$, $P2Y_2$, $P2Y_4$, $P2Y_6$, $P2Y_{11}$, $P2Y_{12}$, $P2Y_{13}$ and $P2Y_{14}$) receptor subtypes have been cloned and characterized in human cells (Figure 3.1). P2X receptors are formed by three P2X receptor subunits, either as homomeric or heteromeric receptors. P2X receptors are non-selective cation channels. Under normal physiological conditions, P2X receptor activation will result in $Na^+$ and $Ca^{2+}$ influx and $K^+$ efflux across the cell membrane, leading to depolarization of the plasma membrane and increase in intracellular $Na^+$ and $Ca^{2+}$ concentrations. Membrane depolarization can activate voltage-gated channels, causing firing of action potentials. P2Y receptors are highly diverse in their amino acid sequences and their profiles for endogenous ligands [White et al., 2006]. Alignment of the human receptor sequences of $P2Y_1$, $P2Y_2$, $P2Y_4$, $P2Y_6$, $P2Y_{11}$, $P2Y_{12}$, $P2Y_{13}$ and $P2Y_{14}$ shows an amino acid identity of 21% to 61% [Abbracchio et al., 2017]. P2Y receptors contain seven transmembrane domains, a typical structure of G-protein coupled receptors (GPCRs) with an extracellular N-terminus and an intracellular C-terminus. Several signaling pathways are mediated by P2Y receptors [White et

al., 2006]. The common signaling pathway of P2Y receptors is associated with $G_q$ proteins, an increase in phospholipase C (PLC) activity, leading to IP3 (inositol 1, 4, 5 trisphosphate) generation and the release of $Ca^{2+}$ from the endoplasmic reticulum [Schultze-Mosgau et al., 2000].

It has been demonstrated that different subtypes of receptors can be expressed on the same cell and that different receptor profiles can have opposite effects on cell proliferation. Thus, control of cell proliferation by extracellular nucleotides might be regulated by receptor subtypes mediating a balance between mitogenic and apoptotic processes [Burnstock, 2006].

To date $P2Y_1$, $P2Y_2$, $P2Y_{11}$, $P2X_5$ and $P2X_7$ receptors have been reported to be involved in cancers [White et al., 2006 and Klalid et al., 2017]. $P2Y_1$ and $P2Y_2$ receptor subtypes are the most widely studied among other subtypes of receptors. The effects of P2 receptor activation are reported to vary depending on the cancer cell types. Activation of $P2Y_2$ in melanoma and lung cancer led to an increase in cellular proliferation [White et al., 2005 and Schafer et al., 2003] whereas in esophageal cancer and some colorectal cancers, cellular proliferation was decreased [Hopfner et al., 1998 and Maaser et al., 2002]. $P2Y_2$ activation can lead to the release of epidermal growth factor receptor (EGFR) ligand TGF-α and transactivation of EGFR, through a mechanism involving mitochondrial production of reactive oxygen species [Myers et al., 2009 and Stagg et al., 2010]. Another study reported that the ability of $P2Y_2$ to induce reactive oxygen species in prostate cancer cells, resulting in increased tumor growth [Sauer et al., 2001 and Stagg et al., 2010]. A study in HCT8 and Caco-2 colon cancer cells demonstrated that $P2Y_2$ receptor activation stimulates cell proliferation [Coutinho-Silva et al., 2005]. $P2Y_2$ receptor activation increases cell growth in highly metastatic breast cancer [Jin et al., 2014]. $P2Y_2$, $P2Y_1$ and $P2Y_6$ receptor activations were found to be responsible for driving resistance of an anaplastic lymphoma kinase (ALK) inhibitor in the lung [Wilson et al., 2015]. In ovarian cancer cells OVCAR-3, ATP causes an increase in the rate of cell proliferation [Popper et al., 1993] consistent with another study in human ovarian EFO-21 and EFO-27 carcinoma cells reporting that activation of $P2Y_2$ receptors induced cell proliferation [Schultze-Mosgau et al., 2000]. $P2X_7$ receptor activation is implicated in apoptosis mediated through the caspase enzyme system [Humphreys et al., 2000]. In contrast, inhibition of $P2X_7$ in lymphocytic leukemia cells, suppressed cell proliferation [Adinolfi et al., 2002]. Even though, there are a number of studies on P2 receptors-associated and cancer, further investigations are needed to clarify these effects in different kinds of tumors.

### 3.3.2 P1 receptors

Main agonist of this receptor family is adenosine, a degradation product of ATP via membrane enzymes. CD39 is a member of ectonucleoside triphosphate diphosphohydrolase (E-NTPDase) and metabolizes ATP to ADP or AMP while 5'- ectonucleotidase enzyme CD73 convert AMP to adenosine [Di Virgilio et al., 2017]. P1 receptors are also labeled as adenosine receptors because adenosine is the main ligand of these receptors. P1 receptors are G-protein coupled receptors (GPCRs) and can be divided into four subtypes: A1, A2A, A2B and A3 (Figure 3.1). They are distributed throughout the body. A1, A2A and A3 receptors display high affinity for adenosine while the A2B receptors display low affinity [Gessi et al., 2011]. A1 receptors interact with pertussis toxin-sensitive G-proteins ($G_i$ and $G_o$) inhibiting adenylyl cyclase (AC), and modulating calcium and potassium channels and phospholipase C (PLC). A2A receptors are coupled to $G_s$/$G_{olf}$ proteins stimulating AC and thus increasing intracellular cyclic adenosine monophosphate (cAMP) concentration. A2B receptors are coupled to $G_s$/$G_q$ proteins, increasing AC activity and stimulating PLC. Finally, A3 receptors couple to $G_i$ and $G_q$ proteins leading to inhibition of AC and stimulating PLC [Gessi et al., 2011]. A1 receptor activation has been reported to support breast cancer cell growth and melanoma cell chemotaxis [Gessi et al., 2011, Mirza et al., 2005]. Stimulation of A2A receptors in MCF-7 breast cancer cells enhances cell proliferation [Etique et al., 2009] whereas in A375 melanoma cells, A2A receptor activation can trigger cell death [Merighi et al., 2002]. Activation of A2B receptors in MDA-MB-231 breast cancer cells resulted in the inhibition of cell proliferation via the ERK pathway [Gessi et al., 2011]. In the ovarian cancer cell lines OVAR-3, Caov-4 and SKOV-3, A2B receptors are responsible for a cell growth inhibitoty effect and related to the induction of cell apoptosis. [Hajiahmadi et al., 2015]. In prostate cancer cells, the A2B receptor agonist BAY60-6583 induced cAMP accumulation in a concentration-dependent manner confirming functional activity of A2B receptors. NECA-induced proliferation of PC-3 cells was diminished by siRNA knockdown of the A2B receptors and similarly the selective A2B receptor antagonist PSB603 inhibited cell growth [Wei et al., 2013]. A3 receptor stimulation inhibited proliferation of PC3 prostate carcinoma, HCT-116 colon carcinoma and MIA-PaCa pancreatic carcinoma but on the other hand promoted proliferation of HT29 and Caco-2 colon cancer cells [Gessi et al., 2011]. The stimulation and inhibition of adenosine receptors demonstrated a variety of effects on different types of cancer cells and encourage further investigations on adenosine and its receptors and cancer [Di Virgilio et al., 2017].

### 3.3.3 Purinergic ligands: adenosine triphosphate (ATP) and adenosine

Purinergic ligands are defined as ligands acting as agonists for purinergic receptors. In this study, ATP and adenosine were used as ligands to study their effects in ovarian cancer cells. The chemical structures of ATP and adenosine are shown in Figure 3.2 and 3.3, respectively.

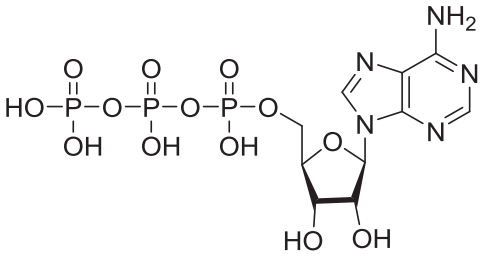

**Figure 3.2. Chemical structure of adenosine triphosphate (ATP)**

*Adenosine triphosphate (ATP)* is an adenine nucleotide found in all living cells. ATP is the molecular result of cellular energy production, involved in metabolic processes, nucleic acid synthesis and it acts as neurotransmitter [Di Virgilio et al., 2017]. ATP is stored intracellularly at very high concentrations up to 10 mM, it is water soluble and quickly degraded by extracellular nucleotidases [Di Virgilio et al., 2017]. ATP concentrations in the interstitium of resting/healthy tissues are very low, in the nanomolar range, whereas in stimulated or diseased tissue, ATP can reach hundreds of micromolar [Falzoni et al., 2013 and Yegutkin, 2014]. ATP acts as agonist for many subtypes of P2 receptors [Burnstock et al., 2006] and participates in different cellular responses, including cell proliferation, migration, differentiation and cell death [Di Virgilio et al., 2017]. A study using ATP in combination with cisplatin in the human ovarian cancer cell line A2780 reported that administration of ATP in combination with cisplatin shows additive effect [Rotte et al., 2010].

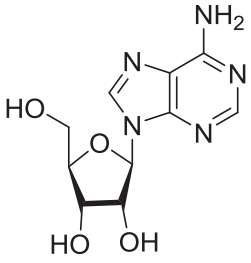

**Figure 3.3 Chemical structure of adenosine**

*Adenosine* is a purine nucleoside and exerts its pharmacologic effects by activation of adenosine receptors. Adenosine relaxes vascular smooth muscles by activation of adenylyl cyclase and reduction of intracellular calcium concentrations in smooth muscle cells. Therefore it acts as a potent vasodilator in most vascular beds [Di Virgilio et al., 2017]. In clinical aspect, adenosine has negative chronotropic and inotropic effects on the heart by slowing the conduction time through the AV node and interrupting AV nodal reentry pathways. US-FDA approved adenosine as intravenous injection solution (3 mg/ml) (Adenocard®) for the conversion to sinus rhythm of paroxysmal supraventricular tachycardia. Methylxanthines such as caffeine and theophylline are competitive antagonists of adenosine whereas the nucleoside transporter inhibitor, dipyridamole inhibits adenosine uptake [USFDA, accessed July 27, 2017]. In biological systems, extracellular adenosine is presented at very low cencentrations (< 1 μM). Its concentration increases under metabolically stressful conditions like inflammation and cancer [Sperlagh et al., 2000 and Martin et al., 2000]. Earlier findings have shown that the extracellular concentration of adenosine carcinomas may reach up to 100 μM (10 to 20-fold higher than normal concentration) which may exert a potent immunosuppressive and cancer growth-promoting effect [Blay et al., 1997 and Kumar, 2013]. In contrast, a study in the ovarian cancer cell line OVCAR-3 demonstrated that adenosine inhibits cell proliferation in a concentration-dependent manner, induces G0/G1 cell cycle arrest as well as induction of apoptosis [Shirali et al., 2013]. Moreover, many studies in prostate cancer [Virtanen et al., 2014], cervical cancer [Mello et al., 2014], hepatocellular carcinoma [Yang et al., 2011 and Wu et al., 2006] and gastric cancer cell lines [Soitoh et al., 2004 and Tsuchiya et al., 2015] also supported inhibitory effects of adenosine on cancer cell proliferation and its ability to induce apoptosis. In addition, a study in endothelial HUVEC cells demonstrated that adenosine-induced phosphorylation of AMPK was not mediated by P1 receptors but required adenosine uptake by equilibrative nucleoside transporters followed by its intracellular metabolism to AMP [da Silva et al., 2006]. In addition to this data, a study in gastric cancer cells demonstrated that extracellular adenosine is transported into cells through adenosine transporters and converted by adenosine kinase to AMP which then activates AMPK [Tsuchiya et al., 2015]. Similarly, a study in the hepatocellular cell line HuH-7 reported that adenosine-activated AMPK was associated with apoptosis induction [Yang et al., 2011].

## 3.4 Adenosine uptake inhibitors

Adenosine mainly exerts its activity via adenosine receptors and most studies focused on adenosine signaling through adenosine receptors. However, adenosine is also taken up from the extracellular space into cells through specific transport proteins called nucleoside transporters located on the cell membrane [Thorn et al., 1996 and Noji et al., 2004]. Extracellular adenosine is rapidly taken up into cells with a half-life of less than 30 s and disappears within 1 min via nucleoside transporters [Yeung, 1991 and Noji et al., 2004]. Nucleoside transport occurs via two distinct families of nucleoside transporter proteins (NTs); SLC28 and SLC29 [Baldwin et al., 2004]. Nucleoside transporters are divided into two main categories based on their functional characteristics and molecular structure: (i) equilibrative and (ii) concentrative nucleoside transporters (ENTs and CNTs) [Lane et al., 2010]. ENTs facilitate passive diffusion of nucleosides across the membranes in either direction depending on intra- and extracellular nucleoside concentrations while CNTs use energy derived from the sodium gradient to influx nucleosides against their concentration gradients. ENTs are found throughout the body but CNTs are found in special tissue or organs such as small intestine epithelium, macrophages, kidney, liver and brain [Noji et al., 2004]. Human equilibrative nucleoside transporter subtype-1 (hENT1), is the major plasma membrane NT [Rehan et al., 2015]. hENT1 is expressed in all tissue types. Cellular hENT1 protein levels have been shown to approximately double between G1 and G2-M phases of the cell cycle [Pressacco et al., 1995 and Rehan et al., 2015]. Elevated hENT1 expression has been found in a variety of cancers including pancreatic adenocarcinoma [Greenhalf et al., 2014] and breast cancer [Lane et al., 2010].

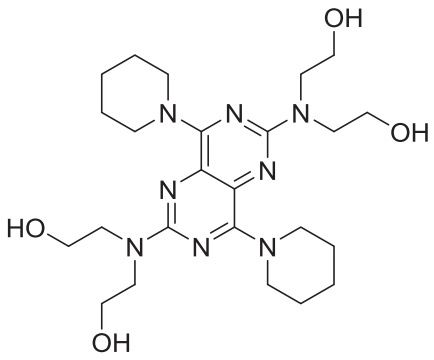


**Figure 3.4. Chemical structure of dipyridamole**

Dipyridamole (DPM) is widely used as nucleoside transporter inhibitor in experimental studies [Noji et al., 2004]. The chemical structure of DPM is shown in Figure 3.4. DPM inhibits the cellular uptake of adenosine into platelets, red blood cells and endothelial cells, leading to increased extra-cellular concentrations of adenosine [Vasu et al., 2013 and Ge et al., 2016]. In pharmacological aspect, DPM is known to inhibit phosphodiesterase enzymes with normally breakdown cAMP, thus resulting in an increase in cellular cAMP levels and blocking of platelet response to ADP [Ge et al., 2016]. In addition, dipyridamole has been shown to lower pulmonary hypertension without a significant drop of systemic blood pressure [Gomez et al., 2013 and Vasu et al., 2013]. DPM inhibits proliferation of smooth muscle cells in vivo and has been shown to prevent AV-shunt failure in dialysis patients [Vasu et al., 2013]. DPM has further been found to increase the concentrations of the anticancer drugs (5-fluorouracil, methotrexate, and vincristine) and thus enhance the efficacy of these drugs [Wang et al., 2013, Spano et al., 2013 and Goda et al., 2008]. A study in vincristine (VCR)-resistant and multidrug-resistant (MDR) cells showed that DPM at a concentration of 10 to 100 μM enhanced uptake of vincristine and inhibited P-glycoprotein. Moreover, DPM also inhibited the enhanced efflux out of MDR cells [Asoh K et al., 1989 and Wang et al., 2013].

## 3.5 AMP-activated protein kinase (AMPK) and mechanistic target of rapamycin (mTOR)

### 3.5.1 AMPK subunit structure

The AMPK structure exists as a heterotrimer of catalytic α and regulatory β and γ subunits. In mammals, α- and β- subunits contain two subtypes, α1, α2, β1 and β2, while γ subunits consist of three subtypes: γ1, γ2 and γ3 [Davies et al., 1994 and Mitchelhill et al., 1994]. There are several possibilities that each of the subtypes in each subunit can form an AMPK complex. Different kinds of AMPK complexes were found in different tissues. The N-terminus of the α-subunit contains the catalytic domain as well as phosphorylation sites for upstream kinases such as liver kinase B1 (LKB1) and Calcium/calmodulin-dependent protein kinase kinase (CaMKKs) regulating AMPK activity [Crute et al., 1998 and Dasgupta et al., 2016]. The γ-subunits are nucleotide binding regulatory subunits binding AMP or ADP. The conserved C-terminus of β-subunits interacts with both α- and γ-subunits and plays an obligatory role in AMPK complex formation [Dasgupta et al., 2016]. In addition, the β-

subunits contain a conserved carbohydrate-binding domain that perhaps allows AMPK to function as a glycogen sensor. AMPK subunits are expressed more or less ubiquitously, and the αβγ AMPK complex exists in 12 different flavors. The expression of particular AMPK complexes displays considerable variation and tissue-specific expression in human [Quentin et al., 2011 and Dasgupta et al., 2012].

### 3.5.2 AMPK regulation and function

AMPK is an evolutionary conserved cellular energy sensor. It is essential for embryonic growth and development and its full impact in adult tissues is revealed under stressful situations [Dasgupta et al., 2016]. AMPK is traditionally thought to play a major role in regulation of cellular metabolism. It is now widely recognized to have antineoplastic efficacy and thus as a target of chemotherapy. The first hint that AMPK may be linked to cancer was provided by the finding that liver kinase B1 (LKB1), a known tumor suppressor, acts as an upstream kinase at AMPK activating AMPK [Woods et al., 2003 and Kim et al., 2013].

AMPK was originally identified in rat liver preparation as a contaminant of its now well-known substrate acetyl-CoA carboxylase (ACC), the rate-limiting enzyme in fatty acid synthesis. AMPK was also found to inhibit 3-hydroxy-3-methylglutaryl CoA (HMG-CoA) reductase, the rate-limiting enzyme in cholesterol biosynthesis. AMPK is inhibited by ATP and activated by AMP and by phosphorylation and was thus named AMP-activated protein kinase or AMPK [Dasgupta et al., 2016]. To date, activation of AMPK by a high AMP/ATP ratio and $Ca^{2+}$ are well studied activation mechanisms. When the cellular AMP/ATP ratio increases, AMP or ADP bind to γ subunits of AMPK. This interaction causes allosteric activation and conformational change in the catalytic α subunits, enabling activating phosphorylation at Thr172 in α1 and/or α2 by upstream kinases (e.g. LKB1) and also inhibition of Thr172 dephosphorylation by phosphatases [Gowans et al., 2013]. It was later found that binding of ADP can also activate AMPK [Xiao et al., 2011]. At least three kinases can phosphorylate AMPK at Thr172: liver kinase B1 (LKB1), also known as serine/threonine kinase (STK11), calcium/calmodulin-dependent kinase kinase (CaMKKβ), and transforming growth factor β (TGFβ)-activated kinase (TAK1) [Dasgupta et al., 2016]. Of these, LKB1 and CaMKKβ are the major upstream kinases of AMPK. LKB1 activates AMPK in response to AMP/ADP while CaMKKβ activates AMPK in response to $Ca^{2+}$, and both pathway work independently or synergistically [Fogarty et al., 2010].

Activation of AMPK inhibits anabolism and activates catabolism, inhibiting cell growth and proliferation by (i) inhibiting protein synthesis through mechanistic target of rapamycin complex 1 (mTORC1) (ii) blocking fatty acid biosynthesis through direct phosphorylation of acetyl-CoA carboxylase (ACC) [Zadra et al., 2015]. AMPK can phosphorylate tuberous sclerosis complex 1 and 2, leading to the suppression of mTORC1 [Yoshida et al., 2011 and Wang et al., 2017]. Alongside with the metabolic effects, AMPK can also induce cell cycle arrest and apoptosis [Zadra et al., 2015 and Dasgupta et al., 2016].

While LKB1/AMPK pathway can act as tumor suppressor through its ability to retard tumor cell growth, it can also behave as tumor promoter, allowing tumor cells to be more resistant to metabolic stress[Zadra et al., 2015], so called " metabolic adaptation" [Liang et al., 2013 and Zadra et al., 2015]. Noteworthy, it was reported that active AMPK can provide stress resistance in human cancers [Koumenis et al., 2014], eventually leading to chemoresistance. This is an undesired effect of AMPK activation since cellular stress arising from pathological cellular conditions such as cancer, lack of nutrients, energy, and oxygen and most important from chemotherapy and radiotherapy should result in the induction of apoptosis. Activation of AMPK in malignant cells might promote their survival especially in the initial stages of tumor development [Yung et al., 2016]. Therefore, AMPK is a double-edged sword of whose activation or inhibition in a particular treatment needs to be considered**.**

### 3.5.3 Role of AMPK in cancer

Metformin, a biguanide anti-diabetic agent which inhibits complex I of mitochondrial electron transport chain [Forgarty et al., 2010] is reported for anti-cancer effect by activation of AMPK [Hawley et al., 2002]. Metformin was shown to inhibit cell proliferation and induce apoptosis in triple-negative breast cancer cell lines as well as estrogen receptor (ER) α-positive and human epidermal receptor (HER) 2-positive cell lines through AMPK activation. Moreover, the combination treatment of metformin and chemotherapeutic agent carboplatin, paclitaxel or doxorubicin showed synergistic inhibition of the G1-phase [Liu et al., 2012]. Phenformin, a more potent biguanide than metformin, also activates AMPK and it is effective in the prevention and treatment of estrogen receptor (ER)-positive and triple-negative breast cancer xenografts in immunocompromised mice [Appleyard et al., 2012]. In NSCLC patients, a significant association was found between high phosphorylated AMPK (pAMPK) expression and increased overall survival and recurrence-free survival [William et al., 2012]. Metformin treatment increased apoptosis in human lung cancer cell lines A549 and NCI-H1299 and significantly inhibited cell proliferation in a dose and time-dependent

manner which was confirmed by results from A549 tumor xenografts in nude mice [Wu et al., 2011]. In acute lymphoblastic leukemia (ALL) cell lines, the AMPK-activating AMP-analogue AICAR induced dose- and time-dependent cell growth inhibition leading to increased AMPK phosphorylation and decreased mTOR phosphorylation [Kuznetsov et al., 2011 and Leclerc et al., 2010]. A similar study in breast cancer cell lines treated with metformin, remarkably repressed cell proliferation as a result of AMPK activation and inhibition of mTOR and S6K [Zakikhani et al., 2006]. A further study confirmed that such effects of meformin were AMPK-dependent, since AMPK knockdown in breast cancer cells prevented metformin-induced inhibition of mTOR signaling and rescued cells from metformin-induced cell growth inhibition [Zakikhani et al., 2006 and Yung et al., 2016]. In the panel of gynecological cancers, it has been demonstrated that A23187, an CaMKKβ-dependent AMPK activator was able to inhibit cervical cancer cell growth [Yu et al., 2009]. Similarly, a the study in LKB1-deficienct HeLa cell lines, treatment with A23187 inhibited cell proliferation significantly stronger than treatment with AICAR, an LKB1-dependent AMPK activator [Zakikhani et al., 2006]. Moreover, cotreatment of AICAR and A23187 enhanced inhibition of cell growth in the cervical cancer cell lines HeLa, CaSki and C41 by suppressing the AMPK/mTOR signaling pathway [Zakikhani et al., 2006 and Yung et al., 2016]. Resveratrol, a well known AMPK activator [Baur et al., 2006] promoted cell death via autophagy in five ovarian cancer cell lines [Opipari et al., 2004]. A study in ovarian cancer cells has found that resveratrol enhanced chemosensitivity of cisplatin and prevent the development of resistance against cisplatin [Engelke et al., 2016]. Again through AMPK activation, bitter melon extract significantly inhibited tumorigenicity and overcame cisplatin resistance in ovarian cancer cells [Yung et al., 2015]. All together, these studies demonstrate a prominent role of AMPK in several kinds of cancers including ovarian cancer.

### 3.5.4 Mechanistic target of rapamycin (mTOR)

One of the major growth regulatory pathways controlled by LKB1-AMPK is the mechanistic target of rapamycin (mTOR) [Kim et al., 2013]. mTOR is an evolutionary conserved serine/threonine kinase integrating signals from multiple pathways including nutrients (e.g. amino acids and glucose), growth factors (e.g. insulin and insulin-like growth factor), hormones (e.g. leptin) and stress (e.g. starvation, hypoxia and DNA damage) to regulate a wide variety of eukaryotic cellular functions such as transcription, translation, protein turnover, cell growth and differentiation, energy balance and stress response [Watanabe et al.,

2011]. mTOR consists of two functionally and structurally distinct complexes, rapamycin-sensitive mTOR complex 1 (mTORC1) and rapamycin-insensitive mTOR complex 2 (mTORC2). mTOR1 phosphorylates S6K and 4E-BP1 and regulates translation, autophagy, growth, lipid biosynthesis, mitochondria biogenesis and ribosome biogenesis whereas mTOR2 phosphorylates SGK1, Akt (S473), Rac1 and PKCα and regulates survival, metabolism, proliferation and cytoskeletal organization [Wullschleger et al., 2006 and Ma et al., 2009].

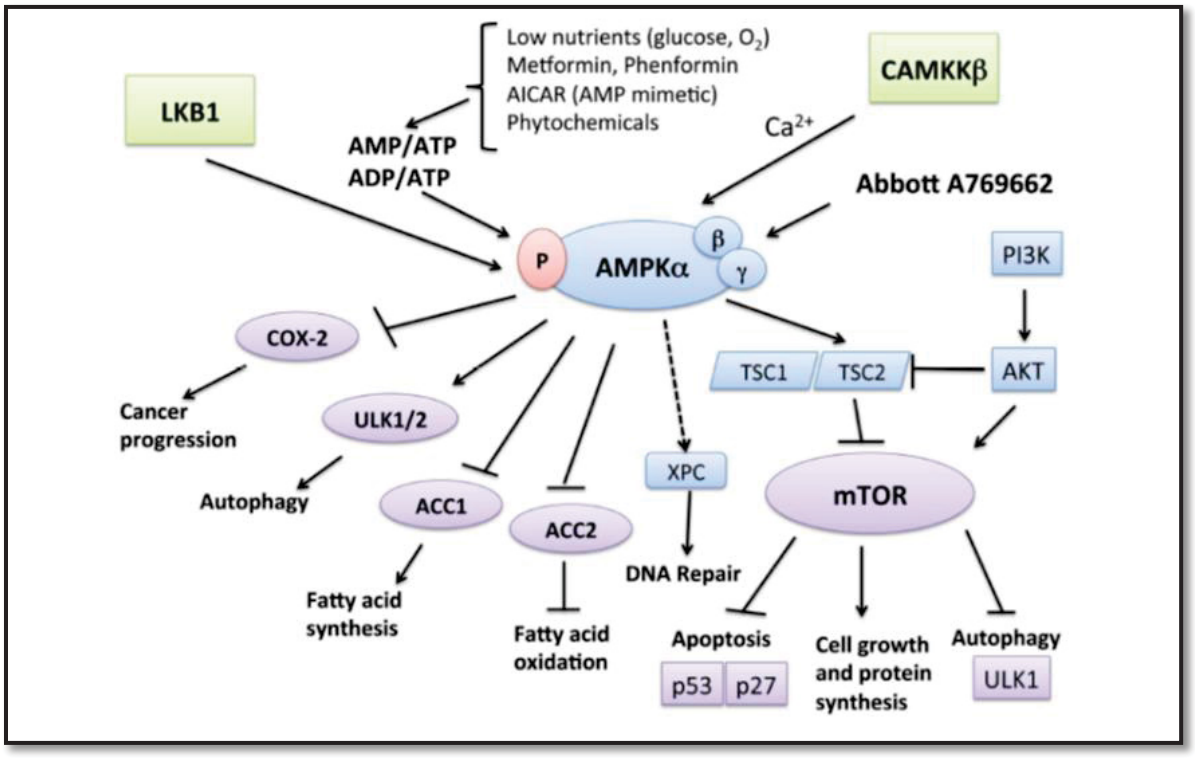


**Figure 3.5. Function and regulation of AMPK leading to tumor suppression** [Kim et al., 2013]
AMPK is activated when cellular AMP/ATP or ADP/ATP ratios rise due to various physiological stresses. One of the most well-known pathways of AMPK is through the TSC1/TSC2 complex, leading to the inhibition of mTOR. The mTOR pathway suppresses apoptosis via its effect on the tumor suppressor p53 and p27.

Based on the information shown in Figure 3.5, mTOR plays a role downstream of AMPK. Under low energy (high AMP/ATP ratio), AMPK is activated in an LKB1-dependent manner and phosphorylates TSC2, leading to mTOR inhibition. However, AMPK also directly phosphorylates Raptor at S792 in an LKB1-dependent manner, which is required for inhibition of mTOR1 and growth arrest under energy stress [Ma et al., 2009 and Watanabe et

al., 2011]. Similarly, Gwinn et al. has proposed a relationship between AMPK and mTOR in TSC2-deficient cells which remain responsive to energy stress [Gwinn et al., 2008]. This study reported that AMPK directly phosphorylates the mTOR binding partner raptor on two well-conserved serine residues, and this phosphorylation induces 14-3-3 binding to raptor. The phosphorylation of raptor by AMPK is required for the inhibition of mTORC1 and cell-cycle arrest induced by energy stress. These findings uncovered a conserved effector of AMPK mediating its role as a metabolic checkpoint coordinating cell growth with energy status [Gwinn et al., 2008].

# 4. Objective

Ovarian cancer is the most lethal gynecologic cancer [Coward et al., 2015]. One of the reasons is a resistance development to platinum-based chemotherapy currently used as first-line chemotherapy of ovarian cancer. A number of studies attempted to reinforce the sensitivity of platinum chemotherapy by changing the schedule of administration or combining platinum drugs with other chemotherapeutic agents. However the success is moderate and a therapeutic ceiling is being reached with these approaches [Coward et al., 2015].

Purinergic signaling pathways have been proposed since the 1970s [White et al., 2006] and the presence of high concentrations of purinergic ligands in the extracellular tumor environment has been found. Purinergic ligands have extensively been studied in several types of cancer including ovarian cancer. Encouraging effects of purinegic ligands on cancer cell growth, proliferation, and metastasis as well as cell death [Stagg et al., 2010] suggest purinergic signaling pathways as new targets to improve cancer treatment. Even though the beneficial effects of purinergic ligands have been investigated in several types of cancers, their effects on ovarian cancer remain mostly unclear.

Therefore, this study aimed to clarify the contribution of the purinergic ligands ATP and adenosine to chemosensitization in ovarian cancer cells of different platinum sensitivity and unravel underlying mechanisms in single and in combination treatments with cisplatin. Cisplatin is regarding its pharmacodynamical effects and platinum-DNA adduct formation equivalent to carboplatin, the platinum drug used as first-line chemotherapy [Bookman et al., 2003, Ozols et al., 2003, du Bois et al., 2003 and Neijt et al., 2000]. More specifically, the following topics should be investigated in ovarian cancer cells in the framework of this thesis:

- expression and functional activity of purinergic receptors
- cytotoxicity of the purinergic ligands ATP and adenosine
- underlying molecular mechanisms of the cytotoxic effects of the purinergic ligands ATP and adenosine
- investigation of combinations of ATP or adenosine, respectively, and cisplatin for increasing platinum sensitivity.

# 5. Materials and Methods

## 5.1 Materials

**Table 5.1. List of chemical reagents**

| Chemical reagents | Manufacturer |
|---|---|
| 2-Mercaptoethanol 99% (analytical grade) | Carl Roth GmbH & Co.KG, Karlsruhe |
| 2X QuantiTect-SYBR® Green master mix | Qiagen, Germany |
| Acetyl-Coenzyme A | AppliChem, Darmstadt |
| Adenosine | Sigma Aldrich, Steinheim |
| Adenosine 5'-(α,β-methylene)diphosphate sodium salt (APCP) | Tocris bioscience |
| Adenosine triphosphate-Disodium salt hydrate (ATP) | Sigma Aldrich, Steinheim |
| Agarose gel for electrophoresis | Carl Roth GmbH & Co.KG, Karlsruhe |
| Ammonium persulfate (APS), $(NH_4)_2S_2O_8$ | Merk KGaA, Darmstadt |
| Bromophenol blue sodium salt | Acros Organic/Thermo Fisher Scientific Inc., USA |
| BSA (Bovine Serum Albumin) | AppliChem, Darmstadt |
| Calcium chloride ($CaCl_2$) | Sigma Aldrich, Steinheim |
| Calcium Chloride dehydrate ($CaCl_2 \times 2H_2O$) | KHF Laborchemie, Leipzig |
| Cisplatin | Sigma Aldrich, Steinheim |
| Copper (II) sulfate pentahydrate ($CuSO_4 \times 5H_2O$) | Sigma Aldrich, Steinheim |
| CRE-luciferase transporter plasmid | Stratagene, Germany |
| Dimethyl sulfoxide (DMSO) (analytical grade) | VWR® BDH PROLAB®, Darmstadt |
| Dipyridamole | Sigma Aldrich, Steinheim |
| Disodiumhydrogenphosphate dihydrate ($Na_2HPO_4 \times 2H_2O$) | VWR® BDH PROLAB®, Darmstadt |
| Dithiothreitol (DTT) | Carl Roth GmbH & Co.KG, Karlsruhe |

| Chemical reagents | Manufacturer |
|---|---|
| D-Luciferin sodium salt | AppliChem, Darmstadt |
| DNase-free RNase A | AppliChem, Darmstadt |
| Dulbecco's Modified Eagle Medium (DMEM) | PAN Biotech GmbH, Aidernbach |
| EDTA | Carl Roth GmbH & Co.KG, Karlsruhe |
| EDTA disodium salt, dihydrate | AppliChem, Darmstadt |
| Eosin B (C.I. 45400) | Carl Roth GmbH & Co.KG, Karlsruhe |
| Ethanol analytical grade | VWR® BDH PROLAB®, Darmstadt |
| FBS (Fetus Bovine Serum) | PAN Biotech GmbH, Aidernbach |
| GeneRuler 50 bp DNA ladder | Thermo Scientific, Germany |
| Glucose ($C_6H_{12}O_6$) | Sigma Aldrich, Seelze |
| Glycerol water-free , analytical grade | Carl Roth GmbH & Co.KG, Karlsruhe |
| Glycine | AppliChem, Darmstadt |
| Helipur® | B. Braun Melsungen AG, Melsungen |
| HEPES free base | AppliChem, Darmstadt |
| High Capacity cDNA Reverse Transcription Kit | Applied Biosystems, California, USA |
| Hydrochloric acid 37% (HCl) | VWR® BDH PROLAB®, Darmstadt |
| Isopropanol tech. | Obtained from Central Chemical Unit HHU |
| Magnesium acetate tetrahydrate | AppliChem, Darmstadt |
| Magnesium sulfate ($MgSO_4$) | Fluka , USA |
| Magnesium sulfate heptahydrate | Fluka Chemie AG, Buchs, Schweiz |
| Metformin HCl | Tokyo chemical, Zwijndrecht, Belgium |
| Methanol (analytical grade) | VWR® BDH PROLAB®, Darmstadt |
| Milk powder (Blotting grade) | Carl Roth GmbH & Co.KG, Karlsruhe |
| MTT (3-(4,5-Dimethylthiazol-2-yl)-2,5-diphynyltetrazoliumbromide | SERVA, Electrophoresis GmbH, Heidelberg |
| My Budget RNA Mini Kit | Qiagen, Germany |
| N-Tris(hydroxymethyl)-methyl-glycin (Tricine) | AppliChem, Darmstadt |
| Oligo$(dT)_{23}$ anchored primer | Invitrogen, Germany |
| Oregon Green™ 488 BAPTA-1 AM | Thermo Fisher Scientific, Rockford, USA |

| Chemical reagents | Manufacturer |
|---|---|
| Paclitaxel | Biotrend chemikalien GmbH, Cologne |
| PageRuler™ Plus prestained protein ladder | Thermo Scientific, Rockford, USA |
| PageRuler™ prestained protein ladder | Thermo Scientific, Rockford, USA |
| Penicillin-Streptomycin (10,000 U/ml ; 10 mg/ml) | PAN Biotech GmbH, Aidenbach |
| Pierce™ Reagent A for BCA assay | Thermo Scientific, Germany |
| Pluronic F-127 | Sigma Aldrich, Steinheim |
| PolyFect transfection reagent | Qiagen, Germany |
| Potassium Chloride (KCl) (analytical grade) | Carl Roth GmbH & Co.KG, Karlsruhe |
| Potassium dihydrogen phosphate ($KH_2PO_4$) | Carl Roth GmbH & Co.KG, Karlsruhe |
| Propidium iodide | Santa Cruz Biotechnology, Heidelberg |
| Protease/phosphatase inhibitor mini tablets | Thermo scientific, Rockford |
| Q-VD-OPh hydrate | Sigma Aldrich, Steinheim |
| RNase-free DNase set | Qiagen, Germany |
| Roswell Park Memorial Institute Medium (RPMI) | PAN Biotech GmbH, Aidenbach |
| Rotiphorese® Gel 30 (37.5:1) | Carl Roth GmbH & Co. KG, Karlsruhe |
| Sodium azide ($NaN_3$) 99% | Acros Organic/Thermo Fisher Scientific Inc., USA |
| Sodium Chloride (analytical grade) | Fisher Chemicals, Themo Scientific, Rockford, USA |
| Sodium Chloride solution 0.9% (w/v), sterile | Fresenius Kabi Deutschland GmbH, Bad Homburg |
| Sodium citrate tribasic dihydrate | Fisher Chemicals, Themo Scientific, Rockford,USA |
| Sodium deoxycholate | Carl Roth GmbH & Co.KG, Karlsruhe |
| Sodium dodecyl sulfate (SDS) Ultra-pure | SERVA, Electrophoresis GmbH, Heidelberg |
| Sodium hydrogen carbonate ($NaHCO_3$) | VWR® BDH PROLAB®, Darmstadt |
| Sodium hydroxide (NaOH) | Mallinkrodt Baker, Griesheim |
| Tetramethylethylenediamine (TEMED) | Carl Roth GmbH & Co.KG, Karlsruhe |
| Tris(hydroxymethyl)-aminomethane (Tris) | AppliChem, Darmstadt |

| Chemical reagents | Manufacturer |
|---|---|
| Triton® X-100 | AppliChem, Darmstadt |
| Trypsin-EDTA in PBS | PAN Biotech GmbH, Aidenbach |
| Tween®20 | Carl Roth GmbH & Co.KG, Karlsruhe |
| UDP (Uridine diphosphate) | Sigma Aldrich, Steinheim |
| UTP (Uridine triphosphate) | Sigma Aldrich, Steinheim |
| Verapamil | Sigma Aldrich, Steinheim |
| Western Blotting Luminol Reagent | Santa Cruz Biotechnology, Heidelberg |

**Table 5.2. List of cell lines**

| Cell type | Cell lines | Medium | Manufacturer |
|---|---|---|---|
| Ovarian cancer cells | A2780<br>A2780CisR<br>HEY | RPMI1640 | European Collection of Cell Cultures (ECACC, UK) |
| Human Embryonic Kidney cells | HEK293 | DMEM | German Collection of Microorganisms and Cell Cultures (DSMZ, Germany) |

**Table 5.3. List of selective agonists and antagonists of purinergic receptors**

| Agonist/Antagonist | Selectivity | Manufacturer |
|---|---|---|
| **P1 receptor** | | |
| BAY 60-6583 | A2B receptor agonist | Tocris bioscience |
| (±)-5'-Chloro-5'-deoxy-ENBA | A1 receptor agonist | Tocris bioscience |
| SLV320 | A1 receptor antagonist | Tocris bioscience |
| SCH 442416 | A2A receptor antagonist | Tocris bioscience |
| PSB 603 | A2B receptor antagonist | Tocris bioscience |
| **P2 receptor** | | |
| A 740003 | P2X7 receptor antagonist | Tocris bioscience |
| AR-C 118925 | P2Y2 receptor antagonist | Tocris bioscience |
| 5 BDBD | P2X4 receptor antagonist | Tocris bioscience |
| MRS 2179 | P2Y1 receptor antagonist | Tocris bioscience |

**Table 5.4. List of antibodies for western blot analysis**

| Antibodies | Manufacturer | Concentration |
|---|---|---|
| Goat Anti-PARP | R&D system, Wiesbaden | 1:2500 |
| Mouse Anti-β-Actin (C4) | Santa Cruz Biotechnology, Heidelberg | 1:2000 |
| Mouse Anti-pS6K (Thr389) | Cell signaling technology | 1:1000 |
| Rabbit Anti-A1 adenosine receptor | Alomone labs, Jerusalem | 1:200 |
| Rabbit Anti-A2A adenosine receptor | Alomone labs, Jerusalem | 1:200 |
| Rabbit Anti-A2B adenosine receptor | Alomone labs, Jerusalem | 1:200 |
| Rabbit Anti-A3 adenosine receptor | Alomone labs, Jerusalem | 1:200 |
| Rabbit Anti-Akt1/2/3 | Santa Cruz Biotechnology, Heidelberg | 1:200 |
| Rabbit Anti-p-Akt1/2/3 | Santa Cruz Biotechnology, Heidelberg | 1:2000 |
| Rabbit Anti-pAMPK (Thr172) | Santa Cruz Biotechnology, Heidelberg | 1:200 |
| Rabbit Anti-$P2X_4$ receptor | Santa Cruz Biotechnology, Heidelberg | 1:200 |
| Rabbit Anti-$P2X_7$ receptor | Santa Cruz Biotechnology, Heidelberg | 1:200 |
| Rabbit Anti-$P2Y_1$ receptor | Santa Cruz Biotechnology, Heidelberg | 1:200 |
| Rabbit Anti-$P2Y_2$ receptor | Santa Cruz Biotechnology, Heidelberg | 1:200 |
| Rabbit Anti-$P2Y_6$ receptor | Alomone labs, Jerusalem | 1:200 |
| Rabbit Anti-$P2Y_{11}$ receptor | Alomone labs, Jerusalem | 1:200 |
| Rabbit Anti-$P2Y_{13}$ receptor | Alomone labs, Jerusalem | 1:200 |

**Table 5.5. List of equipment**

| Equipment | Manufacturer |
|---|---|
| Biosphere® Pipette tips with aerosol filter 10 µl, 100 µl, 1000 µl | Sarstedt AG & Co., Nümbrecht |
| Cell culture flask T25, T75, T175 | Sarstedt AG & Co., Nümbrecht |
| Chromatography paper Whatman® | International Ltd, Maldstone, UK |
| Cryovial for cell storage (Cryo Pure) | Sarstedt AG & Co., Nümbrecht |
| Immobilon®-P Transfer Membrane, Pore size 0.45 µm | Millipore Corporation, Billerica, USA |
| Parafilm® | Pechiney Plastic Packaging, Chicago, USA |
| PCR-reactions micro tubes 0.2 ml | Applied Biosystems/Applera, Darmstadt |
| Pipette tips 10 µl, 200 µl, 1000 µl, 5 ml | Sarstedt AG & Co., Nümbrecht |
| Reaction tube 1.5 ml, 2 ml | Sarstedt AG & Co., Nümbrecht |
| Round-bottom cleared 96-well plate | Sarstedt AG & Co., Nümbrecht |
| Sterile cell culture micro plate 6-well and 24-well | Sarstedt AG & Co., Nümbrecht |
| Sterile cell culture microplate 96-well (Costar®) | Corning Inc., Corning, USA |
| Sterile cell culture microplate 96-well -PS Clear-flat bottom, white-border Cellstar® | Greiner Bio-One GmbH, Frickenhausen |
| Sterile filter from Cellulose acetate 0.2 µm | VWR, Darmstadt |
| Sterile single used pipette 10 ml | VWR, Darmstadt |
| Conical tube 15 and 50 ml | Sarstedt AG & Co., Nümbrecht |
| Cell scraper | Sarstedt AG & Co., Nümbrecht |

**Table 5.6. List of instrument**

| Instrument | Manufacturer |
|---|---|
| Analytical balace ABS 220-4 | Kern & Sohn GmbH, Balingen-Frommen |
| Analytical balance BP 221S | Sartorius AG, Göttingen |
| Autoclave Systec V-65 | Systec GmbH, Wettenberg |

| Instrument | Manufacturer |
|---|---|
| Centrifuge:<br>MIKRO 200R<br>ROTINA 420R | Hettich Zentrifugen, Tuttlingen |
| Drying cabinet | Heraeus Instrument GmbH, Hanau |
| Flow cytometer (CyFlow space) | Partec GmbH, Münster |
| Gel electrophoresis chamber Bio-Rad MINISUB® Cell GT | Bio-Rad Laboratories GmbH, München |
| Incubator Heraeus® Function-line Heraeus®/ | Thermo Electron Corporation, Dreieich |
| Laminar air flow<br>Werkbank MSC advantage | Thermo Scientific, Dreieich |
| Magnetic Stirrer IKA® RCT basic | IKA-Werke GmbH & Co.KG, Staufen |
| Microplate reader FLUOstar for absorption detection | BMG Labtechnologies, Offenburg |
| Microplate reader LUMIstar for luminescence detection | BMG Labtechnologies, Offenburg |
| Microplate reader NOVOstar for fluorescence detection | BMG Labtechnologies, Offenburg |
| Axio Vert.A1 Inverse microscope | Zeiss, Oberkochen |
| Nano cuvette IMPLEN | Implen GmbH, München |
| Nano Photometer P300 | Implen GmbH, München |
| Hemocytometer for cell counting | LO-Laboroptik GmbH, Bad Homburg |
| PCR working bench | Envirco Corporation, Sandorf, US |
| pH-Meter 713 | Metrohm GmbH & Co. KG, Filderstadt |
| Roller mixer SRT6 | Bibby Scientific LTD, Stone(Staffordshire), UK |
| Semi-dry-blotting apparatus | Carl Roth GmbH & Co. KG, Karlsruhe |
| Shaking machine Duomax 1030 | Heidolph Instruments, Schwalbach |
| Themo cycler for RT-PCR | Eppendorf, Jülich |
| Ultra sonicator<br>Sonorex Super RK514BH | Bandelin electronic GmbH & Co. KG, Berlin |
| UV-Vis-Spectrometer<br>Spectronic Genesys10 Bio | Thermo Electron GmbH, Dreieich |

| Instrument | Manufacturer |
|---|---|
| Voltage source :<br>Power Pack 3000<br>Standard Power Pack P25 | Bio-Rad Laboratories GmbH, München<br>Biometra GmbH, Göttingen |
| Vortex-Genie® | VWR, Darmstadt |
| Water bath<br>Julabo 19/ED | JULABO Labortechnik GmbH, Seelbach |
| Western Blot-Detections system INTAS ChemiLux ECL Imager HR16 Pro | INTAS Science Imaging Instruments GmbH, Göttingen |

**Table 5.7. List of software**

| Software | Manufacturer |
|---|---|
| CalcuSyn version 2.1 | Biosoft, Cambridge, U.K. |
| Compusyn version 1.0 | ComboSyn, Inc. , New Jersey, USA |
| FloMax 2.82 | Partec GmbH, Münster |
| GraphPad Prism® version 4.00 for windows | GraphPad Software, San Diego, USA |
| ImageJ 1.47v | Wayne Rasband, National Institutes of Health, USA |
| INTAS ChemoStar | INTAS Science Imaging Instruments GmbH, Göttingen |

## 5.2 Buffers and solutions

### 5.2.1 Cell culture

**Phosphate Buffer Saline (PBS) 10X**

| | | |
|---|---|---|
| NaCl | 81.8 | g |
| KCl | 2.2 | g |
| $Na_2HPO_4$ x $2H_2O$ | 14.2 | g |
| $KH_2PO_4$ | 2.04 | g |
| Distilled $H_2O$ q.s. to | 1000 | ml |

5 N of NaOH was used to adjust pH of the buffer to 7.4. Then, final volume of buffer was adjusted to 1000 ml using volumetric flask. The 50 ml aliquot part of PBS 10X in conical tube was stored at -20°C.

**PBS 1X**

| | | |
|---|---|---|
| NaCl | 140 | mM |
| KCl | 3 | mM |
| $Na_2HPO_4$ x $2H_2O$ | 8 | mM |
| $KH_2PO_4$ | 1.5 | mM |

PBS 10X was diluted 1:10 to obtain PBS 1X. The PBS 1X solution in a glass bottle was then sterilized at 121°C for 15 min using autoclave and stored at 2-8°C.

**Eosin solution 0.4% (w/v) for cell counting**

50 mg of eosin was dissolved in 15 ml of NaCl 0.9% (w/v) solution. The eosin solution was then stored at 2-8°C.

### 5.2.2 RT-PCR

**Tris-EDTA (TE) 10X**

| | | |
|---|---|---|
| Tris-Cl pH 7.5 | 10 | mM |
| EDTA | 1 | mM |

TE 10X was prepared from 1 M stock solution of Tris-Cl (pH 7.5) and 500 mM stock solution of EDTA (pH 8.0) by mixing 10 ml of 1 M Tris-Cl stock solution and 2 ml of 500 mM EDTA stock solution then final volume was adjusted to 1000 ml with distilled water.

**1 M Tris (free base) stock solution**

60.57 g of Tris (hydroxymethyl) aminomethane (MW 121.4 g/mole) was dissolved in 500 ml of distilled water. pH was adjusted to 7.5 using HCl (18.5 % v/v).

**500 mM EDTA stock solution**

18.6 g of EDTA (MW 372.2 g/mole) was dissolved in 100 ml of distilled water. pH was adjusted to 8.0 using 5 N NaOH. **Note;** EDTA was not able to soluble until pH reached 8.0 thus vigorous stirring with moderate heat and time are recommended.

**TAE 10X**

| | | |
|---|---|---|
| Tris base | 24.2 | g |
| Acetic acid | 5.7 | ml |
| EDTA disodium salt | 1.85 | g |
| Distillated $H_2O$ q.s. to | 500 | ml |

Tris base and EDTA disodium salt were weight and 400 ml of distilled water was added into beaker. Mixture was mixed well until became a clear solution then acetic acid was added. Final volume was adjusted to 500 ml with distilled water in a volumetric flask.

### 5.2.3 Western blot analysis

**Radioimmunoprecipitation assay (RIPA) lysis buffer**

| | | |
|---|---|---|
| Tris HCl (pH 8.0) | 50 | mM |
| EDTA | 2 | mM |
| Sodium Chloride | 150 | mM |
| SDS | 0.1 | % (w/v) |
| Triton X-100 | 1 | % (w/v) |
| Sodium deoxycholate | 0.5 | % (w/v) |
| Distilled $H_2O$ q.s. to | 100 | ml |

RIPA lysis buffer was prepared according to the recipe then 1 tablet of protease/phosphatase inhibitor was added. 1 ml aliquot part of RIPA lysis buffer plus protease/phosphatase inhibitor in 1.5 ml reaction tube was stored at -20°C. The lysis buffer was freshly thawed before using and avoided to repeat another freeze/thaw process.

**Loading buffer 2X**

| | | | |
|---|---|---|---|
| Tris | 0.197 | g | (125 mM) |
| Sodium dodecyl sulfate (SDS) | 0.6 | g | (6% w/v) |
| 2-Mercaptoethanol | 1 | ml | (10 % (v/v) |
| Glycerol | 3 | ml | (30 % v/v) |
| Bromophenol blue | 1 | pipet tip | |
| Distilled $H_2O$ q.s.to | 10 | ml | |

Tris and SDS were dissolved in 5 ml of distilled water then the mixture was mixed until became a clear solution. After that, glycerol and 2-Mecaptoethanol were added into the solution then pH was adjusted to 6.7 with 5 N NaOH. Final volume was adjusted to 10 ml with distilled water. Finally, Bromophenol blue was added into buffer solution and buffer was stored at 2-8°C.

**10% (w/v) ammonium persulfate (APS) solution**

1 g of ammonium persulfate was dissolved in 10 ml of distilled water and stored at -20°C.

**Collecting gel buffer 4X**

| | | | |
|---|---|---|---|
| Tris | 60.6 | g | (0.5 M) |
| Sodium dodecyl sulfate (SDS) | 4.0 | g | (0.4 % w/v) |
| Distilled $H_2O$ q.s. to | 1000 | ml | |

pH of buffer was adjusted to 6.8 with 18.5% (v/v) of HCl. Buffer was stored at room temperature.

**Separating gel buffer 4X**

| | | | |
|---|---|---|---|
| Tris | 181.8 | g | (1.5 M) |
| Sodium dodecyl sulfate (SDS) | 4.0 | g | (0.4 % w/v) |
| Distilled $H_2O$ q.s. to | 1000 | ml | |

pH of buffer was adjusted to 8.8 with 18.5% (v/v) HCl. Buffer was stored at room temperature.

**SDS running buffer 10X**

| | | | |
|---|---|---|---|
| Tris | 30 | g | (25 mM) |
| Glycine | 144 | g | (192 mM) |
| Sodium dodecyl sulfate (SDS) | 10 | g | 1 % (w/v) |
| Distilled $H_2O$ q.s. to | 1000 | ml | |

SDS running buffer 10X was stored at 2-8°C.

**SDS running buffer 1X**

SDS running buffer 10X was diluted 1:10 in distilled water to obtain SDS running buffer 1X and stored at room temperature.

**TBS 10X**

| | | | |
|---|---|---|---|
| Tris | 24.228 | g | (200 mM) |
| Sodium Chloride (NaCl) | 90.0 | g | (9 % w/v) |
| Distilled $H_2O$ q.s. to | 1000 | ml | |

pH was adjusted to 7.4 with 18.5% (v/v) HCl. Buffer was stored at 2-8°C.

**TBST 10X**

Buffer was prepared from TBS 10X plus 1% (w/v) of Tween20 and stored at 2-8°C.

**TBS 1X and TBST 1X buffers**

TBS 10X and TBST 10X were diluted 1:10 in distilled water to obtain TBS 1X and TBST 1X, respectively. Buffers were stored at 2-8°C.

**Semi-dry buffer**

Buffer contained 10% (v/v) of methanol in SDS running buffer 1X and was stored at room temperature.

**Blocking solution**

Solution contained 3% non-fat milk in TBST 1X. Solution was freshly prepared and should be used within 24 h.

## 5.2.4 Calcium assay

**Krebs-HEPES buffer 5X (calcium and magnesium free)**

| | | | |
|---|---|---|---|
| NaCl | 17.330 | g | (593 mM) |
| KCl | 0.876 | g | (23.5 mM) |
| $KH_2PO_4$ | 0.408 | g | (6 mM) |
| $NaHCO_3$ | 0.882 | g | (21 mM) |
| Glucose | 5.269 | g | (58.5 mM) |
| HEPES (free acid) | 5.958 | g | (50 mM) |
| Distilled $H_2O$ q.s.to | 500 | ml | |

pH was adjusted to 7.4 with 5 N NaOH. 100 ml aliquot part of the buffer was stored at -20°C.

**Krebs-HEPES buffer 1X (containing $Ca^{2+}$ and $Mg^{2+}$)**

100 ml of Krebs-HEPES buffer 5X was transferred into 500 ml volumetric flask then 650 µl of 1 M $CaCl_2$ and 600 µl of 1 M $MgSO_4$ were added into buffer solution. Final volume was adjusted to 500 ml with distilled water. The 100 ml aliquot part of the buffer was then stored at -20°C.

**20 % (w/w) Pluronic F-127**

0.2 g of Pluronic F-127 was weight in 2 ml reagent tube. Then, dimethylsulfoxide (DMSO) was added until the weight reached 1 g. (approximately 720 µl of DMSO was used). Solution was stored at room temperature.

**Oregon Green stock solution**

39.7 µl DMSO was added into 50 µg Oregon Green 488 BAPTA-1, AM (original package). Then, solution was mixed well with vortex at 1500 rpm for 1 to 2 min. 3 µl aliquot part of Oregon green stock solution in 2 ml reagent tube was stored at -20°C.

## 5.2.5 cAMP reporter gene assay

**Luciferase assay reagent (LAR) pH 7.8**

| | | |
|---|---|---|
| Tricine | 5.376 g | (30 mM) |
| $MgSO_4$ x $7H_2O$ | 1.233 g | (10 mM) |
| EDTA | 0.075 g | (0.5 mM) |
| DTT | 0.771 g | (10 mM) |
| Distillated $H_2O$ q.s. to | 500 ml | |

| | |
|---|---|
| ATP | 0.5 mM |
| Coenzyme A | 0.5 mM |
| D-luciferin | 0.5 mM |

Tricine and EDTA were weight into beaker then 400 ml of distilled water was added. The mixture was mixed for 15 min or until became a clear solution. Then, $MgSO_4$ and DTT were added. pH of a clear solution was adjusted to 7.8 with 5 N NaOH and final volume was adjusted to 500 ml with distilled water. LAR was stored at -20°C. 10 mM stock solution of ATP, Coenzyme A, D-luciferin were prepared in distilled water, stored at -20°C and added into LAR freshly before using.

**Luciferase Lysis Reagent (LLR) pH 7.8**

| | | | |
|---|---|---|---|
| Tricine | 0.717 | g | (8 mM) |
| DTT | 0.077 | g | (1 mM) |
| EDTA | 0.292 | g | (2 mM) |
| Triton X-100 | 25 | g | (5% w/v) |
| Distillated $H_2O$ q.s. to | 500 | ml | |

Tricine and EDTA were weight in the beaker then 400 ml of distilled water was added. Mixture was mixed for 15 min or until became a clear solution. After that, Triton X-100 and

DTT were added into the solution. pH was adjusted to 7.8 with 5 N NaOH then final volume was adjusted to 500 ml with distilled water. LLR was stored at -20°C.

### 5.2.6 MTT assay

**MTT solution**

250 mg of 3-(4,5-Dimethylthiazol-2-yl)-2,5-diphenyltetrazolium bromide (MTT) was dissolved in 50 ml of PBS 1X. The mixture was mixed well until became a yellow clear solution and stored at 2-8°C.

### 5.2.7 Cell cycle analysis

**70% ethanol solution for cell fixation**

Absolute ethanol was diluted in distilled water to prepare 70% (v/v) then the solution was stored at 2-8°C.

**Filtered distilled water**

Distilled water was filtered through 0.2 µm-cellulose filters and stored at -20°C.

**Propidium iodide (PI) stock solution**

Propidium iodide was dissolved in filtered distilled water to obtain the concentration of 500 µg/ml. A stock solution was stored at 2-8°C and protected from light.

**Sheath fluid**

Sheath fluid is a commercial sterile 0.9% NaCl plus 0.01% of sodium azide ($NaN_3$). Sheath fluid should be prepared freshly and put in the ultrasonic bath at least 30 min before using.

**DNase-free RNase stock solution (10 mg/ml)**

DNase-free RNase was dissolved in filtered distilled water and stored at -20°C.

**PI staining solution (per 1 well)**

| | | |
|---|---|---|
| Triton X-100 | 0.5 | µl |
| DNase-free RNase (stock solution) | 10 | µl |
| Propidium iodide (stock solution) | 20 | µl |
| Sheath fluid q.s. to | 500 | µl |

Sheath fluid was pipetted into 15 ml conical tube then Triton X-100 was added. The mixture was mixed well until became a clear solution then PI stock solution and DNase-free RNase stock solution were added. PI staining solution should be prepared freshly before staining the cells, protected from light and always kept on ice.

### 5.2.8 Apoptosis assay

**Propidium iodide (PI) stock solution**

Propidium iodide was dissolved in filtered distilled water to obtain the concentration of 500 µg/ml. The stock solution was stored at 2-8°C and protected from light.

**Sheath fluid**

Sheath fluid is a commercial sterile 0.9% NaCl plus 0.01% of sodium azide ($NaN_3$). Sheath fluid should be prepared freshly and put in the ultrasonic bath at least 30 min before using.

**Filtered distilled water**

Distilled water was filtered through 0.25 µm-filters and stored at -20°C.

**Hypotonic PI staining buffer**

| | |
|---|---|
| Sodium citrate | 0.1% (w/v) |
| Triton X-100 | 0.1% (v/v) |
| PI stock solution | 100 µg/ml |

Sodium citrate was dissolved in filtered distilled water and the mixture was mixed until became a clear solution before Triton X-100 was added. PI stock solution was added at the last step and final volume was then adjusted with filtered distilled water. Buffers was protected from light and stored at 2-8°C.

## 5.3 Methods

### 5.3.1 Cell culture

**General cell culture**

Cell culture was performed under laminar airflow with aseptic technique. All the materials and reagents for cell culture were sterilized at 121°C for 20 min by autoclave in order to avoid bacterial contamination.

A2780, A2780CisR and HEY cell lines were cultivated in Roswell Park Memorial Institute 1640 (RPMI1640) while HEK293 cell line was cultivated in Dulbecco Modified Eagle Medium (DMEM). The RPMI1640 and DMEM were supplemented with 10% fetal bovine serum (FBS) and 1.2% penicillin/streptomycin (10,000 IU/ml penicillin and 10,000 mg/ml streptomycin). Cell lines were grown in T75 cell culture flask at 37 °C in a humidified atmosphere containing 5% $CO_2$ until cells reached 80% to 90% confluence. Then, cells were washed one time with 6 ml of PBS 1X and detached with 3 ml of 0.05% trypsin/0.02% EDTA in PBS. Cells were then incubated in the incubator for 2 min (A2780, A2780CisR and HEK293 cells) or 4 min (HEY cells) in order to allow cells to detach from the flask. After 2 to 4 min incubation time, 7 ml of complete medium was added into the flask to stop the reaction of trypsin then all the cells were harvested from the flask and transferred to 50 ml conical tube. Cell suspension was then centrifuged at 266 g, 4°C for 4 min. Finally, supernatant was gently removed and cell pellet was suspended with 5 ml complete medium. This cell suspension can be used for further experiments.

**Cell counting**

In order to count the exactly number of cells in cell suspension, a hemocytometer was used for cell counting. 10 µl of harvested cell suspension was diluted in 90 µl of 0.4% eosin solution. 10 to 15 µl of cell suspension in eosin solution were filled in between hemocytometer and coverslip until all four quadrants of hematocytometer (Figure 5.1) were totally filled with cell suspension without appearance of bubbles. Then, cells were counted under microscope. The total cell numbers obtained from four quadrats of hemocytometer was used to calculate the exactly amount of cells per microliter using the equation below. The dilution factor was 10.

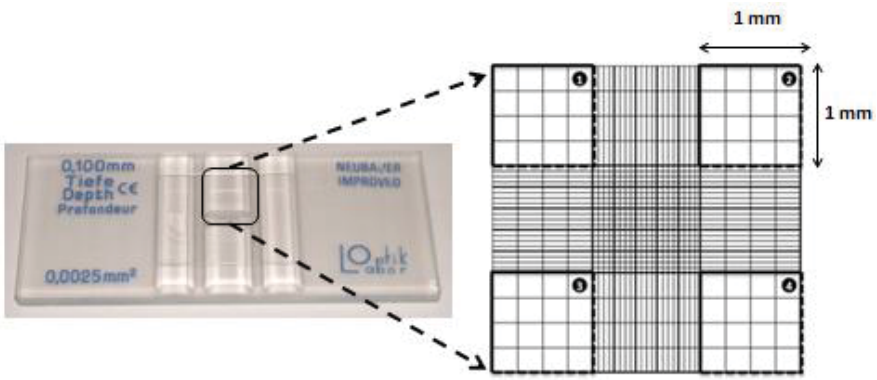


**Figure 5.1. Hemocytometer**

$$\text{Cell number per } \mu l = (n \div 0.4) \times DF$$

n = Total cell number from four quadrats

DF = Dilution Factor

The cell number per microliter was then used to calculate the exactly amount of cells per well for further experiments. Some of cell suspension was put in a new T75 flask for a backup. Cell lines were cultured at least once a week and the medium was changed every 48 to 72 h.

## 5.3.2 Reverse Transcriptase – Polymerase Chain Reaction (RT-PCR)

### RNA extraction

Cell lines were cultivated in T25 flask to reach 80% to 90% confluence then RNA was extracted using My-Budget RNA Mini Kit (Bio-budget, Germany) followed the protocol for eukaryotic cells**.** Briefly, cells pellet was harvested as described before in general protocol for cell culture. Then, cell pellet was lysed with lysis buffer (from the RNA Mini Kit) after that genomic DNA was selectively removed by adhering to a first centrifugation filter. RNA was bound to a second centrifugation filter; contaminants were removed by washing steps. The total RNA was eluted through RNase-free water. The purification and concentration of RNA were determined by Nano Photometer. The 1 µg aliquot part of purified RNA in 0.2 ml PCR-reaction tube was stored at -20°C.

**Reverse Transcription (RT) from RNA to cDNA**

1µg of purified RNA was used to prepare cDNA using High Capacity cDNA Reverse Transcription Kit and Oligo$(dT)_{23}$ anchored Primer (See Table 5.8) with the following program setting in the thermo cycler: 10 min at 25°C followed by 120 min at 37°C. The 20 µl of cDNA was diluted in 100 µl of TE buffer 1X, pH 7.5 and stored at -20°C for the further PCR reaction.

**Table 5.8. Components for reverse transcription**

| Component | Weight/volume |
|---|---|
| Purified RNA | 1 µg |
| Reaction buffer 1X | 1 µl |
| dNTP 25X | 0.4 µl |
| Oligo(dT)23-Primer [0.5 µg/µl] | 0.5 µl |
| Reverse Transcriptase [1:5 in Ampuwa water] | 2.5 µl |
| Ampuwa water q.s. to | 20 µl |

**Primer design**

Specific primers of purinergic receptors were designed using primer design tool from the website www.ncbi.nlm.nih.gov/tools/primer-blast/ [Ye et al., 2012]. Then, the primer sequences were produced by Eurofins Genomics (Ebersberg, Germany). The 125 µM primer stock solutions were prepared in TE buffer 1X and stored at -20°C. All the primers sequences are shown in Table 5.9.

**Table 5.9. Sequences of forward and reverse primers for PCR**

| Receptor | Sequences | | Product size (bp) |
|---|---|---|---|
| | Forward Primer (5'-3') | Reverse Primer (5'-3') | |
| **Housekeeping Gene** | | | |
| ACTB | TCCTTCCTGGGCATGGAGT | GCACTGTGTTGGCGTACAG | 103 |
| **P1 receptor (adenosine receptor)** | | | |
| A1 | CCCTCTCCGGTACAAGATGG | GCAGCACCCACACAAAGAAG | 239 |
| A2A | ATCCCGCTCCGGTACAATGG | GAGTGGTTCTTGCCCTCCTT | 146 |
| A2B | ATCTGTGTCCCGCTCAGGTAT | ATAAGCAGTGGGGGCAGAAC | 272 |
| A3 | CTGGGAAAGACCTATCAGGCA | GCTTCAAAGTGTTGCCTACCC | 195 |
| **P2 receptor** | | | |
| P2X1 | AATGACCACCATCGGCTCTG | CCCCATGTCCTCAGCGTATT | 133 |
| P2X2 | GACCCTTGCCCGTGTATTGG | CCACACTCTGCCCCTTGTTG | 111 |
| P2X3 | TCCGTTTCCCCCTCTTCAAC | CAAGATGGGGCAGAAAGGGT | 113 |
| P2X4 | GTCATCGGGTGGGTGTTTGT | AGAAGTGTTGGTCACAGCCA | 105 |
| P2X5 | TGATGGACGTCAAGGACAGA | ATTCCTATCACGCCACCCTC | 148 |
| P2X6 | CGTGGTCTATGTGGTAGGGT | TGAGTGACGGAAACCCCTTTG | 111 |
| P2X7 | ACACCGCAGACTACACCTTC | GGGATATCGGGACACACAACC | 104 |
| P2Y1 | TTACGACACCACCTCAGACG | TGAAAGTATCTCCCGCCAAG | 115 |
| P2Y2 | CGACTGCTAAACCAGCCTA | ATGTTGATGGCGTTGAGGGT | 188 |
| P2Y4 | ACAACCAGCAACAAAGGGACCACC | AGCAAACAAGAGTGACCAGGCAGG | 136 |
| P2Y6 | ACGGCAGCATCCTCTTCCTCACC | CAGCAGGAAGCCGATGACAGTGA | 256 |
| P2Y11 | GCCAACGTCTCGGGTGCCAAG | CGGCCACCAGGAACTCAACCAC | 121 |
| P2Y12 | ATGCCAAACTGGGAACAGGACCAC | AATGGCCTGGTGGTCTTCTGGTAG | 139 |
| P2Y13 | ACTCACACCTGGCACCCTGG | AGCCCTAACAGCACGATGCCC | 100 |
| P2Y14 | AGTAGCATTGTGTTCTTTGGGC | AACAGCAAGGAGGAGCATGAGC | 146 |

**Polymerase Chain Reaction (PCR)**

cDNA from reverse transcription reaction and specific forward and reverse primers were pipetted into 20 µl PCR-reaction tubes together with 2X QuantiTect-SYBR®-Green master mix and Ampuwa water as shown in Table 5.10.

**Table 5.10. Components for PCR**

| Reagent | Volume |
|---|---|
| cDNA in TE 1X buffer | 1.5 µl |
| 125 µM Forward primer stock solution | 0.8 µl |
| 125 µM Reverse primer stock solution | 0.8 µl |
| 2X QuantiTect-SYBR®-Green master mix | 10 µl |
| Ampuwa water q.s. to | 20 µl |

PCR program consisted of an initial denaturation step at 95°C 120 s for 1 cycle then continued with 94°C for 20 s followed by 57°C for 30 s and 72°C 60 s for 40 cycles.
10 µl of PCR products was diluted in 15 µl of ampuwa water and 5 µl of loading dye. PCR product solution of purinergic receptors and ACTB as housekeepting gene were then separated using 2% agarose gel in TAE 1X buffer as running buffer with the constant 125 V for 45 min. The separated DNA bands were detected under Intas Gel iX Imager UV system. GeneRuler 50 bp was used as DNA ladder.

### 5.3.3 Western blot analysis

**Protein preparation**

Cells were cultivated in T25 flask overnight before treated with test compounds. After appropriate incubation time, cells were washed twice with PBS1X then 50 µl of RIPA lysis buffer were added onto the cells. Cells were detached from the flask using scraper and transferred into 1.5 ml reagent tube. Cell lysate was incubated with RIPA lysis buffer on a roller mixer for 30 min at 4 to 8°C. After that, cell lysate was centrifuged at 14,000 g for 15 min at 4°C. Supernatant containing protein sample was pipetted into new 1.5 ml reagent tube. 10 µl of protein sample was used for protein concentration assay (BCA assay) and the rest was mixed 1:1 with loading buffer 2X. The protein sample in loading buffer was heated at 95 °C for 10 min and stored at -80°C.

**Bicinchoninic acid (BCA) assay for protein concentration**

The principle of BCA assay is protein bonds in the protein samples can reduce $Cu^{2+}$ to $Cu^{1+}$ which then forms a complex with bicinchoninic acid. The $Cu^{1+}$ - bicinchoninic acid complex is purple-colored and can be detected at an absorption wavelength of 566 nm. The amount of reduction is proportional to protein in the sample.

Bovine Serum Albumin (BSA) stock solution (2 mg/ml) was diluted in distilled water to prepare protein standard in a concentration of 1500, 1000, 750, 500, 250, 125 and 25 µg/ml. While, protein samples were diluted 1:10 in distilled water. 25 µl of either BSA standard dilutions or protein samples were added in wells of a 96-well plate in replicate. The BCA working reagent was prepared in a ratio 50:1 of Reagent A (Thermo Scientific, Germany) to Reagent B (4% w/v $CuSO_4$). 200 µl of BCA working reagent were then added into each well of protein standards and protein samples and incubated at 37°C. After 30 min, absorption was measured at 544 nm using a FLUOstar microplate reader. BSA calibration curve was used to calculate protein concentration of each protein sample.

**Gel preparation**

Gels were prepared at least one day before electrophoresis. All the components were pipetted according to Table 5.11 into 50 ml conical tube. APS solution and TEMED were added at the last. Separating gel solution was firstly poured in between glass plates separated by spacers of 1 mm thickness. Bubbles on the surface of the separating gel solution were removed by adding isopropanol then separating gel solution was allowed to polymerize for 10 to 15 min. After that, isopropanol was discarded then collecting gel solution was poured in the upper part of the separating gel. Bubbles should be avoided. Then, comb was inserted into the collecting gel solution in between two glass plates in order to make pockets for protein samples. The collecting gel solution was allowed to polymerize for 10-15 min. Gels were stored in aluminum foil with wet paper towel at 2-8°C overnight. The separating gel was prepared based on molecular mass of proteins of interest. In this study, the 8 to 12% of separating gel and 5% of collecting gels were used. The components for preparing one gel are shown in Table 5.11.

**Table 5.11. Gel components for one gel preparation**

| Component | Separating gel | | | Collecting gel |
|---|---|---|---|---|
| | 8% | 10% | 12% | 5% |
| Rotiphorese®Gel 30 | 1.6 ml | 2.0 ml | 2.4 ml | 0.5 ml |
| Distilled $H_2O$ | 2.9 ml | 2.5 ml | 2.1 ml | 1.75 ml |
| Separating gel buffer 4X | 1.5 ml | 1.5 ml | 1.5 ml | - |
| Collective gel buffer 4X | - | - | - | 0.75 ml |
| 10 % APS solution | 60 µl | 60 µl | 60 µl | 30 µl |
| TEMED | 6 µl | 6 µl | 6 µl | 3 µl |

**Sodium dodecyl sulfate polyacrylamide gel electrophoresis (SDS-PAGE)**

The protein samples in loading buffer were loaded onto the gel placed in electrophoresis chamber filled with running buffer 1X. Electrophoresis was performed at 80 V for 15 min or until all samples were entered to the separating gel. Then, voltage was increased to 160 V and electrophoresis was performed until the bromophenol blue band of the loading buffer left the separating gel. Separated proteins were then transferred onto a PVDF membrane using semi-dry blotting for 1 hour at room temperature (constant electric current at 40 mA per membrane). The PVDF membrane was activated by immersing in 100% methanol for a few seconds, until the entire membrane is translucent then soaked in semi-dry buffer for at least 15 min prior to protein blotting. After blotting, PVDF membrane was blocked with 3% non-fat milk in TBST 1X for 1 h at room temperature. Then, the membrane was incubated with specific primary antibodies overnight at 4 to 8°C on a shaking machine. The specific primary antibodies were prepared in 3% non-fat milk in TBST 1X plus 0.01% $NaN_3$ at a dilution of 1:2500 up to 1: 200.

On the next day, the membrane was washed twice with TBST 1X for 30 min and once with TBS 1X for another 30 min before incubation with a HRP-coupled secondary antibody (concentration 1:3000 in blocking solution) for 1 h at room temperature. Then, membrane was washed again twice with TBST 1X and once with TBS 1X for 30 min in each washing step. Finally, the membrane was then incubated in 1 ml of Luminol reagent (Reagent A to Reagent B, 1:1) for 2 min. The luminescence of labeled protein bands was detected by Intas Chemochem system using INTAS ChemiLux ECL Imager HR16 Pro.

### 5.3.4 Calcium assay

This assay was used to study the activity of G-protein coupled receptors (GPCR). Activation of Gq-coupled receptors, a subtype of GPCR results in the release of intracellular calcium from intracellular calcium stores. By using Oregon Green BAPTA-1 AM which can penetrate cell membrane into intracellular space and binds with $Ca^{2+}$, resulting in increase of fluorescence which correlates with intracellular calcium released upon receptors activation. Schematic diagram for GPCR-induced calcium releases is shown in Figure 5.2.

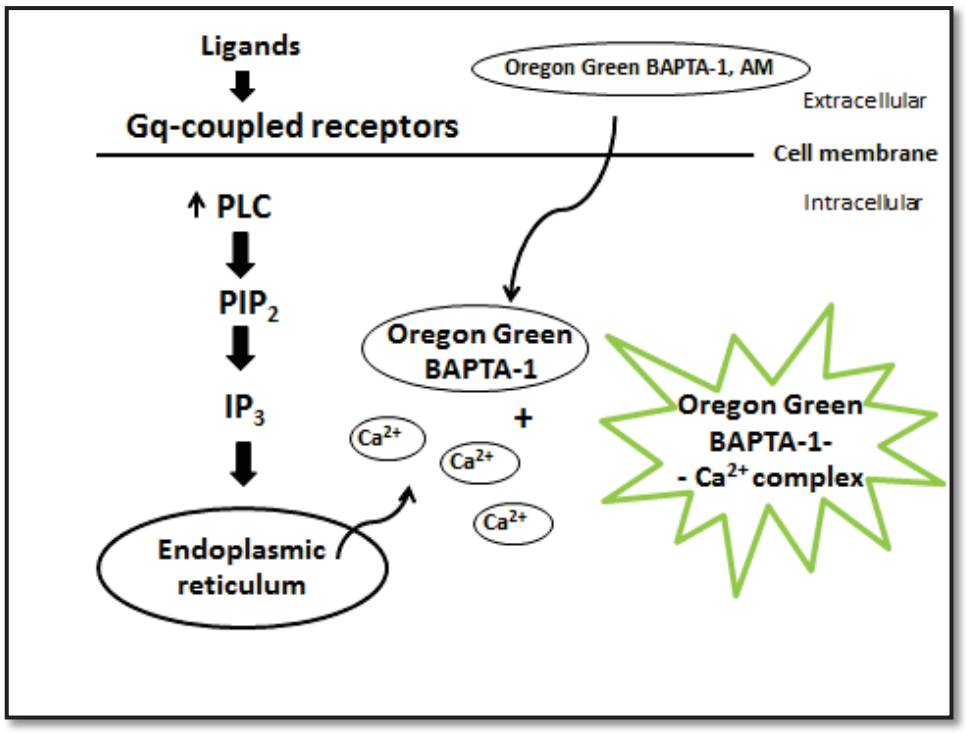


**Figure 5.2. Monitoring of GPCR-induced calcium releases**

The specific ligands activate Gq-coupled receptors at the cell membrane leading to activation of phospholipase C (PLC) converting phosphatidylinositol-4,5-bisphosphate ($PIP_2$) to the second messenger inositol-1,4,5-trisphosphate ($IP_3$). $IP_3$ then stimulates calcium channels at the membrane of endoplasmic reticulum resulting in calcium ion releases into the cytoplasm. Oregon Green BAPTA-1 AM penetrates into the cells then is cleaved by cytosolic esterase to Oregon Green BAPTA-1 which then is able to form a chelate with calcium ion, resulting in the increase of fluorescence correlates with intracellular free calcium released upon GPCR activation.

Cell lines were seeded at a density of 30,000 cells per well into 96-well plates and incubated at least overnight before treatment. At the measurement day, cells should reach 80% to 90% confluence in each well. Cells were then washed twice with Krebs-HEPES buffer 1X to avoid cleavage of Oregon Green BAPTA-1 AM by esterase in complete medium. Then, Oregon Green working solution was prepared by mixing 3 µl of Oregon Green BAPTA-1 AM stock solution and 3 µl of 20% Pluronic F-127 in 2 ml of Krebs-HEPES buffer 1X. 20 µl of Oregon Green working solution was added onto the cells in each well and incubated for 1 h in an incubator. During the incubation time, reagent plate containing 80 µl per well of either increased concentrations of agonist (for "agonist mode") or a constant concentration of agonist (3 to 5-fold of EC50 of agonist for "antagonist mode") was prepared in a clear round-bottom 96-well plate. After cells were labeled with Oregon green BAPTA-1 for 1 h, the Oregon green working solution was gently removed from the wells to reduce a high background then 180 µl of Krebs-HEPES buffer 1X was replaced in each well ("agonist mode"). In case of "antagonist mode", 20 µl of increased concentrations of antagonist and 160 µl of Krebs-HEPES buffer 1X were incubated in the cells for 30 min (in an incubator) after removal of Oregon green working solution. A 96-well plate containing cells labeled with Oregon green BAPTA-1 and a round-bottom 96-well plate containing agonist solutions were placed in NOVOstar fluorescence microplate reader on a measurement plate position and reagent plate position, respectively. The 20 µl of agonist solution (in reagent plate) was then injected into each well of 96-well plate containing cells labeled with Oregon green BAPTA-1 (measurement plate) by NOVOstar fluorescence microplate reader injector. Fluorescence was monitored according to the instrument setting shown in Table 5.12. The fluorescence-time curves of untreated control, agonist alone or in combination with antagonist are shown in Figure 5.3. Baseline fluorescence intensity (average fluorescence intensity between 1 to 4 s) was subtracted from maximum fluorescence intensity (maximum fluorescence intensity between 5 to 53 s) then was used to calculate respective $EC_{50}$ or $IC_{50}$ values of test compounds using GraphPad Prism version 4.0 for windows.

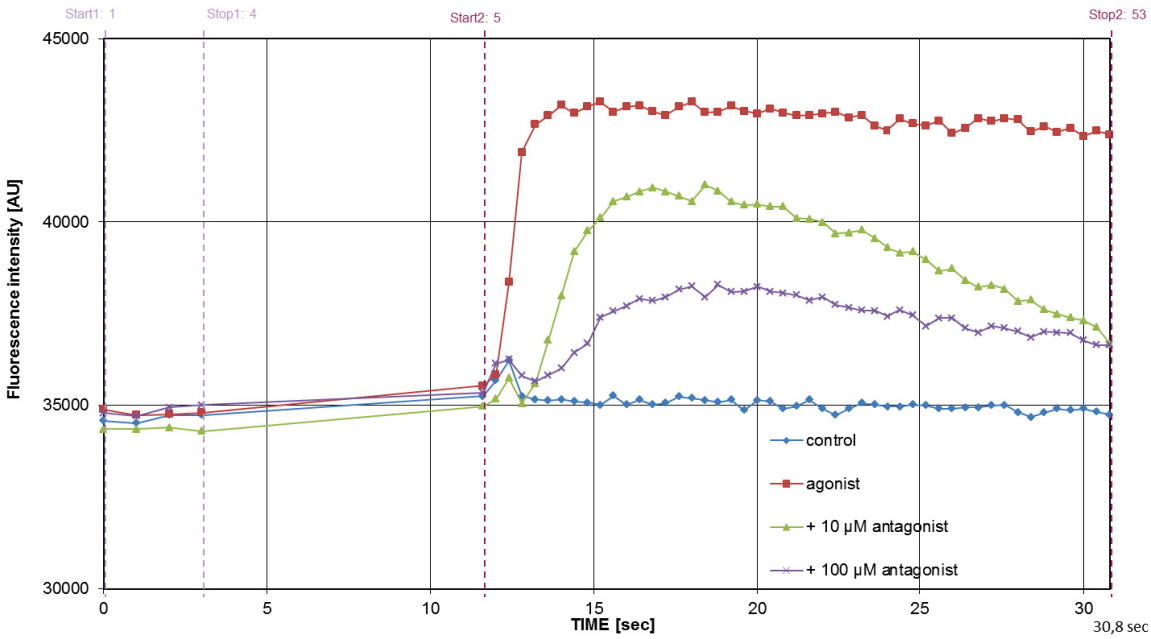


**Figure 5.3. Fluorescence-time curves obtained from calcium assay after treatment with agonist in a presence or absence of antagonist compared with untreated control.**

Fluorescence intensity is increased upon time after injection of agonist onto the cells whereas fluorescence intensity is decreased in a presence of antagonist.

**Table 5.12. NOVOstar microplate reader instrument setting for calcium assay**

| Fluorescence | Well mode |
|---|---|
| Measurement plate | COSTAR 96 |
| Reagent plate | COSTAR 96 |
| Gain | 1895 |
| Excitation filter | 485-P |
| Emission filter | 520 |
| Required value | 55% |
| Positioning delay | 0.5 s |
| Air volume to aspirate | 10 µl |
| Air volume to dispense | 10 µl |
| Target temperature | 37 °C |
| Injection speed | 33 µl/s |
| Dispense depth | 6.5 mm |
| Use air gap | Yes |

| Wash cycle | | 1 |
|---|---|---|
| Rinse cycle | | 3 |
| Pump | | 1 |
| Injection start time | | 11.6 s |
| | Kinetic window 1 | Kinetic window 2 |
| Staring time | 0 s | 11.6 |
| Number of interval | 4 | 49 |
| Number of flash | 10 | 10 |
| Interval time | 1 s | 0.4 s |
| End time | 4 s | 31.2 s |

### 5.3.5 cAMP reporter gene assay

The assay was performed in order to evaluate functional activity of adenosine receptors by using reporter gene system. Upon receptors activation, a stimulation or inhibition of adenylyl cyclase results in increase or decrease of cyclic AMP (cAMP) levels, respectively. According to G-protein coupling of each subtype of adenosine receptors, $G_s$-coupled receptors activation results in increase of cAMP levels. Whereas activation of $G_i$-coupled receptors, resulting in decrease of cAMP levels. cAMP activates protein kinase A (PKA) which in turn phosphorylates cAMP response element binding protein (CREB). Phosphorylated CREB (pCREB) together with other transcription factors can bind to promoter regions containing 5'-TGACGTCA-3' sequence of cAMP response element (CRE), and in consequence induce downstream gene transcription. [Shan et al., 2010]. In this study, human ovarian cancers cells A2780, A2780CisR and HEY were transiently transfected with CRE-luciferase reporter gene (CRE-luc gene). Therefore, cell signaling after an activation of adenosine receptors leads to transcription of CRE-luciferase reporter gene, resulting in conversion of D-luciferin to oxy-luciferin which exhibits luminescence in correlates to cAMP levels. Theory of cAMP reporter gene assay upon $G_s$-coupled receptors activation is shown in Figure 5.4.

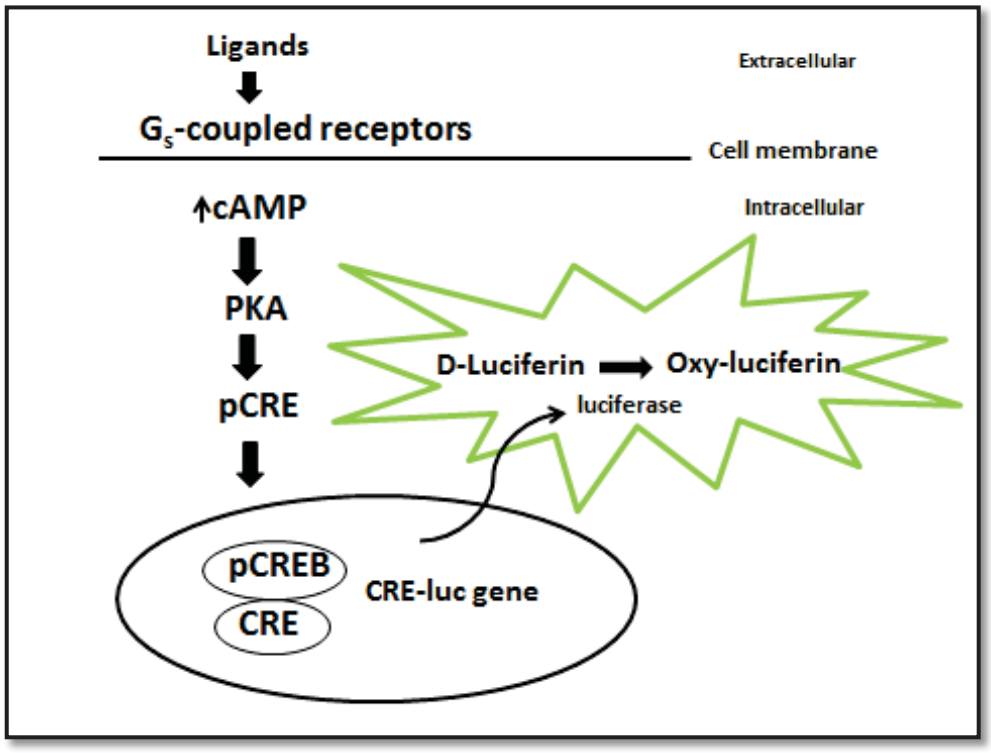


**Figure 5.4. Theory of cAMP reporter gene assay.**

Once ligands activate Gs-coupled receptors, cAMP levels are increased. cAMP then activates protein kinase A (PKA) leading to phosphorylation of cAMP response element binding protein (CREB). Then, pCREB binds to CRE initiating the transcription of luciferase. Luciferase then converts D-luciferin to oxyluciferin, generating a luminescence signal.

### Transient transfection

According to a protocol for transient transfection of PolyFect transfection reagent (Qiagen, Germany) Briefly,

1. The day before transfection, cells were seeded in a 6-well plate (in a density of 400,000 cells per well) with 3 ml of complete medium per well. Cells should have 40 to 80% confluence on the day of transfection. Then, cells were incubated at 37 °C and 5% $CO_2$ in an incubator overnight.
2. Next day, 1.5 µg of CRE-luc plasmid were diluted in medium without FBS, total volume should be 100 µl. Then, 12 µl of PolyFect transfection reagent was added and solution was mixed well by pipetting up and down then incubated for 10 min at room temperature (20-25°C) to allow complex formation. Note: this amount of plasmid and transfection reagent is for one well.

3. While complex formation took place, old medium was gently aspirated from the cell plate and cells were washed once with 2 ml PBS 1X. Then, 1.5 ml of new complete medium was added per well.
4. After 10 min incubation time, 600 µl of complete medium was added into the reaction tube containing transfection complexes. Transfection complex solution was mixed well by pipetting up and down twice and immediately transferred to the cells in 6-well plate. Cell plate was gently swirled to ensure uniform distribution of the complexes.
5. Cells with transfection complexes solution were incubated in the incubator to allow gene expression for 24 h.

**Treatment and luminescence measurement**

1. After 24 h transfection, cells were harvested and seeded into a white, clear-bottom 96-well plate and allowed to grow for 48 h in the incubator. Cells should grow until reach 80 to 90% confluence after 48 h incubation. For A2780 cell line, transfected cells were seeded at a density of 60,000 cells per well.
2. To test for agonist activity, old medium was gently aspirated then 90 µl of freshly medium without FBS and 10 µl of increased concentrations of adenosine were added. Adenosine dilutions were then incubated for 3 h. In case of antagonist mode, 80 µl of medium without FBS and 10 µl of increased concentrations of selective antagonists were added. The selective antagonists were incubated 30 min before 10 µl of adenosine (200 µM) was added. Adenosine was then incubated for another 3 h in the incubator.
3. LUMIstar Galaxy plate reader was switched on and temperature was set at 25°C. LUMIstar instrument setting is shown in Table 5.13.
4. After 3 h incubation time, medium containing adenosine and/or selective antagonists was removed then 100 µl of LLR was added per well. LLR was incubated on the cells for 20 min at 4 to 8°C in order to lyse the cells.
5. After cells were completely lysed (by observing under a microscope). The cells plate was placed in LUMIstar Galaxy microplate reader for 10 min.
6. ATP, Coenzyme A and D-luciferin were added into LAR. Then, an injector of LUMIstar Galaxy microplate reader was primed by flushing LAR solution twice to allow the LAR solution filled in an injection tube. Luminescence was measured after injection of LAR solution into the wells. Average luminescence intensity from 4 to 13 s which displayed stable luminescence intensity were used to calculate respective

$EC_{50}$ or $IC_{50}$ values of test compounds using GraphPad Prism version 4.0 for windows. The luminescence-time curves obtained from cAMP reporter gene assay are shown in Figure 5.5.

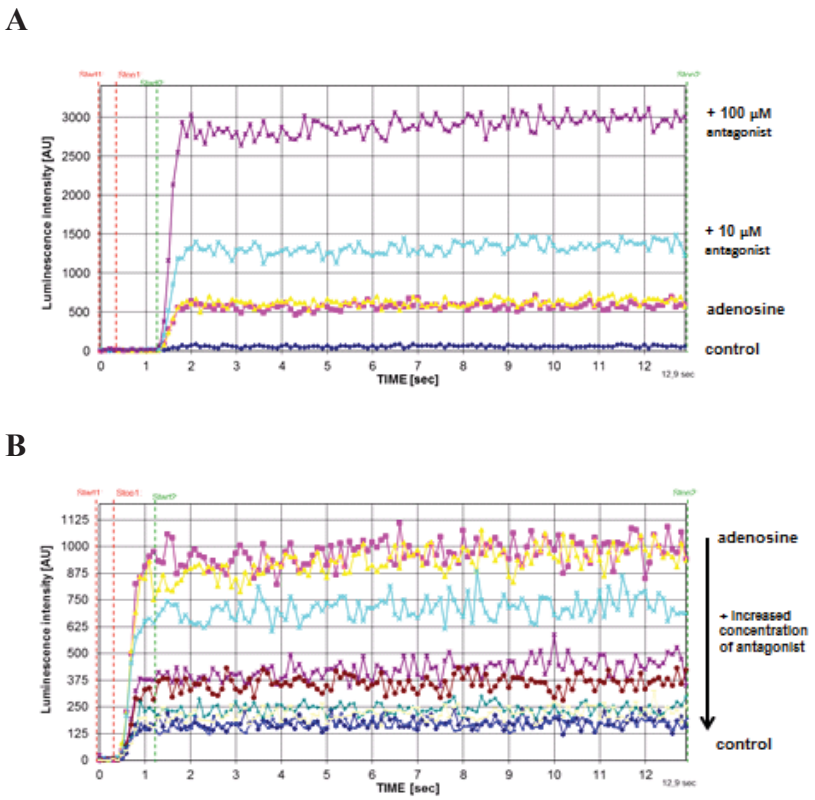


**Figure 5.5. Luminescence-time curves obtained from cAMP reporter gene assay after treatment with non-selective agonist (adenosine) alone or in combination with antagonists compared to untreated control.**

(A) Adenosine treatment increases luminescence intensity according to an activation of both $G_s$- and $G_i$-coupled receptors and a presence of selective $G_i$-coupled receptors antagonist further increases luminescence intensity achieved from adenosine alone. (B) A presence of selective $G_s$-coupled receptors antagonist decreases luminescence intensity achieved from adenosine alone in a concentration-dependent manner.

**Table 5.13. LUMIstar luminescence plate reader instrument setting for cAMP assay**

| | |
|---|---|
| Measuring mode: | Luminescence, well-mode |
| Measuring plate: | Greiner µClear®-plate 655098 |
| Spectrum range: | 290-700 nm |
| Positioning delay: | 0.5 sec |
| Temperature: | 25 °C |

| | |
|---|---|
| Reading direction: | Horizontal |
| Number of interval: | 130 |
| Measuring interval time: | 0.1 sec |
| Start measuring: | 0 sec |
| Time to start injection: | 0.3 sec |
| Total time per well: | 13 sec |

### 5.3.6 MTT assay

3-(4,5-dimethylthiazol-2-yl)-2,5-diphenyltetrazolium bromide (MTT) is a substance used for study of cell viability. Yellow MTT solution is converted by mitochondrial dehydrogenase enzyme in the living cells to violet formazan precipitate. Then, the formazan precipitate is solubilized in dimethyl sulfoxide (DMSO) or isopropanol. Absorption derived from formazan solution correlates with cell viability.

Cells were seeded into 96-well plates (in a density of 8,000 cells per well for a total 72 h incubation time) and incubated overnight. Next day, 90 µl of complete medium and 10 µl of test compounds were added on the cells. After appropriate time of incubation, 25 µl of 5 mg/ml of MTT in PBS 1X was added directly to each well. MTT solution was incubated in the cells in an incubator until violet formazan precipitate appeared. Supernatant containing MTT solution was aspirated and the formazan precipitate was then dissolved in 75 µl dimethyl sulfoxide (DMSO). Absorption was measured at 544 nm (test wavelength) and 690 nm (background wavelength) using the FLUOstar absorption plate reader. Background absorption at 690 nm was subtracted from the absorption at 544 nm then a concentration-effect curve was plotted and the respective $IC_{50}$ was calculated using GraphPad Prism version 4.00 for Windows according to the equation below.

$$\mathbf{Y = Bottom + (Top - Bottom)/ 1 + 10^{(log\ EC50 - X) \times Hill\ slope}}$$

**X** = logarithm of concentration

**Y** = the response

Y starts at Bottom and goes to Top with sigmoidal shape: this is identical to the four parameter logistic equation.

**Combination treatment using MTT assay**

Combination treatment was performed by MTT assay. Cells were seeded in a density of 4,000 cells per well into 96-well plates and incubated overnight. A confluence of the cells in untreated control wells should be reached 80 to 90 % at a measurement day (A2780 and HEY cell lines were seeded 4,000 cells per well while A2780CisR cell was seeded 4,500 cells per well and HEK293 was seeded 5,000 cells per well). Next day, ATP or adenosine was added and incubated 48 h prior to 72 h co-incubation with increased concentrations of cisplatin. Selective antagonists or dipyridamole were incubated 60 min and 30 min, respectively prior to ATP or adenosine administration. Absorption was measured in the same manner as MTT assay for single treatment.

The combination index (CI) values indicate synergism (CI < 0.9), additive effect (CI = 1.0) or antagonism (CI > 1.1) of drug interaction in the combination treatments were calculated according to Chou-Talalay method [Chou TC., 2006] using Calcusyn software version 2.1 and Compusyn software version 1.0 for windows. The obtained absorption from MTT assay was used to calculate "Fraction affected" (see formula below) which indicates inhibitory effect of ATP/adenosine alone or in combination with cisplatin on cell lines.

$$\textit{Fraction affected} = \left[100 - \left[\left[\frac{\textit{mean absorption of treatment}}{\textit{mean absorption of } 0.9\%\ \textit{NaCl}}\right] \times 100\right]\right] \div 100$$

Concentrations of ATP, adenosine, cisplatin and fraction affected values of certain treatment condition (single and combination treatments) were used for calculation of "CI values" by the software according to an equation below.

$$\mathrm{CI} = \frac{(\mathrm{D})_1}{(\mathrm{D_x})_1} + \frac{(\mathrm{D})_2}{(\mathrm{D_x})_2} = \frac{(\mathrm{D})_1}{(\mathrm{D_m})_1[f_a/(1-f_a)]^{1/m_1}} + \frac{(\mathrm{D})_2}{(\mathrm{D_m})_2[f_a/(1-f_a)]^{1/m_2}}$$

$(D)_1$ and $(D)_2$ refer to Concentration of drug 1 or drug 2, $(D_m)_1$ and $(D_m)_2$ refer to median-effect dose of drug 1 or 2, $f_a$ is a fraction affected of certain combination treatment and $m_1$ and $m_2$ are slope of median-effect plot of drug 1 or 2.

### 5.3.7 Cell cycle analysis

Cell lines were seeded at a density of 100,000 to 150,000 cells per well in 6-well plates overnight before treatment. At the day of cell fixation, cells should reach 60 to 80% confluence. Reference wells included untreated control and 50 nM of paclitaxel for 24 h which was served as G2/M phase-arrest control.

**Cell fixation**

After appropriate treatment time, supernatant and PBS 1X which was used to wash cells in each well were transferred to 15 ml conical tubes. Afterward, cells were detached from the wells with 0.02% typsin and transferred to the same 15 ml conical tube containing supernatant and PBS 1X. Cell suspension was then centrifuged at 266 g, 4°C for 4 min. Cell pellet was suspended in 1 ml of PBS 1X and centrifuged at 266 g, 4°C for 4 min. Then, cell pellet was re-suspended with 1 ml of cold PBS 1X (2 to 8°C) then cell suspension was slowly dropped into 9 ml of cold 70% ethanol (-20°C) and stored at -20°C overnight before analysis by flow cytometer.

**Cell cycle analysis by flow cytometer**

Cells suspension in 70% ethanol fixation was centrifuged at 266 g, 4°C for 30 min to separate all the cells out of ethanol solution. Then, supernatant was aspirated carefully without removing some floating cells which remained at the surface of cell suspension. After that, cells were washed with cold PBS 1X (2 to 8°C) and centrifuged for another 30 min. This washing step was performed twice in order to get rid of ethanol solution from cell suspension. After washing step, cell pellet was stained with 500 µl of PI staining solution and incubated for 15 min at 37°C in an incubator. PI staining cells were then diluted in sheath fluid to limit the cell number injected into flow cytometer (cell count should less than 1,000 cells per second in order to obtain accurate cell counting through flow cytometer). A minimum total cells count was 10,000 cells. The intact cells with propidium iodide staining can be separated into G1, S and G2/M phase depending on DNA content. Cells that are in S phase will have more DNA than cells in G1. They will take up proportionally more dye and will fluoresce

more brightly until they have doubled their DNA content whereas cells in G2/M will be approximately twice as bright as cells in G1. Fluorescence derived from PI-staining cells was shown in the histogram of FL2-PI (PI staining channel). Particular range of G2/M phase can be estimated by G2/M phase arrest-inducing by paclitaxel treatment (Figure 5.6A). G1-phase peak can clearly be seen and separated from S phase based on a histogram of untreated control (Figure 5.6B). Percentages of cells in each phase from FL2 channel histogram were used for cell cycle evaluation.

**A** **B**

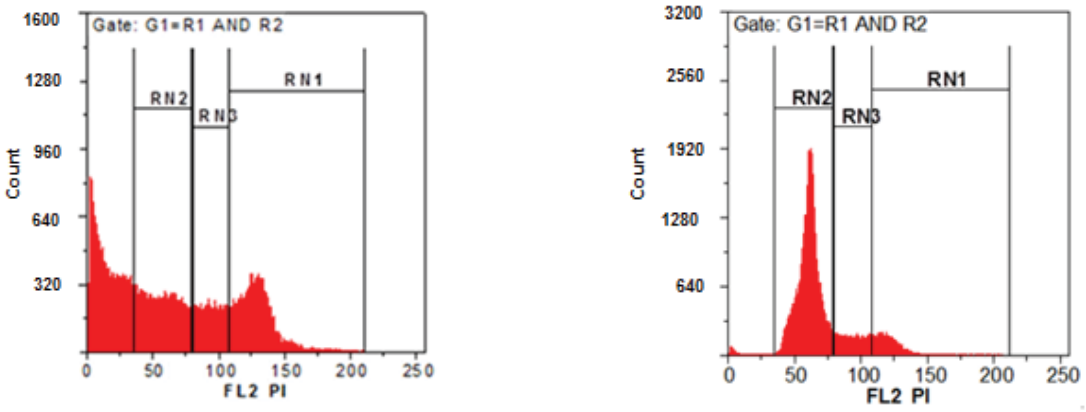


**Figure 5.6. Histogram of PI staining cells in FL2 channel obtained from obtained from cell cycle analysis.**

(A) Histogram of cells treated with 50 nM paclitaxel as a reference for G2/M phase arrest. (B) Histogram of untreated control cells as a reference for G1 and S phase. RN1, RN2 and RN3 indicate G2/M, G1 and S-phase, respectively.

## 5.3.8 Apoptosis assay

Cell lines were seeded at a density of 50,000 cells per well in 24-well plates overnight before treatment. The day after, old complete culture medium was replaced by new complete medium containing test compounds then cells were incubated for certain stated incubation times. Controls included untreated cells, 10% DMSO-treated cells and cisplatin-treated cells. After appropriate incubation time, the whole 6-well plate was centrifuged at 1200 rpm, 4°C for 5 min to settle down the entire apoptotic floating cells to bottom of the wells. Afterward, supernatant was gently removed and 500 µl of hypotonic PI staining buffer was then added into each well. The PI staining buffer was incubated in the cells at least 6 h before analysis by

flow cytometer. The homogenous PI-stained cells suspension was diluted in sheath fluid to obtain a final volume of 1 ml in a flow cytometer cuvette. Cell count should less than 1,000 cells per second in order to obtain accurate cell counting through flow cytometer. The minimum total cells count was 10,000 cells. The histogram of cells in FL2-PI channel will clearly show apoptotic cells populations in the subG1 phase (apoptosis cells) which containing nuclear DNA fragments (Fig. 5.7). Cell debris was excluded from the interested populations. Percentage of apoptosis cells in subG1 phase was used for the evaluation.

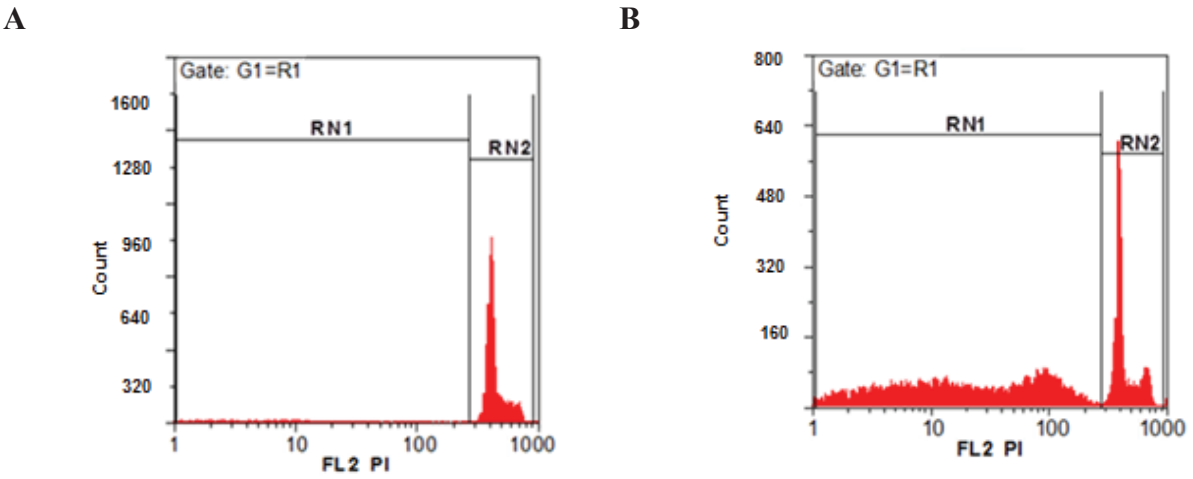


**Figure 5.7. Histogram of PI staining cells in FL2 channel obtained from apoptosis assay.** Histogram of untreated control cells showed no cells populations in the subG1 region (A) whereas cells treated with apoptotic-inducing compounds showed an increasing subG1 region (B). RN1 and RN2 indicate subG1 region and normal cell cycle region.

## 5.4 Statistics

$EC_{50}$ or $IC_{50}$ values were estimated after fitting the data from at least three-independent experiments to the four-parameter logistic equation using GraphPad Prism version 4.00 for Windows. Data were presented with standard error of the mean ($P$ value < 0.05). Statistical comparison was analyzed using Student's *t-test*. (*), (**) and (***) indicate $P$ value < 0.05, < 0.01 and < 0.001, respectively.

# 6. Results

*Effect of purinergic ligands on chemosensitivity of cisplatin*

Purinergic ligands used in this study are adenosine triphosphate (ATP) and adenosine, ligands for P2 nucleotide and P1 receptors, respectively. Parental A2780, cisplatin-resistant subline A2780CisR and HEY served as models for human ovarian cancer cells for the evaluation of ATP and adenosine effects on cisplatin sensitivity.

**Note:** P2 receptor expression and function, including ATP effects on cisplatin sensitivity in HEY cells were mainly studied in another Ph.D. project and are thus not presented here.

## 6.1 Characterization of ovarian cancer cells for purinergic receptor expression

In order to obtain an overview on purinergic receptor expression in ovarian cancer cell lines, parental A2780, cisplatin-resistant subline A2780CisR and HEY cell lines were characterized by reverse-transcription polymerase chain reaction (RT-PCR) and western blot analysis for gene and protein expression.

### 6.1.1 P2 receptor expression

**A**

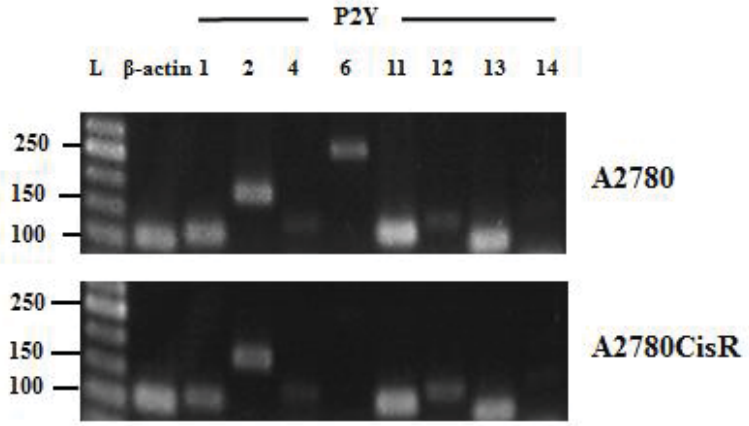

**B**

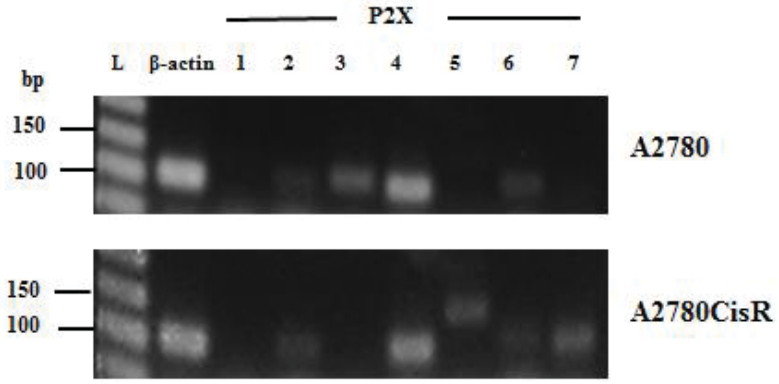


**Figure 6.1. Gene expression of P2Y** (A) **and P2X** (B) **receptors in A2780 and A2780CisR cells obtained from RT-PCR.**

"L" indicates DNA ladder and β-actin was used as housekeeping gene. Data shown are representative data from at least two-independent experiments.

Gene expression profiles in Figure 6.1A and 6.1B demonstrated that $P2Y_1$, $P2Y_2$, $P2Y_{11}$, $P2Y_{13}$ and $P2X_4$ receptors are expressed in both A2780 and A2780CisR cells whereas $P2Y_6$ receptors are expressed only in A2780 cells while $P2X_7$ receptors are slightly detected only in A2780CisR cells.

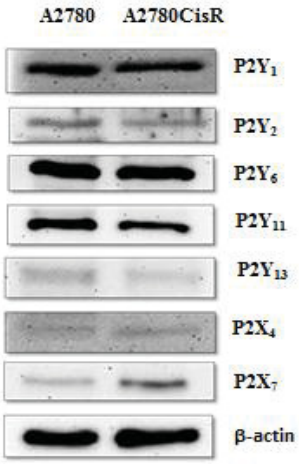


**Figure 6.2. Protein expression of P2Y receptors ($P2Y_1$, $P2Y_2$, $P2Y_6$, $P2Y_{11}$ and $P2Y_{13}$) and P2X receptors ($P2X_4$ and $P2X_7$) in A2780 and A2780CisR cells obtained from western blot analysis.**

β-actin was used as a loading control. Data shown are representative data from at least two-independent experiments.

Protein expression profiles shown in Figure 6.2 confirmed the expression of $P2Y_1$, $P2Y_2$, $P2Y_6$ and $P2Y_{11}$ receptors in A2780 and A2780CisR cells as well as a higher protein expression of $P2X_7$ in A2780CisR than in A2780 cells which is an agreement with RT-PCR results. Protein expression of $P2Y_{13}$ and $P2X_4$ are relatively lower compared to their higher expression found by RT-PCR.

### 6.1.2 P1 receptor expression

Next, gene and protein expression profiles of adenosine receptors were analyzed in human ovarian cancer cells A2780, A2780CisR and HEY by RT-PCR and western blot analysis.

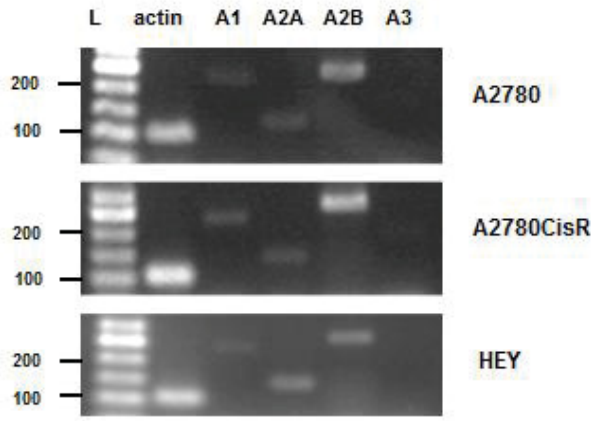


**Figure 6.3. Gene expression profile of adenosine receptors A1, A2A, A2B and A3 subtypes in A2780, A2780CisR and HEY cell lines obtained from RT-PCR.**

"L" indicates DNA ladder and β-actin was used as housekeeping gene. Data shown are representative data from at least two-independent experiments.

Gene expression profile shown in Figure 6.3 exhibited that A1, A2A and especially A2B adenosine receptor subtypes are expressed in A2780, A278CisR and HEY cells whereas the A3 receptor subtype cannot be detected by RT-PCR.

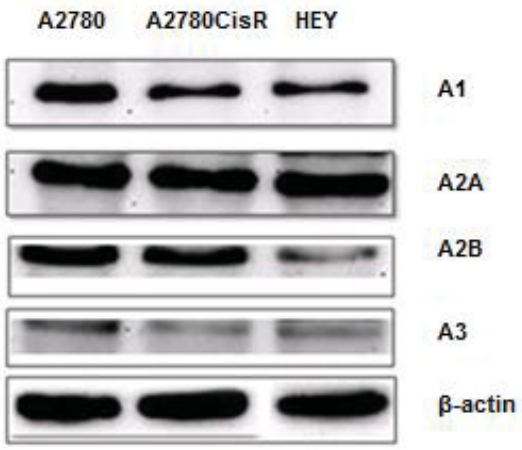


**Figure 6.4. Protein expression of A1, A2A, A2B and A3 adenosine receptors in A2780, A2780CisR and HEY cells obtained from western blot analysis.**
β-actin was used as loading control. Data shown are representative data from at least three-independent experiments.

Protein expression profile shown in Figure 6.4 confirmed the expression of A1, A2A and A2B adenosine receptors in A2780, A2780CisR and HEY cells. A small band for the A3 receptors pointed at a slight protein expression of the A3 receptor subtype.

### 6.2 Functional activity of purinergic P2 and P1 receptors

After analysis of receptor expression, functional activity of P2 and P1 receptors was evaluated either by calcium assay or cyclic adenosine monophosphate (cAMP) reporter gene assay, respectively.

#### 6.2.1 Evaluation of P2 receptor functional activity by calcium assay

Upon P2 receptor activation, calcium ions are released from intracellular compartments into the cytoplasm. Oregon Green BAPTA-1 AM is a fluorescent dye which can penetrate through the cell membrane and upon cleavage of ester bonds then binds calcium ions in the cytoplasm. Fluorescence intensity correlates with calcium binding. Thus, P2 receptor activation is correlated with an increase in intracellular fluorescence. In this study, ADP, ATP, UDP and UTP were used as agonists for activation of P2 receptors. Results are shown in Figure 6.5.

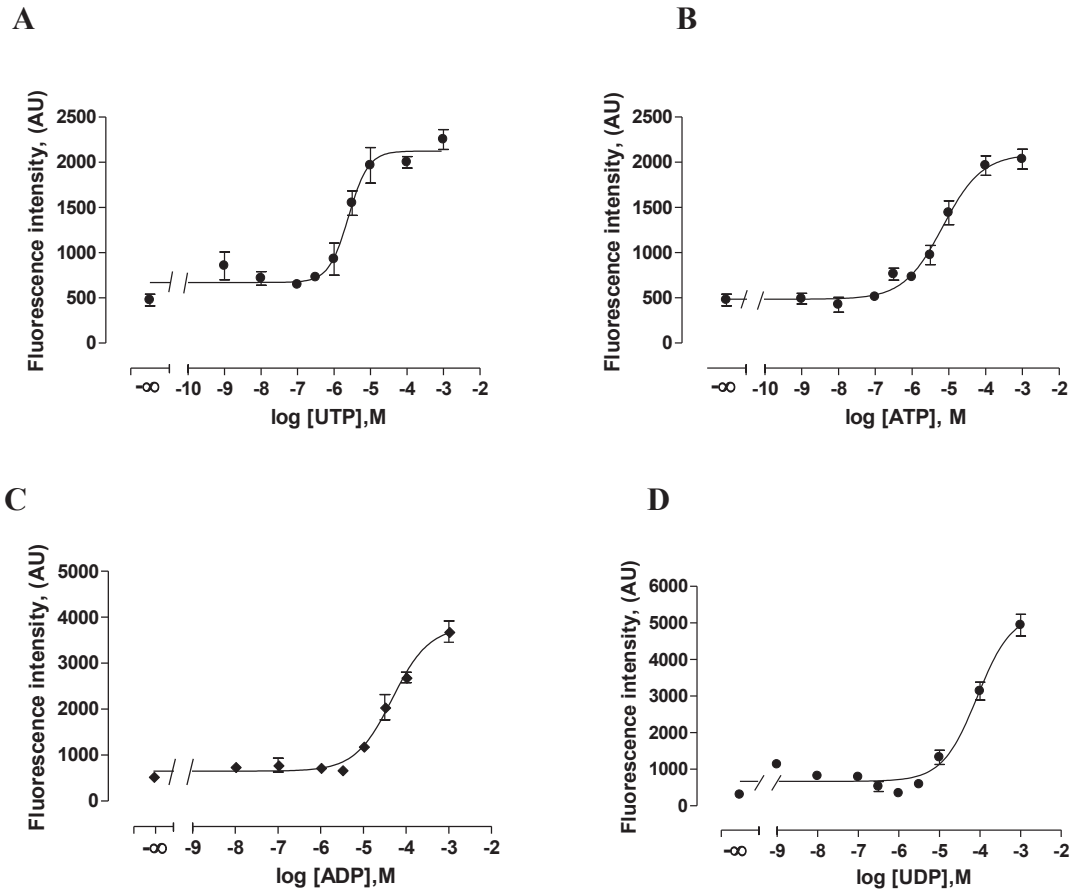


**Figure 6.5. Concentration-effect curves of UTP, ATP, ADP or UDP in A2780 cells monitored by calcium assay.** Increasing concentrations of UTP, ATP, ADP and UDP were injected onto wells containing A2780 cells. Then, fluorescence intensity was measured by NOVOstar plate reader. Data shown are mean ± SEM from a typical experiment out of a set of at least two, each performed in triplicate.

Figure 6.5 demonstrated that calcium ions are released in a concentration-dependent manner after stimulation by UTP, ATP, ADP, or UDP in A2780 cells. These results indicated functional activity of P2 receptors in A2780 cells. The potencies of P2 receptor agonists are shown in Table 6.1 as mean $EC_{50}$ and $pEC_{50}$ ± SEM.

**Table 6.1. Summary of $EC_{50}$ and $pEC_{50}$ ± SEM values of UTP, ATP, ADP and UDP in A2780 cells obtained from calcium assay.**

Increasing concentrations of UTP, ATP, ADP or UDP were injected into wells containing A2780 cells. Then, fluorescence intensity was measured by NOVOstar plate reader. Data shown are from at least two-independent experiments.

| Agonist | $EC_{50}$ (µM) | $pEC_{50}$ ± SEM |
|---|---|---|
| **UTP** | 3.39 | 5.47 ± 0.09 |
| **ATP** | 6.46 | 5.19 ± 0.11 |
| **ADP** | 44.7 | 4.35 ± 0.10 |
| **UDP** | 85.1 | 4.07 ± 0.12 |

As shown in Table 6.1, UTP and ATP exhibit higher potency than ADP and UDP.

Next, P2 receptor antagonists were used to investigate if the increase in fluorescence related to intracellular calcium release induced by UTP or ATP was P2 receptor-mediated. The non-selective P2 receptor antagonist suramin was pre-incubated 30 min prior to addition of UTP or ATP to A2780 cells.

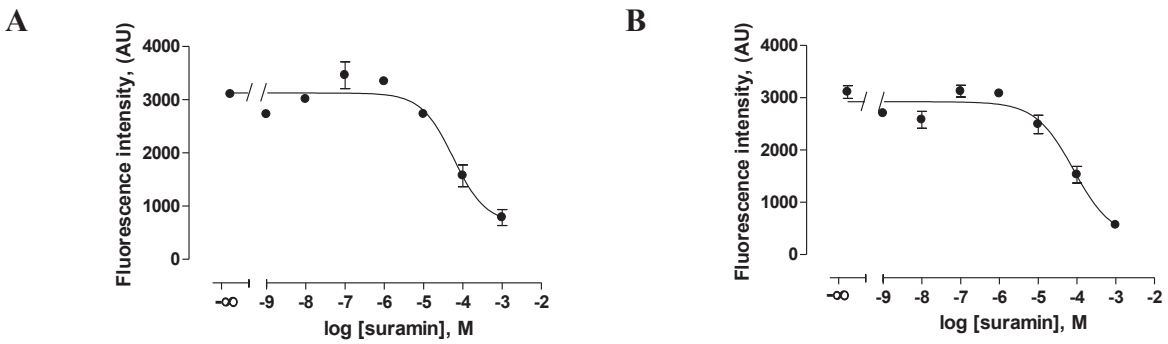


**Figure 6.6. Inhibitory effect of suramin on UTP- or ATP-induced increase in fluorescence in A2780 cells.**

Increasing concentrations of suramin were incubated 30 min prior to injection of 7 µM UTP (A) or 15 µM ATP (B). Data shown are mean ± SEM from a typical experiment out of a set of at least two, each performed in triplicate.

The concentration-effect curves shown in Figure 6.6 demonstrate that suramin inhibits the fluorescence intensity induced by UTP or ATP in a concentration-dependent manner resulting in $pIC_{50}$ values of 4.24 ± 0.16 (Ki = 17.1 µM) and 4.09 ± 0.22 (Ki = 26.0 µM),

respectively, in A2780 cells. These results indicate that the increase in fluorescence intensity upon UTP or ATP injection is mediated via P2 receptors expressed in A2780 cells.

To assess which subtypes of P2 receptors are responsible for ATP and UTP signaling in A2780 cells, selective P2 receptor antagonists were tested. Only antagonists for P2 receptor subtypes shown to be expressed by RT-PCR and western blotting (Figures 6.1 and 6.2) were included in the experiments. Therefore, the selective $P2Y_1$, $P2Y_2$, $P2Y_{11}$, $P2X_4$ and $P2X_7$ receptor antagonists MRS 2179, AR-C118925, NF340, 5-BDBD and A 740003, respectively, were pre-incubated 30 min before injection of either ADP or ATP to A2780 cells. ADP is known as selective agonist for the $P2Y_1$ receptors whereas ATP acts as agonist for many subtypes of P2 receptors [Burnstock, 2006].

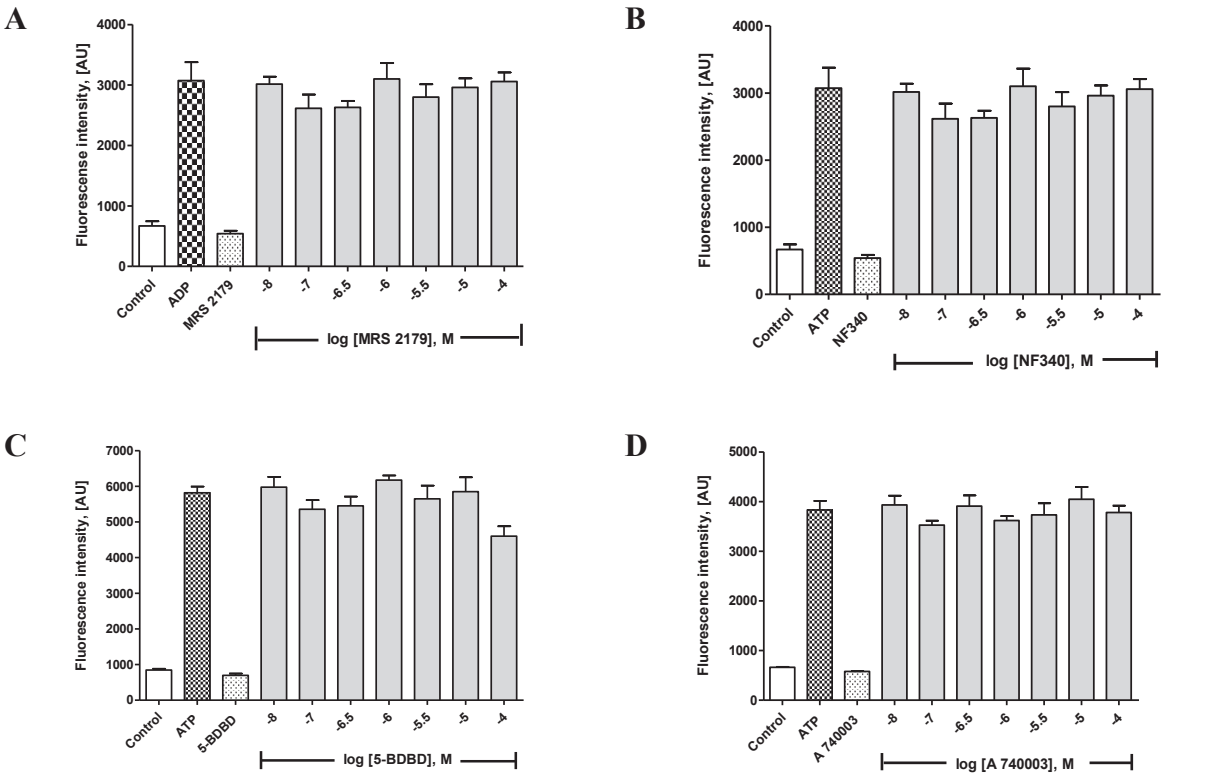


**Figure 6.7. Effects of the selective $P2Y_1$, $P2Y_{11}$, $P2X_4$ and $P2X_7$ receptor antagonists MRS 2179, NF340, 5-BDBD and A 740003 on ADP or ATP-induced P2 receptor activation in A2780 cells.**
The selective antagonists were added 30 min before injection of 36 µM ATP or 150 µM ADP to A2780 cells. Control indicates untreated cells. Data shown are mean ± SEM from at least two-independent experiments, each performed triplicate.

Figure 6.7 shows that none of the selective $P2Y_{11}$, $P2X_4$ and $P2X_7$ receptor antagonists NF340, 5-BDBD and A 740003 can inhibit ATP-induced P2 receptor activation. Similarly, the selective $P2Y_1$ receptor antagonist MRS 2179 does not inhibit ADP-induced $P2Y_1$ receptor activation. Thus, ADP- or ATP-induced receptor activation is not mediated by $P2Y_1$, $P2Y_{11}$, $P2X_4$ or $P2X_7$ receptors. Next, the selective $P2Y_2$ receptor antagonist AR-C118925 was incubated 30 min prior to ATP administration. The result is shown in Figure 6.8.

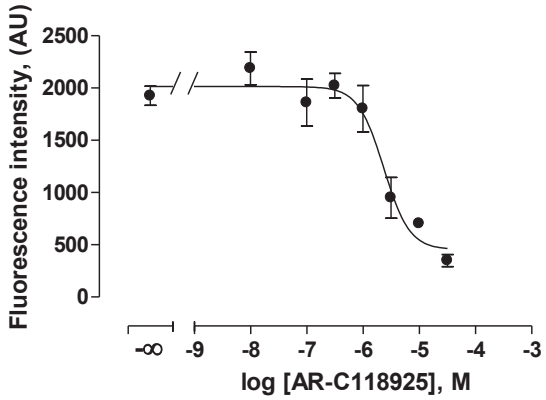


**Figure 6.8. Inhibitory effect of AR-C118925 on ATP-mediated fluorescence increase in A2780 cells.**

The selective $P2Y_2$ receptor antagonist AR-C118925 was pre-incubated 30 min before injection of 100 µM ATP. Data shown are mean ± SEM from a typical experiment out of a set of two, each performed in triplicate.

In contrast to the results obtained with the selective $P2Y_1$, $P2Y_{11}$, $P2X_4$ and $P2X_7$ receptor antagonists, the selective $P2Y_2$ receptor antagonist AR-C118925 is able to inhibit ATP-mediated P2 receptor activation in a concentration-dependent manner (Figure 6.8), yielding a $pIC_{50}$ value of 5.63 ± 0.11 (Ki = 0.13 µM) in A2780 cells. This result indicated that $P2Y_2$ receptors are responsible for ATP-mediated P2 receptor activation in A2780 cells.

To investigate if $P2Y_2$ receptors play a more general role in human ovarian cancer cells, HEY cells were studied for effects of ATP and AR-C118925 by calcium assay. Results are shown in Figure 6.9.

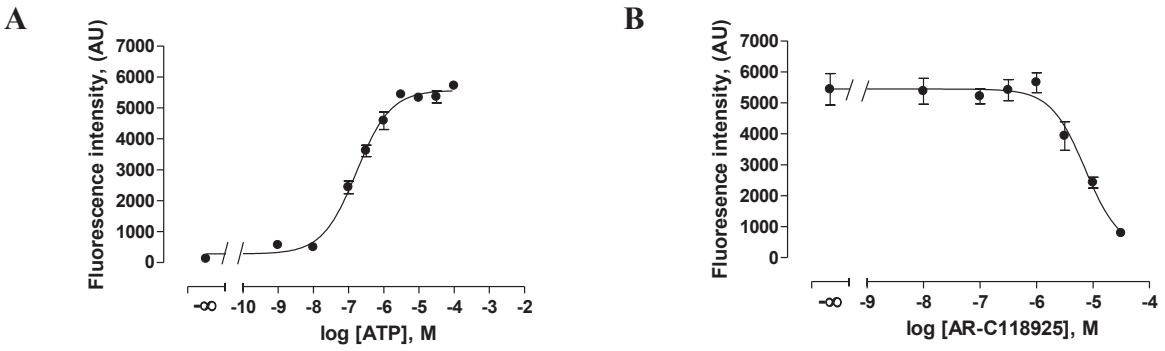


**Figure 6.9. Functional activity of P2 receptors in HEY cells measured by calcium assay**.
(A) Concentration-dependent effect of ATP on fluorescence intensity in HEY cells. (B) Concentration-dependent inhibitory effect of AR-C118925 on ATP-induced receptor activation in HEY cells. AR-C118925 was incubated 30 min before injection of 100 µM ATP. Data shown are mean ± SEM from a typical experiment out of a set of at least two, each performed in triplicate.

Figure 6.9A showed that ATP could activate P2 receptors in HEY cells, giving an $EC_{50}$ value of 0.20 µM which is 32-fold lower than the $EC_{50}$ of ATP achieved in A2780 cells. Moreover, Figure 6.9B showed that the selective $P2Y_2$ receptor antagonist AR-C118925 inhibits ATP-induced receptor activation in a concentration-dependent manner, giving a $pIC_{50}$ value of 5.14 ± 0.15 (Ki 14.4 nM). The inhibitory effect of AR-C118925 on ATP-induced receptor activation in HEY cells is qualitatively similar as in A2780 cells, confirming that the $P2Y_2$ receptor plays a major role for the functional effects of ATP in ovarian cancer cell lines.

To further extend the findings in HEY and A2780 cells, functional studies were undertaken in A2780CisR cells, a cisplatin resistant cell line [Engelke et al., 2016], shown to express P2 receptors (Figure 6.1 and 6.2). Results using ATP and ADP are shown in Figure 6.10.

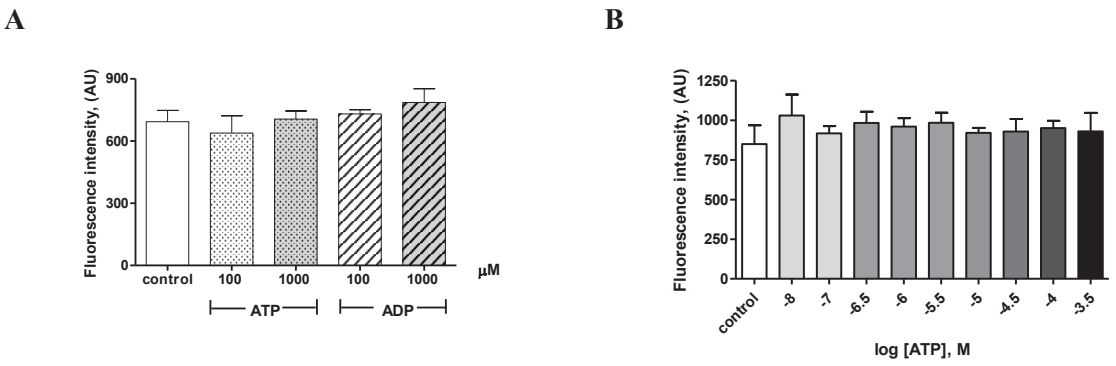

**Figure 6.10. Stimulation by ATP or ADP of P2 receptors in A2780CisR cells measured by calcium assay.**

(A) Fluorescence intensity after injection of 100 or 1000 μM of ATP and ADP. (B) Fluorescence intensity after injecting increasing concentrations of ATP to A2780CisR cells. Fluorescence was measured by NOVOstar microplate reader. Control indicates untreated cells. Data shown are mean ± SEM from at least two-independent experiments.

Figure 6.10 showed that ATP and ADP have no significant effects in A2780CisR cells in the calcium assay compared to untreated cells, suggesting that P2 receptors are expressed in A2780CisR cells (Figure 6.1 and 6.2) but possibly rather few and functionally not active. Further studies with nucleotides were thus not performed in A2780CisR.

### 6.2.2 Evaluation of the functional activity of P1 receptors by cAMP assay

Since A1, A2A, and A2B receptors were found to be expressed in A2780, A2780CisR and HEY cells (Figure 6.3 and 6.4), adenosine-mediated receptor activation was analyzed by a cyclic adenosine monophosphate (cAMP) reporter gene assay.

A2A and A2B receptors are $G_s$-coupled receptors whereas A1 and A3 receptors are $G_i$-coupled receptors. Activation of $G_s$-coupled receptors leads to an increase in cAMP levels whereas $G_i$-coupled receptor activation results in a decrease of cAMP levels. The cAMP reporter gene assay was used to examine luminescence correlating with cAMP levels after receptors activation. The non-selective agonist adenosine was used for activation of adenosine receptors. Forskolin served as a positive control for an increase in cAMP. The luminescence achieved from adenosine-activated receptors in A2780 cell lines is shown in Figure 6.11.

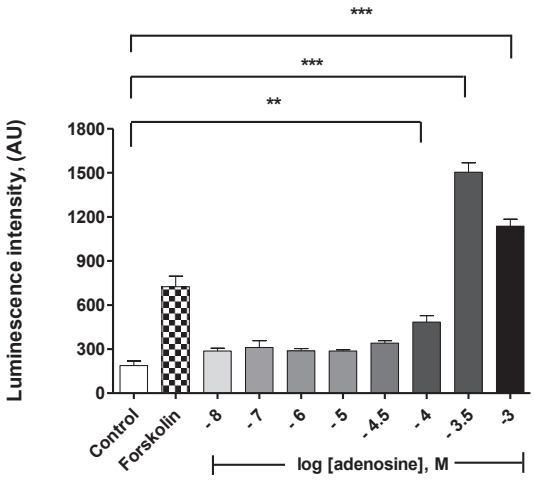


**Figure 6.11. Effect of adenosine on cAMP-dependent luminescence in A2780 cells.**
Increasing concentrations of adenosine or 10 µM forskolin as control were incubated in A2780 cells for 3 h before luminescence was measured by LUMIstar plate reader. Control indicates untreated cells. Data shown are mean ± SEM from a typical experiment out of a set of three, each performed in triplicate. (**), (***) indicate statistical significance compared to untreated control, *P value* < 0.01 and < 0.001, respectively.

Adenosine is able to elevate the luminescence intensity in A2780 cells in a concentration-dependent manner. As of 100 µM adenosine, the increase in luminescence intensity is significant, resulting in an $EC_{50}$ value of 165 µM ($pEC_{50}$ ± SEM = 3.78 ± 0.21). Because adenosine is a non- selective agonist, the luminescence levels are composed of functional activities of $G_s$- and $G_i$-coupled adenosine receptors. To clarify which subtypes of adenosine receptors are involved, potent and selective antagonists of A1, A2A and A2B receptors SLV320, SCH442416, and PSB603, respectively, were incubated 30 min prior to application of adenosine. Results are displayed in Figure 6.12.

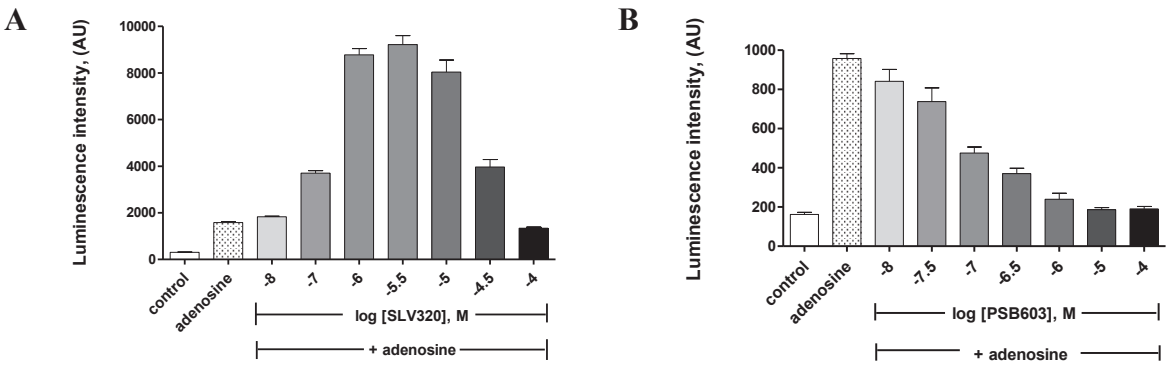

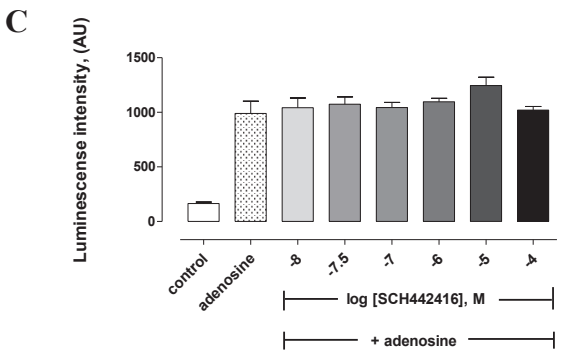


**Figure 6.12. Effects of the selective adenosine receptor antagonists SLV320, PSB603 and SCH442416 on adenosine-induced increase in luminescence in A2780 cells.**

200 µM adenosine was incubated with A2780 cells in the presence or absence of selective adenosine receptor antagonists SLV320 (A1 antagonist), PSB603 (A2B antagonist) or SCH442416 (A2A antagonist). Antagonists were incubated 30 min prior to 200 µM adenosine administration. After 3 h, luminescence intensity was measured by LUMIstar Galaxy plate reader. Data shown are mean ± SEM from a typical experiment out of a set of three, each performed in triplicate.

A1 receptors are $G_i$-coupled receptors. Thus, activation of A1 receptors results in a decrease of cAMP levels. As shown in Figure 6.12A, increasing concentrations of SLV320 up to 10 µM lead to an increase in adenosine-induced luminescence, resulting in an $IC_{50}$ value of 0.16 µM ($pIC_{50}$ ± SEM = 6.81 ± 0.14). Further increase in SLV320 concentrations beyond 31.6 µM results in a decrease of luminescence intensity which can be explained by a loss of selectivity of SLV320 for A1 receptors at high concentrations. As described in the literature, SLV320 has a Ki value of 1 nM at A1 receptors *in vitro* with a selectivity factor of at least 200 over other adenosine receptor subtypes [Kalk et al., 2007]. Thus, increase in SLV320 concentrations beyond 200 nM will result in a loss of selectivity for A1 receptors and subsequent inhibition of other subtypes of adenosine receptors as well. A2A and A2B receptors are $G_s$-coupled receptors. Once these subtypes are activated, cAMP levels increase. As shown in Figure 6.12B, the selective A2B receptor antagonist PSB603 is able to decrease the adenosine-induced luminescence intensity in a concentration-dependent manner, giving an $IC_{50}$ value of 78.5 nM ($pIC_{50}$ ± SEM = 7.10 ± 0.12), whereas the selective A2A receptor antagonist SCH442416 does not show any effects (Figure 6.12C). Since A3 receptors are basically not expressed (see Figures 6.3 and 6.4), A3 antagonists were not studied. Taken together, these results demonstrated that adenosine effects on cAMP levels observed in A2780 cells are mediated via A1 and A2B receptors.

Adenosine-induced increase in cAMP levels is also detected in A2780CisR and HEY cell lines even though the absolute cAMP-related luminescence levels is clearly lower compared to A2780 cells (Figure 6.13). The summary of $EC_{50}$ and $pEC_{50}$ ± SEM of adenosine in A2780, A2780CisR and HEY cell lines is shown in Table 6.2.

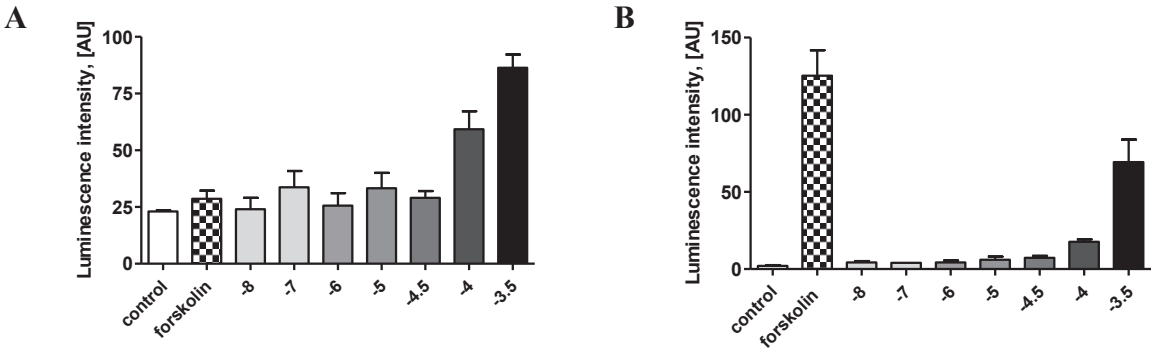


**Figure 6.13. Concentration-dependent effect of adenosine in cAMP reporter gene assay in A2780CisR and HEY cells.**

A2780CisR (A) and HEY (B) cells were incubated with increasing concentrations of adenosine. After 3 h, luminescence was measured by LUMIstar Galaxy plate reader. Control indicates untreated cells. Forskolin served as positive control. Data shown are mean ± SEM from a typical experiment out of a set of three, each performed in triplicate.

**Table 6.2. Summary of $EC_{50}$ and $pEC_{50}$ ± SEM values of adenosine in A2780, A2780CisR and HEY cells obtained from cAMP reporter gene assay.**

Cells were incubated with increasing concentrations of adenosine. After 3 h, luminescence was measured by LUMIstar plate reader. Data shown are from at least three-independent experiments.

| Cell lines | $EC_{50}$ (µM) | $pEC_{50}$ ± SEM |
|---|---|---|
| **A2780** | 165 | 3.78 ± 0.21 |
| **A2780CisR** | 321 | 3.49 ± 0.34 |
| **HEY** | 350 | 3.46 ± 0.33 |

The low adenosine-induced increase in luminescence intensity (Figure 6.13) and $pEC_{50}$ of adenosine (Table 6.2) in A2780CisR and HEY in comparison to A2780 cells, suggests a much lower number of functional active adenosine receptors in A2780CisR and HEY than in A2780 cells.

### 6.3 ATP enhances cisplatin-induced cytotoxicity

The expression and functional activity of P2 receptors have already been evaluated are described in chapter 6.1.1 and 6.2.1. Here, the cytotoxicity of ATP and combinations of ATP and cisplatin were analyzed. Results of MTT assays are shown in Figure 6.14.

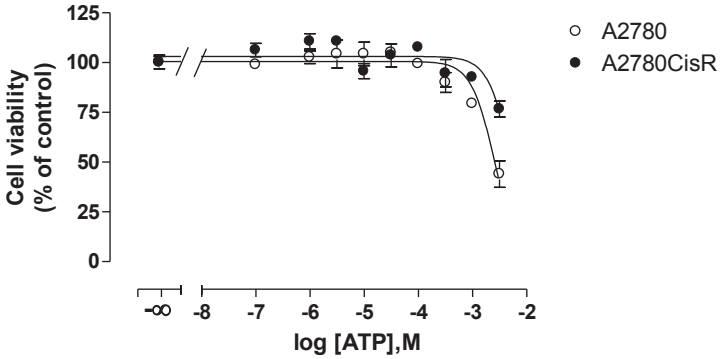


**Figure 6.14. Cytotoxicity of ATP in A2780 and A2780CisR cells (MTT assay).**
A2780 or A2780CisR cell lines were incubated with increasing concentrations of ATP . After 72 h, cell viability was evaluated by MTT assay. Data shown are mean ± SEM from a typical experiment out of a set of three, each performed in triplicate.

ATP treatment for 72 h shows low cytotoxicity to A2780 and A2780CisR cell lines. As shown in Figure 6.14 only starting at a concentration of around 3 mM, ATP decreases cell viability by 30% to 50% compared to untreated control. $IC_{50}$ values of more than 2 mM or 5 mM in A2780 cells or A2780CisR cells, respectively, were estimated.

Next, the combination treatment of ATP and cisplatin was analyzed by MTT assay to investigate if ATP can improve cisplatin cytotoxicity. ATP in a concentration of 100 to 500 µM was incubated 48 h prior to 72 h co-incubation with increasing concentrations of cisplatin. Concentration-effect curves of cisplatin in the absence of ATP were included as control in each experiment and shift factors (Sf) were calculated.

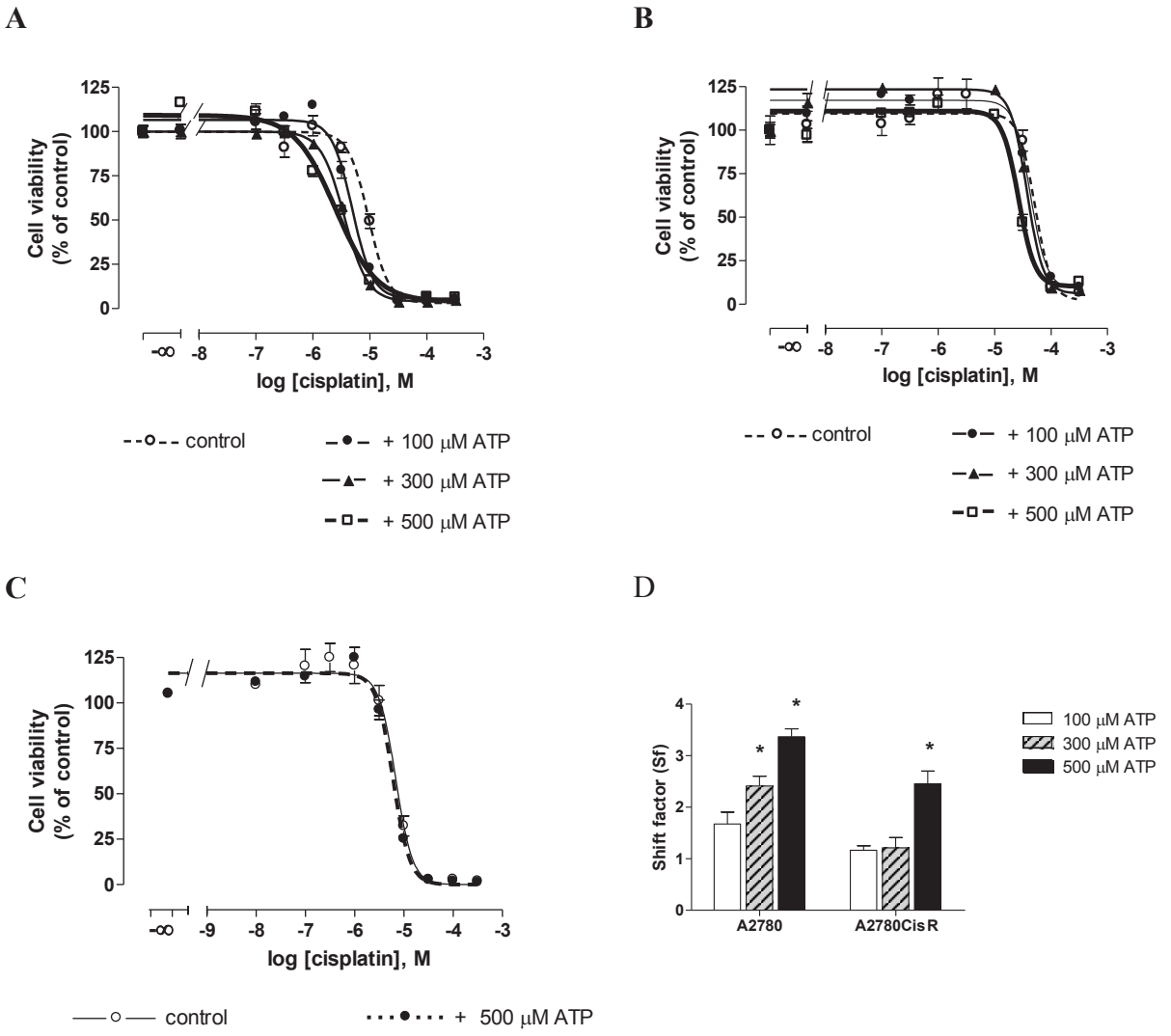


**Figure 6.15. Effect of ATP on cisplatin-induced cytotoxicity in A2780 and A2780CisR cells.**
A2780 (A) and A2780CisR (B) cells were incubated with 100, 300, or 500 μM ATP for 48 h prior to 72 h co-incubation with increasing concentrations of cisplatin. Control indicates cisplatin alone treatment. Data shown are mean ± SEM from a typical experiment out of a set of three, each performed in triplicate. (C) Concentration-effect curves obtained from simultaneous treatment of 500 μM ATP and cisplatin in A2780 cells. Data shown are mean ± SEM from a typical experiment out of a set of three, each performed in triplicate. (D) Summary of shift factors obtained from the combination treatment of ATP and cisplatin. Data shown are mean ± SEM from three-independent experiments. (*) indicates statistical significance compared to cisplatin alone treatment (control), *P value* < 0.05.

**Table 6.3. Summary of $IC_{50}$, $pIC_{50}$ ± SEM values of cisplatin and shift factors (Sf) obtained from combination treatments of ATP and cisplatin in A2780 and A2780CisR cells.**

Data shown are representative data from at least three-independent experiments. (*) indicates statistical significance (*P value* < 0.05) compared to cisplatin alone treatment (control).

| Condition | $IC_{50}$ (µM) | $pIC_{50}$ ± SEM | Shift factor (Sf) |
|---|---|---|---|
| **A2780** | | | |
| control | 9.55 | 5.02 ± 0.03 | - |
| + 100 µM ATP | 5.01* | 5.30 ± 0.05 | 1.91 |
| + 300 µM ATP | 3.46* | 5.46 ± 0.02 | 2.76 |
| + 500 µM ATP | 2.79* | 5.55 ± 0.05 | 3.42 |
| **A2780CisR** | | | |
| control | 52.5 | 4.28 ± 0.07 | - |
| + 100 µM ATP | 42.6 | 4.37 ± 0.04 | 1.23 |
| + 300 µM ATP | 37.2 | 4.43 ± 0.04 | 1.41 |
| + 500 µM ATP | 26.3* | 4.58 ± 0.04 | 2.00 |

Figure 6.15A and 6.15B demonstrate that the combination treatment of ATP and cisplatin (48 h pre-incubation of ATP prior to 72 h co-incubation with cisplatin) is able to shift the concentration-effect curves of cisplatin to the left, i.e., resulting in a decrease of $IC_{50}$ values of cisplatin compared to cisplatin alone treatment (control) and a shift factor of up to 3.4 in A2780 cells. Shift factors in A2780CisR are lower than in A2780 cells but if using 500 µM ATP still significant as shown in Figure 6.15D and Table 6.3. While simultaneous treatment of 500 µM ATP and cisplatin has no effect on cisplatin cytotoxicity (Figure 6.15C).

Based on the results in chapter 6.2.1, ATP calcium signaling is mediated via $P2Y_2$ receptors (Figure 6.8 and 6.9). To determine if ATP-enhanced cisplatin cytotoxicity is also mediated via $P2Y_2$ receptors, the selective $P2Y_2$ receptor antagonist AR-C118925 was pre-incubated 1 h prior to the administration of ATP. Concentration-effect curves of cisplatin in combination with ATP in the presence or absence of AR-C118925 were monitored and are displayed in Figure 6.16. Corresponding $IC_{50}$, $pIC_{50}$ ± SEM and shift factors (Sf) are shown in Table 6.4.

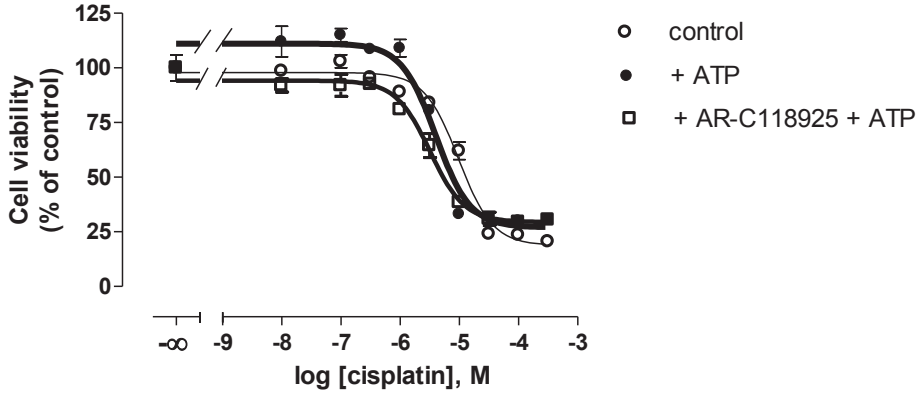


**Figure 6.16. Effect of AR-C118925 on ATP-enhanced cisplatin cytotoxicity in A2780 cells.**
20 μM of AR-C118925 was incubated 1 h prior to 500 μM of ATP for 48 h, followed by 72 h co-incubation with increasing concentrations of cisplatin. Control indicates treatment with cisplatin alone. Data shown are mean ± SEM from a typical experiment out of a set of three, each performed in duplicate.

**Table 6.4. Summary of $IC_{50}$, pIC50 ± SEM values of cisplatin and shift factors (Sf) obtained from combination treatment of ATP and cisplatin in the presence or absence of AR-C118925 in A2780 cells**.
500 μM ATP was incubated 48 h prior to 72 h co-incubation with increasing concentrations of cisplatin in the presence or absence of 20 μM of AR-C118925. Data shown are representative data from three-independent experiments. (*) indicates statistical significance compared to cisplatin alone treatment (Control), *P value* < 0.05.

| | $IC_{50}$ (μM) | $pIC_{50}$ ± SEM | Sf |
|---|---|---|---|
| **Control** | 9.74 | 5.01 ± 0.05 | |
| **+ ATP** | 4.00* | 5.42 ± 0.07 | 2.44 |
| **+ AR-C118925 + ATP** | 3.20* | 5.50 ± 0.05 | 3.04 |

Figure 6.16 and Table 6.4 showed that AR-C118925 does not inhibit ATP-enhanced cisplatin cytotoxicity. $IC_{50}$ of cisplatin in the presence of ATP is significantly lower than in the absence of ATP: 4.00 μM versus 9.74 μM, respectively. Presence of AR-C118925 gave a similar $IC_{50}$ of cisplatin as in the absence of AR-C118925 (3.20 μM), indicating that $P2Y_2$ receptors are not involved in ATP-enhanced cisplatin cytotoxicity. AR-C118925 is known as selective $P2Y_2$ receptor antagonist without any inhibitory effect on nucleotidases such as CD39 or CD73 [Rafehi et al., 2017].

However, extracellular ATP is known to be metabolized by ectonucleotidase CD39 to ADP and AMP. AMP is then further metabolized to adenosine by CD73 [Antonioli et al., 2013]. Therefore, to evaluate if degradation of ATP to adenosine and uptake of adenosine are involved in ATP-enhanced cisplatin cytotoxicity, the adenosine uptake inhibitor dipyridamole (DPM) was pre-incubated 30 min prior to ATP administration followed by addition of cisplatin. Results are shown in Figure 6.17 and Table 6.5.

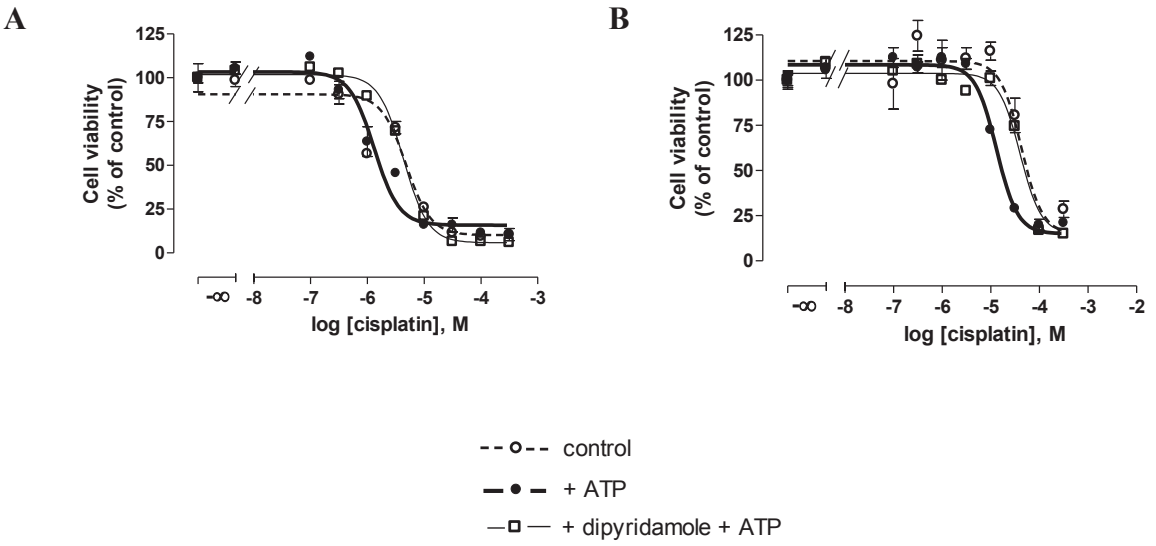


**Figure 6.17. Effect of dipyridamole (DPM) on ATP-enhanced cisplatin cytotoxicity in A2780 and A2780CisR cells.**

A2780 (A) and A2780CisR (B) cells were incubated with 10 µM dipyridamole 30 min prior to 500 µM ATP for 48 h followed by 72 h co-incubation with increasing concentrations of cisplatin . Control indicates cisplatin alone treatment. Data shown are mean ± SEM from a typical experiment out of a set of three, each performed in duplicate.

**Table 6.5. Summary of $IC_{50}$ and $pIC_{50}$ ± SEM values of cisplatin obtained from combination treatments of ATP and cisplatin in the presence or absence of dipyridamole.**

500 µM ATP was incubated 48 h prior to 72 h co-incubation with increasing concentrations of cisplatin in the presence or absence of 10 µM dipyridamole. Data shown are representative data from at least three-independent experiments. (*) and ($^{\#}$) indicate statistical significance compared to cisplatin alone treatment and cisplatin plus ATP treatment, respectively (*P value* < 0.05).

| Cell lines | $IC_{50}$, µM ($pIC_{50}$ ± SEM) | | |
|---|---|---|---|
| | control | + ATP | + dipyridamole + ATP |
| A2780 | **4.80** (5.32 ± 0.10) | **1.32*** (5.88 ± 0.07) | **4.29**$^{\#}$ (5.37 ± 0.03) |
| A2780CisR | **42.7** (4.37 ± 0.08) | **13.2*** (4.88 ± 0.04) | **40.4**$^{\#}$ (4.40 ± 0.04) |

Figure 6.17 showed that the presence of dipyridamole in the combination treatment of ATP and cisplatin abrogates the ATP effect by increasing $IC_{50}$ values of cisplatin to back to the $IC_{50}$ of cisplatin in control (Table 6.5) in both A2780 and A2780CisR cells. These results indicate that ATP-enhanced cisplatin cytotoxicity occurs after degradation of ATP to adenosine. Consequently, these results led to further experiments on adenosine in combination treatment with cisplatin.

## 6.4 Adenosine enhances cisplatin-induced cytotoxicity

Results in Chapter 6.3 showed that dipyridamole is able to diminish ATP-enhanced cisplatin cytotoxicity suggesting a mechanism via ATP breakdown to adenosine. However, to obtain a complete picture of adenosine signaling in ovarian cancer cells, the expression and functional activity of adenosine receptors was examined (see Chapter 6.1.2 and 6.2.2). Here, the cytotoxicity of adenosine and its ability to enhance cisplatin-induced cytotoxicity were evaluated by MTT assay. HEY cells were included in the study in order to extend the understanding of adenosine effects in ovarian cancer cells of different cisplatin sensitivity.

### 6.4.1 Cytotoxicity of adenosine and adenosine effects in combination treatment with cisplatin

The cytotoxicity of adenosine was evaluated by MTT assay. Increasing concentrations of adenosine from 100 to 1000 µM were incubated for 48 h. Results are shown in Figure 6.18.

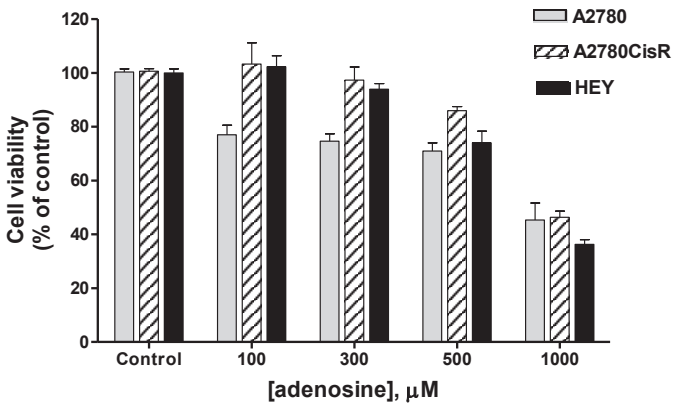


**Figure 6.18. Cytotoxicity of adenosine in A2780, A2780CisR, and HEY cells after 48 h treatment.** 100, 300, 500 and 1000 μM of adenosine were incubated in A2780, A2780CisR and HEY cell lines. After 48 h, cell viability was evaluated by MTT assay. Control indicates untreated cells. Data shown are mean ± SEM from three-independent experiments.

Adenosine shows moderate concentration-dependent cytotoxic effects in A2780, A2780CisR and HEY cell lines. $IC_{50}$ values are between 700 and 900 μM in the three examined cell lines. Further, the combination treatment of adenosine and cisplatin was studied to assess the ability of adenosine to enhance cisplatin-induced cytotoxicity. Adenosine was incubated 48 h prior to increasing concentrations of cisplatin for another 72 h, resulting $IC_{50}$ values of cisplatin in the absence and the presence of adenosine were used to calculate shift factors. Results are shown in Figure 6.19 and Table 6.6.

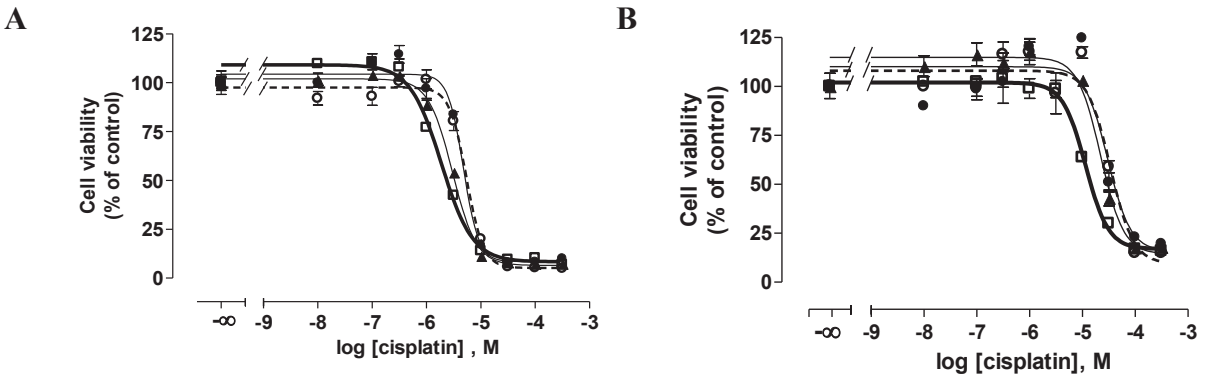

**C**

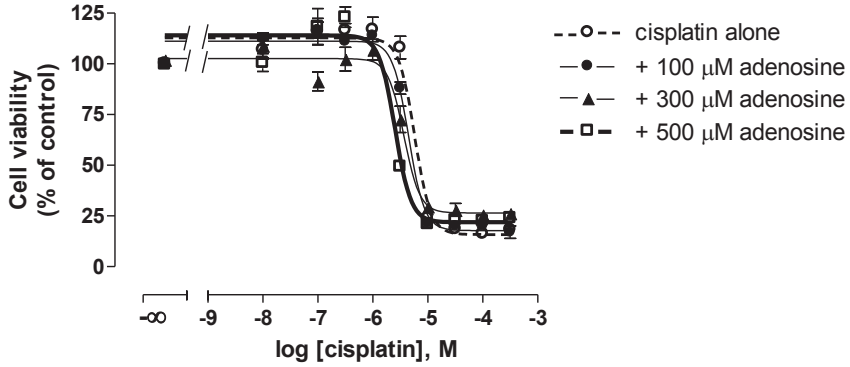


**D**

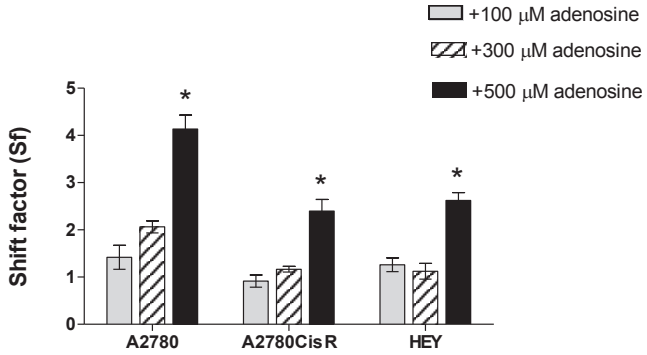


**Figure 6.19. Concentration-effect curves (MTT assay) of cisplatin in the absence and presence of adenosine and resulting shift factors in A2780, A2780CisR and HEY cells.** Adenosine in a concentration of 100, 300, or 500 μM were incubated 48 h prior to addition of increasing concentrations of cisplatin for another 72 h in A2780 (A), A2780CisR (B) and HEY (C) cell lines. Data shown are mean ± SEM from a typical experiment out of three, each performed in triplicate. (D) Mean shift factors from the combination treatment of adenosine and cisplatin in A2780, A2780CisR and HEY cell lines. (*) indicates statistical significance compared to cisplatin alone (*P value* < 0.05). Data shown are mean ± SEM from three-independent experiments.

**Table 6.6. Summary of $IC_{50}$, $pIC_{50}$ ± SEM of cisplatin and shift factors (Sf) derived from combination treatment of adenosine and cisplatin.**

Adenosine in a concentration of 100, 300 and 500 μM was incubated 48 h prior to co-incubation with increasing concentrations of cisplatin for 72 h. Data shown are representative data from at least three-independent experiments. (*) indicates statistical significance (*P value* < 0.05) in comparison to cisplatin alone (control).

| Condition | $IC_{50}$ (µM) | $pIC_{50}$ ± SEM | Shift factor (Sf) |
|---|---|---|---|
| **A2780** | | | |
| control | 5.46 | 5.26 ± 0.03 | - |
| + 100 µM adenosine | 4.77 | 5.32 ± 0.03 | 1.14 |
| + 300 µM adenosine | 3.01* | 5.52 ± 0.02 | 1.81 |
| + 500 µM adenosine | 1.26* | 5.90 ± 0.04 | 4.32 |
| **A2780CisR** | | | |
| control | 34.0 | 4.47 ± 0.07 | - |
| + 100 µM adenosine | 30.1 | 4.52 ± 0.10 | 1.13 |
| + 300 µM adenosine | 22.2 | 4.65 ± 0.06 | 1.53 |
| + 500 µM adenosine | 15.4* | 4.81 ± 0.03 | 2.20 |
| **HEY** | | | |
| control | 5.81 | 5.24 ± 0.05 | - |
| + 100 µM adenosine | 4.46 | 5.35 ± 0.03 | 1.30 |
| + 300 µM adenosine | 3.68* | 5.43 ± 0.04 | 1.58 |
| + 500 µM adenosine | 2.54* | 5.60 ± 0.05 | 2.29 |

The $IC_{50}$ of cisplatin significantly decreases in the presence of adenosine compared to cisplatin alone (Figure 6.19A, 6.19B, 6.19C and Table 6.6). Shift factor is the ratio of $IC_{50}$ values of cisplatin alone and the combination of adenosine with cisplatin. 500 µM of adenosine significantly shifted the $IC_{50}$ of cisplatin by a factor of 4.3 in A2780 cells (Figure 6.19D). Similarly, significant shift factors were obtained in the presence of 500 µM of adenosine in A2780CisR and HEY cells (Figure 6.19B and 6.19C).

### 6.4.2 Synergistic effects of adenosine and cisplatin in combination treatments

In addition, combination index (CI) values were calculated according to the method of Chou-Talalay [Chou, 2006] using Compusyn software to evaluate the mode of interaction between adenosine and cisplatin. Adenosine in a concentration of 100, 300, 500, and 700 µM was incubated 48 h prior to 72 h co-incubation with increasing concentrations of cisplatin. Table 6.7 shows mean CI values for various concentrations in all three ovarian cancer cell lines. CI values $< 0.9$ indicate synergism, $CI = 1$ indicates an additive effect, $CI > 1$, indicates antagonism, respectively [Chou, 2006].

**Table 6.7. Combination index (CI) values derived from combination treatments of adenosine and cisplatin in A2780, A2780CisR and HEY cell lines.**

Adenosine in a concentration of 100, 300, 500 and 700 μM was incubated 48 h prior to 72 h co-incubation with various concentrations of cisplatin. Then, MTT data of a particular combination treatment were used to calculate CI values according to the method of Chou-Talalay using Compusyn software. Data shown are mean CI values from at least three-independent experiments.

| Cell line | Combination Index (CI) value | | | | |
|---|---|---|---|---|---|
| | cisplatin (μM) | plus adenosine (μM) | | | |
| | | 100 | 300 | 500 | 700 |
| **A2780** | **2** | 0.52 | 0.79 | 0.88 | 0.55 |
| | **5** | 0.70 | 0.78 | 0.78 | 0.41 |
| | **10** | 0.49 | 0.42 | 0.46 | 0.25 |
| **A2780CisR** | **25** | 0.95 | 0.91 | 0.95 | 0.82 |
| | **30** | 0.90 | 0.76 | 0.87 | 0.82 |
| **HEY** | **4** | 0.76 | 0.93 | 0.80 | 0.48 |
| | **6** | 0.74 | 0.74 | 0.78 | 0.64 |
| | **8** | 0.83 | 0.79 | 0.83 | 0.80 |

Generally, at higher concentrations of cisplatin and adenosine, CI values were below 0.9, indicating synergism between adenosine and cisplatin. Some combination treatment conditions in A2780CisR and HEY cell lines show CI value ≥ 0.9 indicating an additive effect based on the CI values classification [Chou, 2006].

## 6.5 Adenosine signaling in ovarian cancer cells

Most studies in the literature focus on adenosine signaling pathways via adenosine receptors. However, extracellular adenosine can also be taken up into the cells through nucleoside transporters and initiate many cell response mechanisms [Antonioli et al., 2013 and Mello et al., 2014]. To investigate adenosine signaling in human ovarian cancer cell lines, adenosine receptor antagonists and a nucleoside transporter inhibitor were tested.

### 6.5.1 Role of adenosine receptors and nucleoside transporters in adenosine treatment

To examine the role of adenosine receptors for the observed cytotoxic effects of adenosine, the selective A1 and A2B receptor antagonists SLV320 and PSB603 were incubated 1 h prior to adenosine. Furthermore, the nucleoside transporter inhibitor dipyridamole (DPM) was

incubated 30 min prior to adenosine addition in order to determine role of adenosine uptake via nucleoside transporters. Results are shown in Figure 6.20.

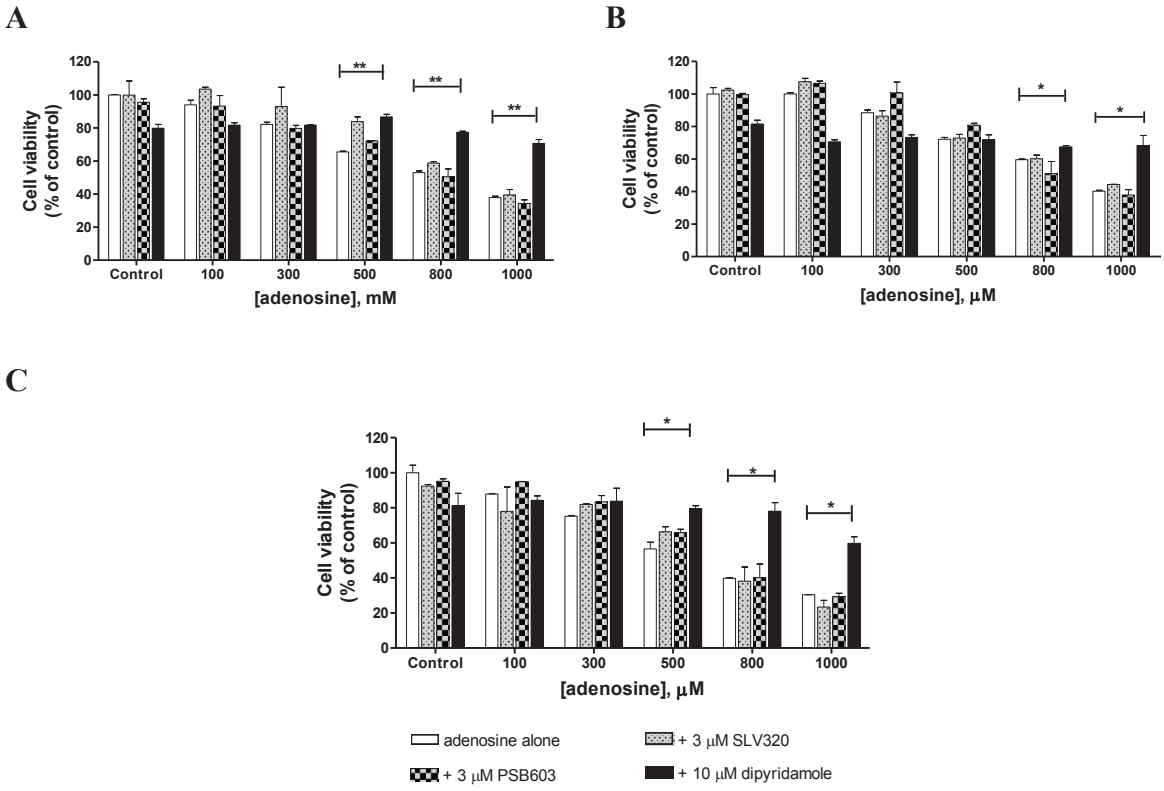


**Figure 6.20. Effect of SLV320, PSB603 and dipyridamole on adenosine cytotoxicity in A2780, A2780CisR and HEY cell lines.** 3 µM of SLV320 or PSB603, respectively were incubated 1 h or 10 µM of dipyridamole (DPM) was incubated 30 min prior to administration of 100 to 1000 µM of adenosine for 48 h in A2780 (A), A2780CisR (B) and HEY (C) cell lines. Control indicates untreated cells or single treatment (no adenosine) of SLV320, PSB603, or DPM. Data shown are mean ± SEM from at least three-independent experiments. (*) and (**) indicate statistical significance compared to adenosine alone treatment, *P value* < 0.05 and < 0.01, respectively.

Figure 6.20 demonstrated that neither SLV320 nor PSB603 are able to inhibit adenosine-induced cytotoxicity whereas dipyridamole, a nucleoside transporter inhibitor, significantly inhibits adenosine-induced cytotoxicity in A2780, A2780CisR and HEY cells.

### 6.5.2 Role of adenosine receptors and nucleoside transporters in the combination treatment of adenosine and cisplatin

According to the inhibitory effect of dipyridamole on the cytotoxicity of adenosine alone (Fig. 6.20), dipyridamole was incubated 30 min prior to adenosine administration for 48 h

followed by co-incubation with cisplatin for another 72 h. Results are shown in Figure 6.21 and Table 6.8.

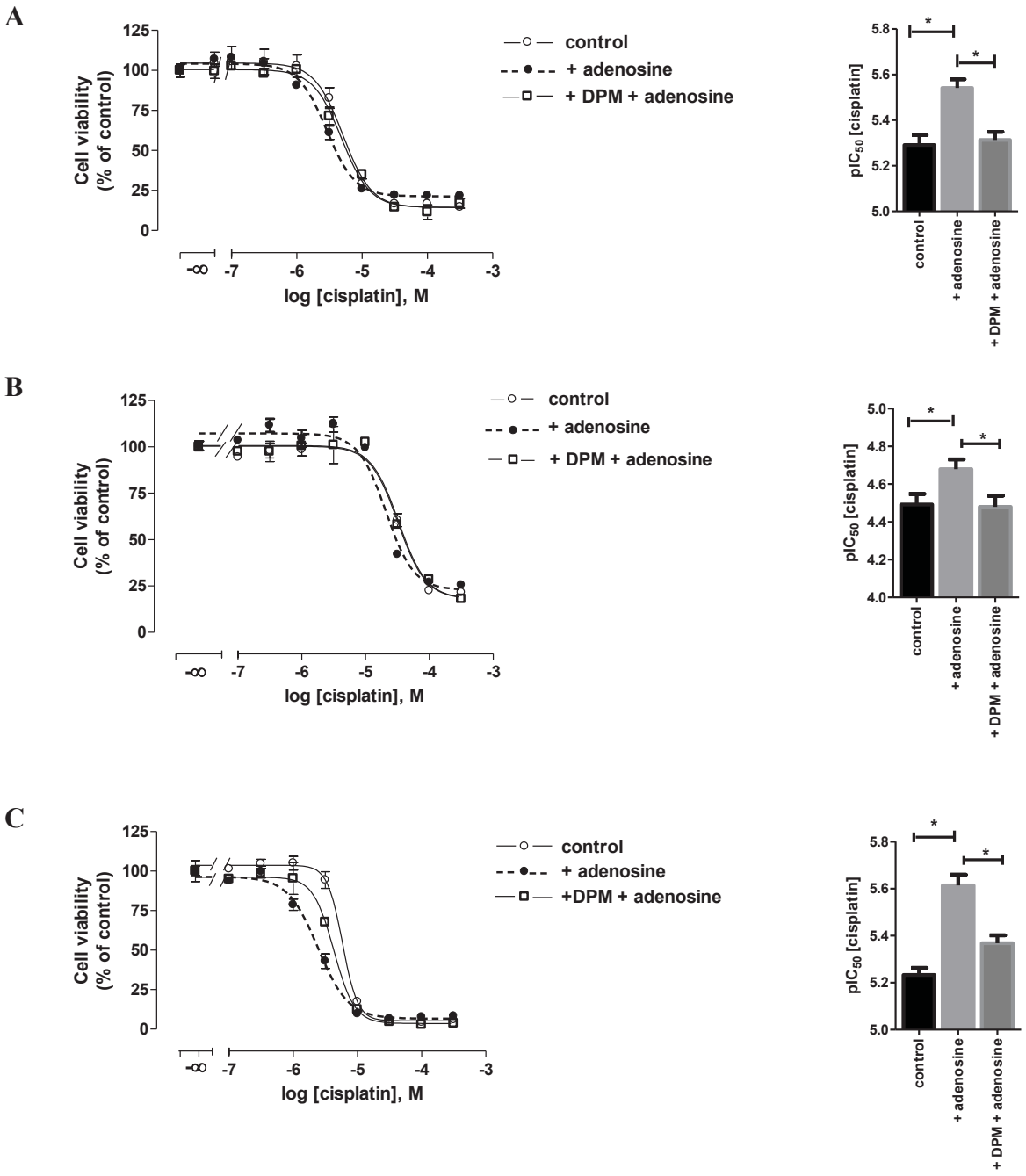


**Figure 6.21. Effect of dipyridmole on adenosine-enhanced cisplatin cytotoxicity in the combination treatment of adenosine and cisplatin (MTT assay).**

10 µM of dipyridamole was incubated 30 min prior to 500 µM of adenosine for 48 h followed by 72 h co-incubation with increasing concentrations of cisplatin in A2780 (A), A2780CisR (B) and HEY (C) cell lines. Bar graphs show comparison of $pIC_{50}$ ± SEM of cisplatin alone or in combination with adenosine in the presence or absence of dipyridamole. (*) indicates statistical significance, *P value* <

0.5. Data shown are mean ± SEM from a typical experiment out of a set of three, each performed in duplicate.

**Table 6.8. Summary of $IC_{50}$, $pIC_{50}$ ± SEM of cisplatin and shift factors achieved from combination treatments of adenosine and cisplatin in the presence or absence of dipyridamole (MTT assay).** 500 µM Adenosine was incubated 48 h prior to 72 h co-incubation with increasing concentrations of cisplatin in the presence or absence of 10 µM dipyridamole. Data shown are representative data from at least three-independent experiments. (*) and ($^{\#}$) indicate statistical significance compared to cisplatin alone (control) and cisplatin plus adenosine, respectively (*P value* < 0.05).

| Cell lines | $IC_{50}$, µM ($pIC_{50}$ ± SEM) | | |
|---|---|---|---|
| | control | + adenosine | + dipyridamole + adenosine |
| **A2780** | **3.13** (5.29 ± 0.04) | **0.88*** (5.54 ± 0.04) | **4.42**$^{\#}$ (5.31 ± 0.04) |
| **A2780CisR** | **32.0** (4.49 ± 0.06) | **20.7*** (4.68 ± 0.05) | **30.8**$^{\#}$ (4.48 ± 0.06) |
| **HEY** | **5.84** (5.23 ± 0.03) | **2.44*** (5.61 ± 0.04) | **4.28**$^{\#}$ (5.37 ± 0.03) |

The presence of dipyridamole abrogated adenosine-enhanced cisplatin cytotoxicity as shown in Figure 6.21 and Table 6.8 by increase in the $IC_{50}$ of cisplatin to nearly the same value as cisplatin alone treatment. These results demonstrated that the uptake of adenosine through nucleoside transporters is important for the cytotoxicity of adenosine and adenosine-enhanced cisplatin cytotoxicity.

Next, to determine a possible role of adenosine receptors in the combination treatment of adenosines and cisplatin, the selective A1 and A2B receptor antagonists SLV320 and PSB603, respectively, were incubated 1 h prior to adenosine administration in the combination treatment of adenosine and cisplatin. Results are shown in Figure 6.22 and 6.23.

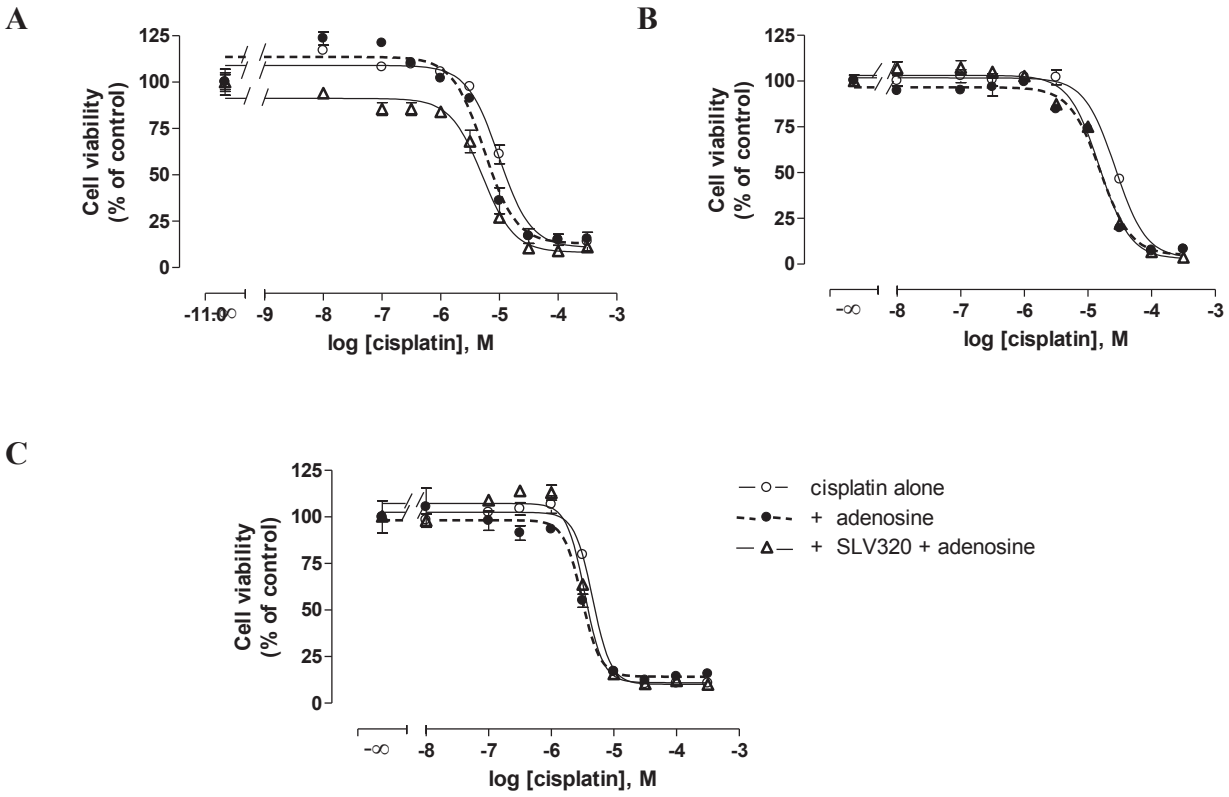


**Figure 6.22. Effect of the selective A1 receptor antagonist SLV320 on adenosine-enhanced cisplatin cytotoxicity in A2780, A2780CisR and HEY cell lines (MTT assay).**

3 μM SLV320 was incubated 1 h prior to 500 μM adenosine for 48 h followed by 72 h co-incubation with increasing concentrations of cisplatin in A2780 (A), A2780CisR (B) and HEY (C). Data shown are mean ± SEM from a typical experiment out of a set of three, each performed in duplicate.

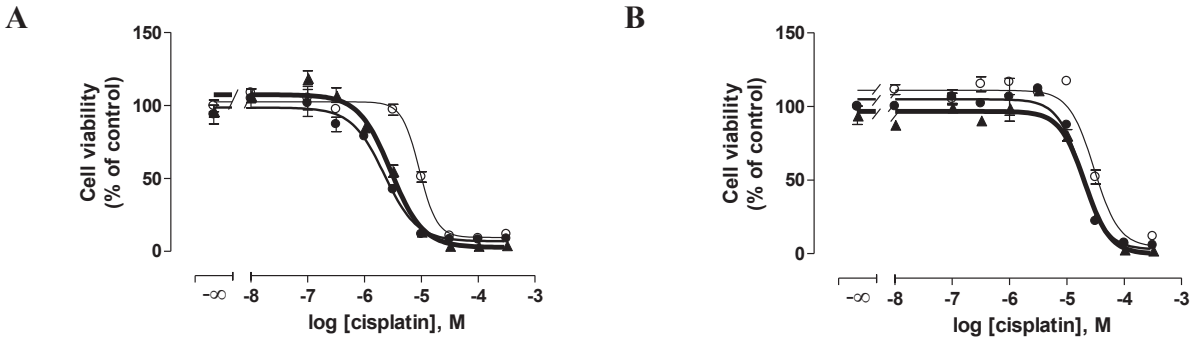

**C**

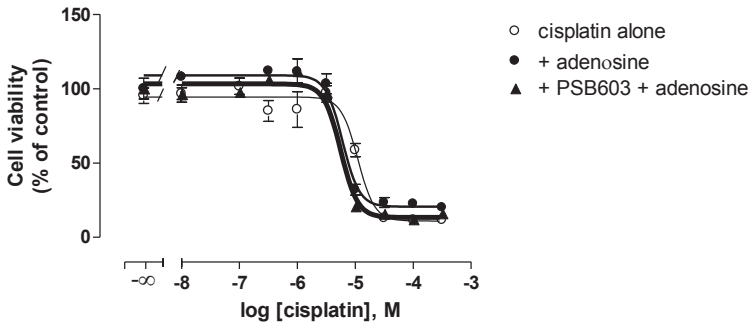


**Figure 6.23. Effect of the selective A2B receptor antagonist PSB603 on adenosine-enhanced cisplatin cytotoxicity in A2780, A2780CisR and HEY cell lines (MTT assay).**
3 µM PSB603 was incubated 1 h prior to 500 µM adenosine for 48 h followed by 72 h co-incubation with increasing concentrations of cisplatin in A2780 (A), A2780CisR (B) and HEY (C). Data shown are mean ± SEM from a typical experiment out of a set of three, each performed in duplicate.

The concentration-effect curves shown in Figure 6.22 and 6.23 showed that SLV320 and PSB603 at a concentration of 3 µM are not able to inhibit adenosine-enhanced cisplatin cytotoxicity in all three examined cell lines, confirming the essential role in adenosine-enhanced cisplatin cytotoxicity of adenosine uptake via nucleoside transporters in A2780, A2780CisR and HEY cell lines. Noteworthy, 3 µM of SLV320 or PSB603 is a concentration which does not show any toxic effects to the cells but inhibits the functional activity of A1 and A2B receptors based on the results from cAMP assay (Figure 6.12).

## 6.6 Effect of ATP and adenosine on cell cycle and apoptosis induction in ovarian cancer cell lines

Next, effects of ATP and adenosine on cell cycle arrest and induction of apoptosis were studied. ATP and adenosive were used at concentrations exhibiting cytotoxicity and enhancing cisplatin sensitivity.

### 6.6.1 ATP and adenosine effects on cell cycle

The cell cycle is an important event for every dividing living cell to control cell division, leading to growth and proliferation. Normal cell cycle consists of three phases: G1, S and G2/M phase. In this study, cells were incubated with 500 µM of ATP or adenosine, concentrations which gave the highest shift factors in the combination treatment of ATP or adenosine and cisplatin. After 48 h, cells were analyzed by flow cytometry. The specific

phases of cell cycle were distinguished in a histogram displaying fluorescence intensity of propidium iodide-stained nuclear DNA. Control included untreated cells and paclitaxel-treated cells which were used to identify the G2/M phase arrest. Results are shown in Figure 6.24.

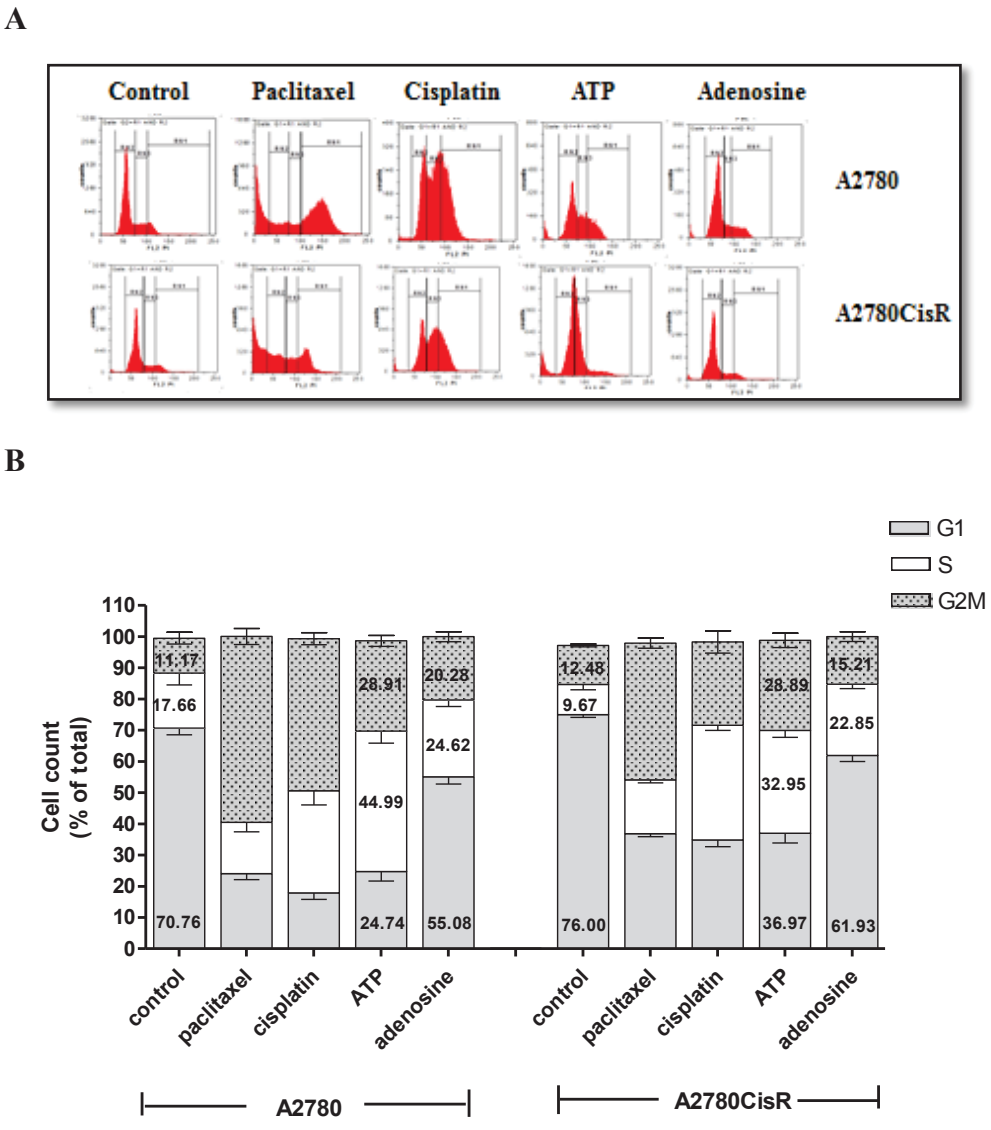


**Figure 6.24. Effect of ATP and adenosine treatment on cell cycle.**

500 µM ATP or adenosine were incubated in A2780 or A2780CisR cells for 48 h. 10 or 60 µM of cisplatin were incubated for 24 h in A2780 and A2780CisR cell lines, respectively as reference. Cells treated with 50 nm of paclitaxel for 24 h was used as positive control for G2/M arrest. Control indicates untreated cells. (A) Representative histograms of cell cycle after treatment with respective conditions. (B) Summary of cell counts in specific phases of cell cycle after treatment. Data shown are mean ± SEM from at least three-independent experiments.

Figure 6.24 showed that treatment with 500 µM ATP or adenosine for 48 h induce cell cycle arrest in S-phase in both, A2780 and A2780CisR cells.

### 6.6.2 ATP and adenosine effects on the induction of apoptosis

Ovarian cancer cells were incubated with various concentrations of ATP or adenosine for 48 h. Propidium iodide (PI) was used to stain DNA at least 6 h before analysis by flow cytometry. Cells undergoing apoptosis can be distinguished from normal cells based on their DNA content in the subG1 region (< 2 C) in PI-stained histograms. Percentage of apoptotic nuclei after ATP or adenosine treatments is shown in Figure 6.25.

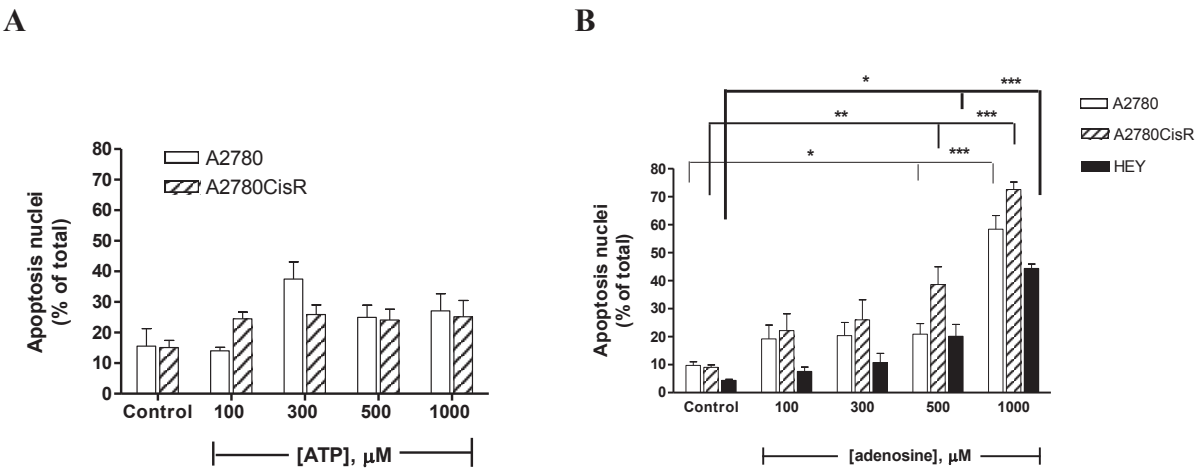


**Figure 6.25. Induction of apoptosis by ATP and adenosine.**
ATP (A) or adenosine (B) in various concentrations of 100 to 1000 µM were incubated in A2780, A2780CisR and HEY cells. After 48 h, cells were analyzed by flow cytometry. Data shown are mean ± SEM from three independent experiments. (*), (**) and (***) indicate statistical significance compared to untreated control, *P value* < 0.05, < 0.01 and < 0.001, respectively.

Treatment with ATP in a concentration of 100 to 1000 µM for 48 h is not able to significantly induce apoptosis neither in A2780 nor in A2780CisR cell lines. However, adenosine is able to induce apoptosis in a concentration-dependent manner. 500 and 1000 µM Adenosine significantly induce apoptosis compared to untreated control in all three examined cell lines.

## 6.7 Adenosine uptake is essential for adenosine-induced apoptosis via caspase pathway

Results from chapter 6.5 demonstrated that adenosine uptake via nucleoside transporters plays a crucial role for the cytotoxicity of adenosine and adenosine-enhanced cisplatin

cytotoxicity. In order to determine if adenosine uptake or adenosine receptors are involved in adenosine-induced apoptosis, dipyridamole and the selective A1 and A2B receptor antagonists SLV320 and PSB603 were incubated for 30 to 60 min prior to adenosine administration. Results are shown in Figure 6.26.

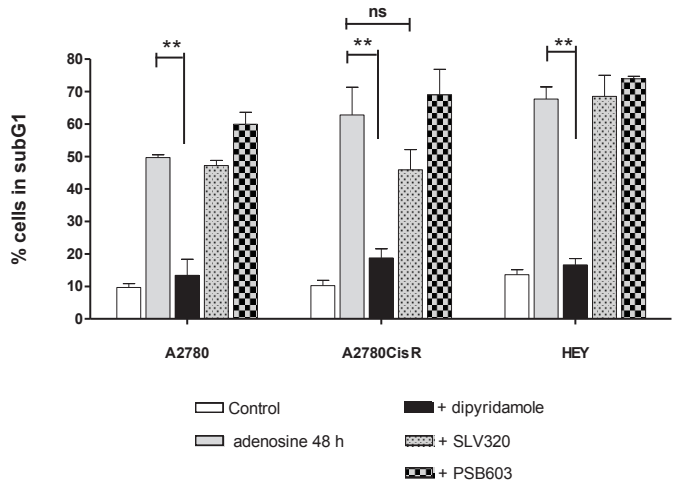


**Figure 6.26. Effect of dipyridamole, SLV320 and PSB603 on adenosine-induced apoptosis in A2780, A2780CisR and HEY cell lines.** 10 μM of dipyridamole and 3 μM of either SLV320 or PSB603 were incubated 30 or 60 min, respectively, prior to addition of 1000 μM adenosine. After 48 h, apoptotic nuclei were analysed by flow cytometry. Control indicates untreated cells. Data shown are mean ± SEM from at least three-independent experiments. (**) indicates statistical significance compared to adenosine alone treated cells (*P value* < 0.01). (ns) means not significant.

Figure 6.26 demonstrated that dipyridamole completely abrogates adenosine-induced apoptosis in all three cell lines whereas the selective A1 and A2B receptor antagonists SLV320 and PSB603 are not able to inhibit adenosine-induced apoptosis. These results indicate that adenosine uptake plays an important role in adenosine-induced apoptosis in A2780, A2780CisR and HEY cells.

Furthermore, to examine if adenosine-induced apoptosis is caspase mediated, the caspase inhibitor QVD-OPh was incubated 1 h prior to adenosine administration. Simultaneously, PARP cleavage after adenosine treatment was examined by western blot analysis. Results are shown in Figure 6.27 and 6.28.

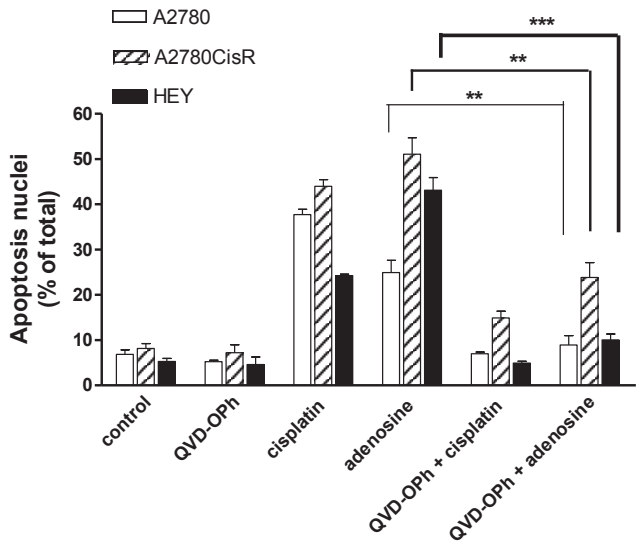


**Figure 6.27. Effect of the caspase inhibitor QVD-OPh on adenosine-induced apoptosis.**
20 µM of the caspase inhibitor QVD-OPh was added 1 h prior to 1000 µM of adenosine for 48 h. 10, 60 and 20 µM of cisplatin were incubated in A2780, A2780CisR, and HEY cell lines for 24 h, respectively. Apoptotic nuclei were analysed by flow cytometry. Control indicates untreated cells. Data shown are mean ± SEM from three-independent experiments. (**) and (***) indicate statistical significance compared to adenosine treatment in the absence of QVD-OPh, *P value* < 0.01 and < 0.001, respectively.

**A**

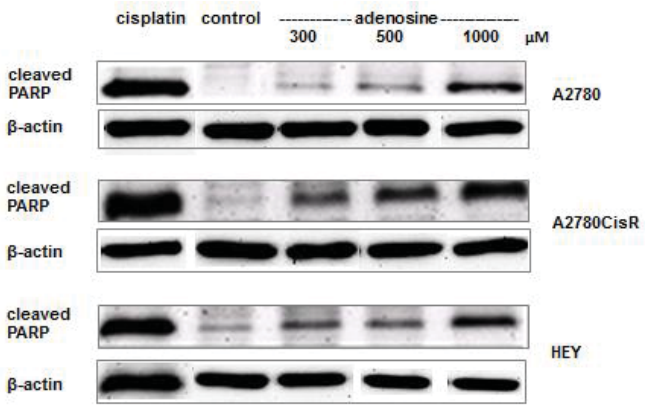

**B**

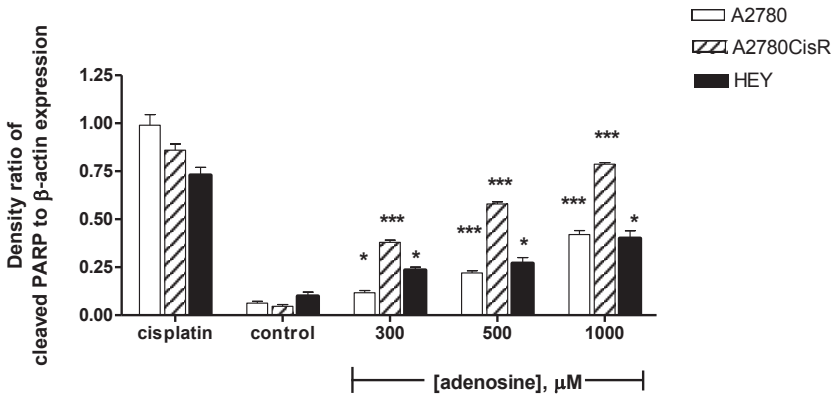


**Figure 6.28. Effect of adenosine on PARP cleavage in A2780, A2780CisR and HEY cell lines.**
(A) Protein expression of cleaved PARP at 24 kDa was detected after 300, 500 and 1000 µM adenosine treatment for 48 h in A2780, A2780CisR and HEY cell lines. 5-fold of cisplatin $IC_{50}$ of each cell line was incubated for 24 h and served as positive control. Control indicates untreated cells. Data shown are representative data from at least three-independent experiments. (B) Quantification of western blots by densitometric analysis and ratio calculation of protein bands of cleaved PARP and β-actin was performed. Data shown are mean ± SEM of density ratio of protein bands analyzed by ImageJ software from three-independent experiments. Statistical significance (*) and (***) was compared to untreated control, *P value* < 0.05 and < 0.001, respectively.

Figure 6.27 showed that QVD-OPh inhibits induction of apoptosis by adenosine similarly as it inhibits cisplatin-induced apoptosis known to be mediated via caspase pathways. Further confirmation that adenosine-induced apoptosis is mediated via caspase pathways came from western blots displaying a concentration-dependent increase in PARP cleavage upon adenosine treatment (Figure 6.28).

Next, the combination treatment of adenosine and cisplatin was assessed for induction of apoptosis compared to cisplatin alone treatment. To mimic the conditions used in MTT assay, 500 µM adenosine were incubated for 48 h prior to 24 h co-incubation of adenosine with a 3-fold $IC_{50}$ of cisplatin. .

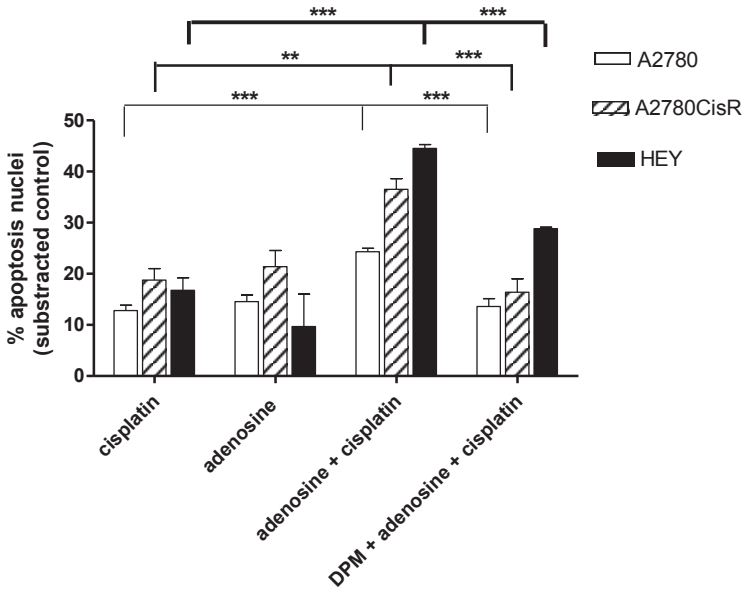


**Figure 6.29. Induction of apoptosis by a combination of adenosine and cisplatin in the presence or absence of dipyridamole.**

500 µM of adenosine was incubated for 48 h prior to 24 h co-incubation with 3-fold $IC_{50}$ of cisplatin in A2780, A2780CisR and HEY cell lines. 10 µM of dipyridamole was incubated 30 min before adenosine administration. The induction of apoptosis was analyzed by flow cytometry. Apoptotic nuclei in untreated control cells were subtracted from all data. Data shown are mean ± SEM from three-independent experiments. (**) and (***) indicate statistical significance compared to cisplatin alone treatment, *P value* < 0.01 and < 0.001, respectively.

Figure 6.29 showed that the induction of apoptosis achieved in combination treatments of adenosine and cisplatin is significantly higher than cisplatin alone treatment in all three cell lines. Moreover, dipyridamole is able to inhibit the adenosine-induced increase in apoptosis in combinations with cisplatin, confirming that adenosine uptake plays a crucial role in adenosine-induced apoptosis in ovarian cancer cells. Western blotting was used to analyse changesin PARP cleavage after combination treatment of adenosine and cisplatin. Results are shown in Figure 6.30.

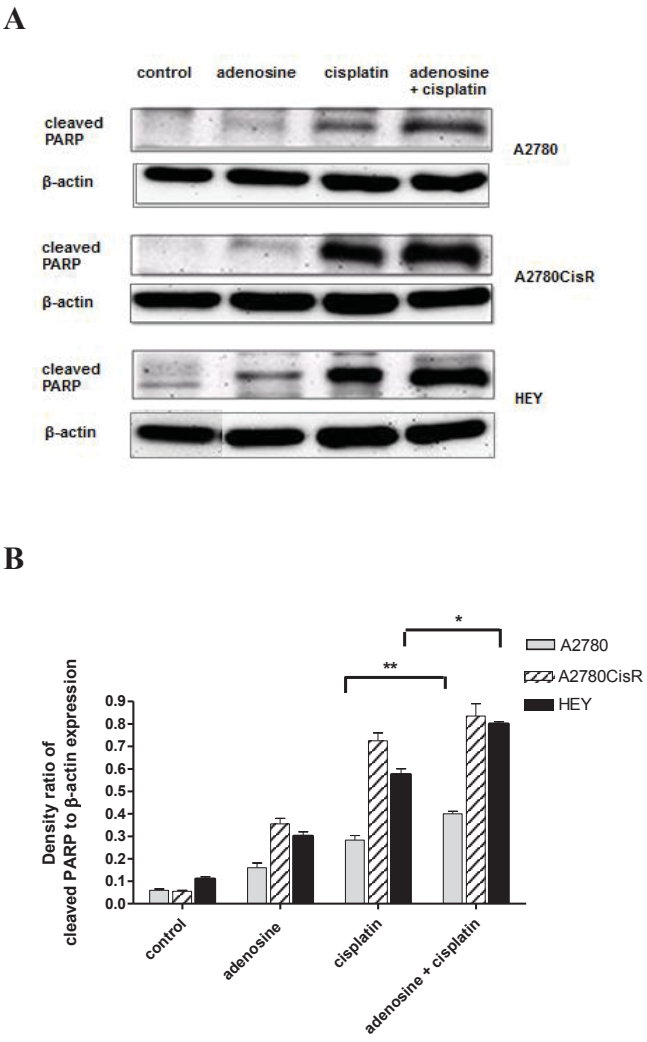


**Figure 6.30. Effect of adenosine in combination with cisplatin on PARP cleavage in A2780, A2780CisR, and HEY cell lines.** (A) Western blot analysis of cleaved PARP at 24 kDa after treatment with 500 µM adenosine for 48 h alone or in combination with 3-fold $IC_{50}$ of cisplatin for another 24 h in A2780, A2780CisR, and HEY cell lines. Control indicates untreated cells. Data shown are representative data from at least three-independent experiments. (B) Quantification of western blots by densitometric analysis and ratio calculation of protein bands of cleaved PARP and β-actin were performed. Data shown are mean ± SEM of density ratio of protein bands analyzed by ImageJ software from three-independent experiments. Statistical significance (*) and (**) was compared to cisplatin alone treatment, *P value* < 0.05 and < 0.01, respectively.

Figure 6.30 demonstrated that adenosine in combination with cisplatin significantly increases PARP cleavage compared to the effect of cisplatin alone in A2780 and HEY cell lines. In A2780CisR cells, this effect was not significant.

## 6.8 Intracellular adenosine activates the AMP-activated protein kinase (AMPK) pathway

The results of this study demonstrated so far that extracellular adenosine reduced proliferation and induced apoptosis and that a pretreatment with adenosine increased cisplatin cytotoxicity and apoptosis in all three examined ovarian cancer cell lines. Further, experiments with dipyridamole and adenosine receptor antagonists revealed that adenosine effects occur after adenosine uptake through nucleoside transporters and not via adenosine receptors. Thus, in the next step the effects of adenosine on AMP-activated protein kinase (AMPK) and downstream signaling were investigated. Results of AMPK activation by adenosine treatment are shown in Figure 6.31.

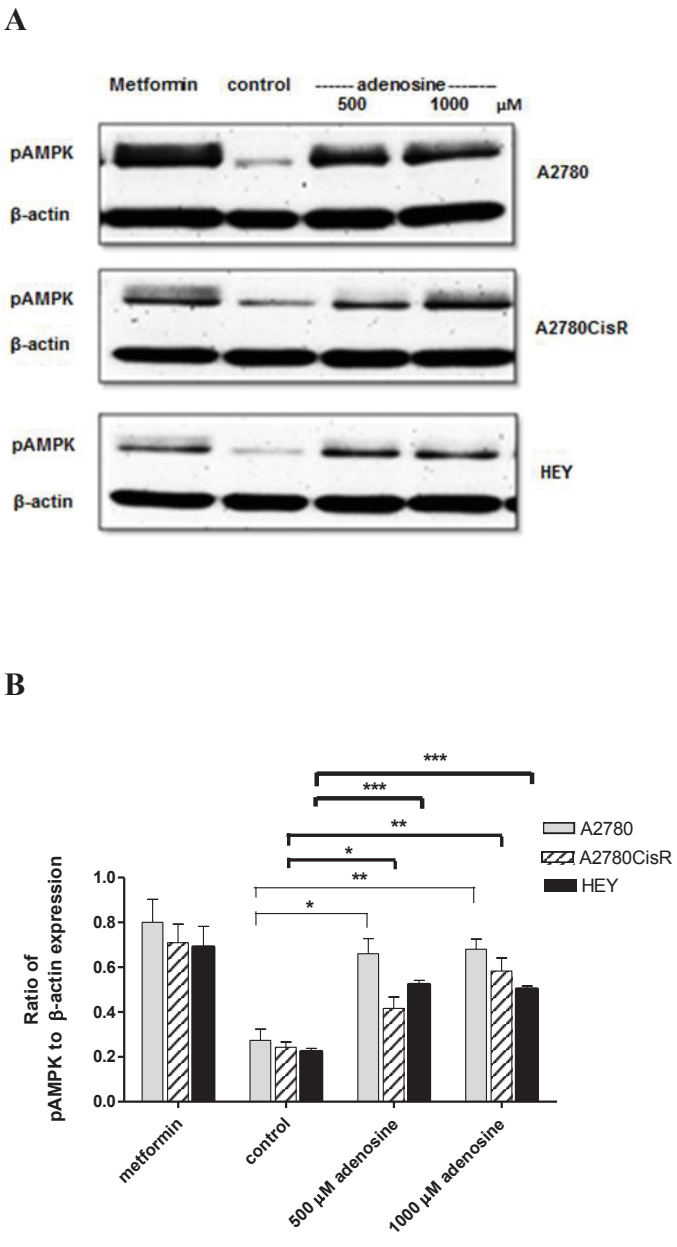

**Figure 6.31. Effect of adenosine on AMP-activated protein kinase (AMPK) activation.**
A2780, A2780CisR and HEY cell lines were incubated for 48 h with 500 or 1000 µM adenosine . After 48 h, phosphorylated AMPK (Thr172) protein was detected by western blotting (A). 30 mM of metformin was incubated for 24 h and served as positive control for AMPK activation. β-actin was used as loading control. Data shown are representative data from at least three-independent experiments. (B) Quantification of western blots by densitometric analysis and ratio calculation of protein bands of pAMPK and β-actin was performed. Data shown are mean ± SEM of density ratio of protein bands analyzed by ImageJ software from three-independent experiments. Statistical significance (*), (**) and (***) was compared to untreated control, *P value* < 0.05, < 0.01 and < 0.001, respectively.

Figure 6.31 showed that treatment for 48 h with adenosine increases the phosphorylation of AMPK at Thr172 in all three examined cell lines similarly to metformin known as AMPK activator [Dasgupta et al., 2016]. Phosphorylated AMPK (pAMPK), the activated form of AMPK, mediates inhibition of the mTOR1 complex by phosphorylation of Raptor [Gwinn et al., 2008]. Thus, the phosphorylation status of S6K (pS6K), a downstream target of mTOR1, was analyzed to unravel the intracellular pathway of the observed adenosine effects – from adenosine uptake over activation of AMPK over inhibition of mTOR1 to inhibition of phosphorylation of S6K. Results of S6K phosphorylation upon adenosine treatment are shown in Figure 6.32.

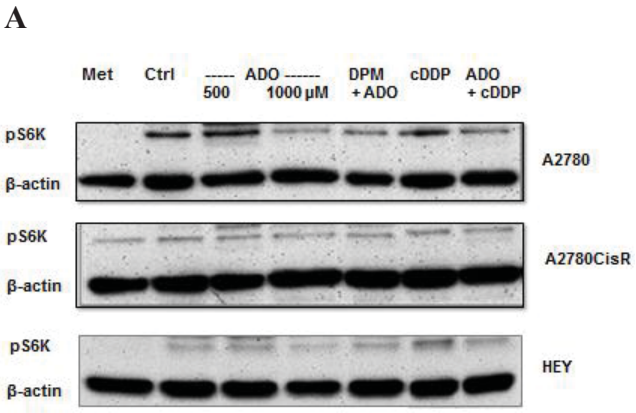

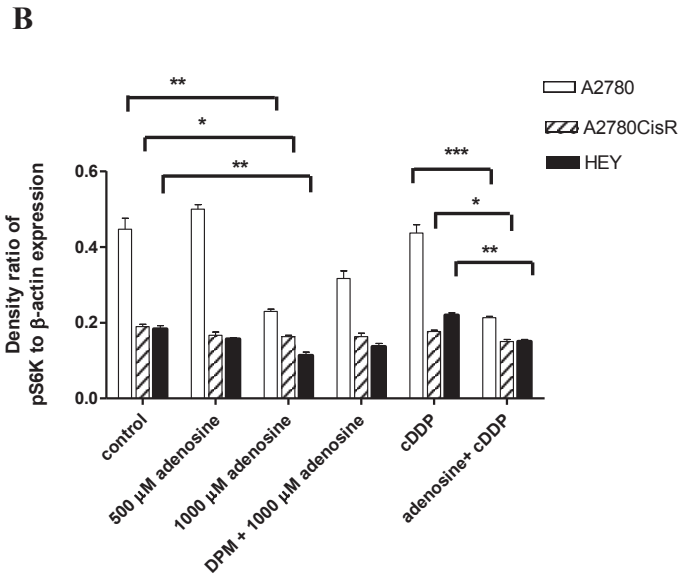


**Figure 6.32. Phosphorylation of S6K at Thr389 after treatment with adenosine alone or in combination with cisplatin in A2780, A2780CisR and HEY cell lines.**

(A) 500 and 1000 µM of adenosine in were incubated for 48 h in the presence or absence of 20 µM dipyridamole 30 min prior to adenosine administration. 3-fold $IC_{50}$ of cisplatin in each cell line was incubated for 24 h alone or in combination with 500 µM of adenosine for 48 h. Control indicates untreated cells. Data shown are representative data from at least two independent experiments. (B) Quantification of western blots by densitometric analysis and ratio calculation of protein bands of pS6K and β-actin was performed. Data shown are mean ± SEM of density ratio of protein bands analyzed by ImageJ software from three-independent experiments. Statistical significance (*), (**) and (***) was compared to untreated control, *P value* < 0.05, < 0.01 and < 0.001, respectively.

Figure 6.32 shows that pS6K was decreased under high dose (1000 µM) adenosine treatment compared to control. Adenosine-induced decrease of pS6K could partially be reversed by dipyridamole. Interestingly, whereas cisplatin has no effect on pS6K (approximately same intensity as untreated control), the combination of adenosine and cisplatin decreases pS6K. Thus, adenosine treatment in ovarian cancer cells leads to activation of AMPK and subsequent inhibition of mTOR1 as estimated by decrease of pS6K. Noteworthy, treatment-induced changes in pS6K were strongest in A2780 whereas slight but still significant differences occurred in HEY and A2780CisR cells. This could partially explain the stronger effect of adenosine in cisplatin sensitization in A2780 compared to A2780CisR and HEY cells (shift factors in Table 6.6).

## 6.9 Effect of adenosine on the HEK293 cell line

The HEK293 cell line was included in the study in order to discriminate the effect of adenosine in tumor cells from non-tumor cells. Adenosine treatment was applied to HEK293 cells in the same experimental setting as to the ovarian cancer cell lines. The ability of adenosine to enhance cisplatin cytotoxicity and induction of apoptosis were analyzed by MTT assay and apoptosis assay using 100, 300 and 500 μM of adenosine alone or in combination with cisplatin. Results are shown in Figure 6.33 and 6.34.

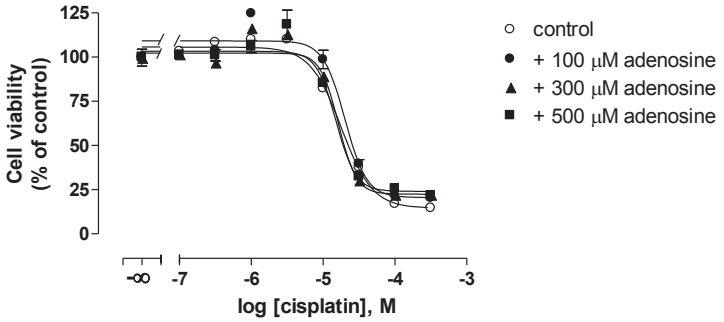


| | $pIC_{50}$ ± SEM | Shift factor |
|---|---|---|
| Control | 4.75 ± 0.04 | - |
| + 100 μM adenosine | 4.70 ± 0.07 | 0.87 |
| + 300 μM adenosine | 4.79 ± 0.06 | 1.09 |
| +500 μM adenosine | 4.82 ± 0.06 | 1.18 |

**Figure 6.33 Concentration-effect curves of cisplatin in the absence or presence of adenosine in HEK293 cells and resulting shift factors.**

Concentration-effect curves including a summary of $pIC_{50}$ ± SEM values and shift factors derived from combination treatment of adenosine and cisplatin in the non-cancer HEK293 cell line. 100, 300 and 500 μM of adenosine were incubated 48 h prior to 72 h co-incubation with increasing concentrations of cisplatin. Control indicates treatment with cisplatin alone. Data shown are mean ± SEM from a typical experiment out of a set of three, each performed in triplicate.

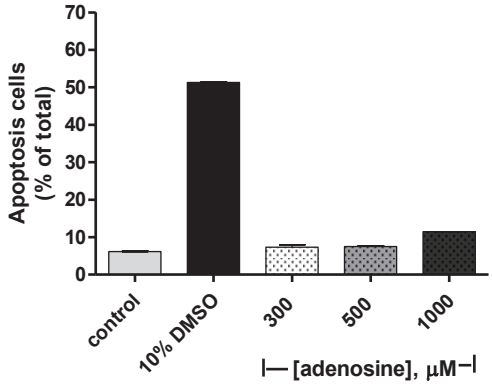


**Figure 6.34. Induction of apoptosis by adenosine in HEK293 cells.**
300, 500 and 1000 µM of adenosine were incubated for 48 h in HEK293 cells. Then, cells were analyzed by flow cytometry. Control indicates untreated cells, and DMSO was used as positive control. Data shown are mean ± SEM from three-independent experiments.

The concentration-effect curves shown in Figure 6.33 exhibited that the combination treatment of adenosine and cisplatin even at the highest concentration of adenosine is not able to significantly increase $pIC_{50}$ values of cisplatin in HEK293 cells. Moreover, adenosine does not induce apoptosis up to 500 µM, and at 1000 µM adenosine only a slight increase in apoptotic cells can be detected (Figure 6.34) whereas 1000 µM adenosine massively induced apoptosis in ovarian cancer cells (Figure 6.25).Taken together, these results indicate the ability of adenosine to increase cisplatin-induced cytotoxicity and induction of apoptosis selectively in ovarian cancer cells and not in non-tumor cells.

# 7. Discussion

## 7.1 Effects of ATP in ovarian cancer cells

Extracellular ATP concentrations are higher in cancer microenvironment than in normal tissue [Pellegatti et al., 2008 and Di Virgilio et al., 2017], leading to an intensive study of the role of ATP in several kinds of cancer. ATP is known as agonist for many subtypes of P2 receptors including $P2Y_2$, $P2Y_{11}$ and most P2X receptors [White et al., 2006]. Among all subtypes of P2 receptors, most studies suggest $P2Y_2$ receptors to be involved in cancer cell growth, proliferation and cell death [Stagg et al., 2010]. There is evidence of $P2Y_2$ receptor overexpression in colon cancer and pancreatic cancer [Kunzli et al., 2007 and Nylund et al., 2007]. Activation of $P2Y_2$ receptors can lead to an increase in cell growth in many types of cancer such as melanoma and lung cancer [Schafer et al., 2003 and White et al., 2005]. A study in breast cancer reported that highly metastatic breast cancer cells displayed high levels of ATP leading through activation of $P2Y_2$ receptors to increased cell proliferation, cell invasion through endothelial cells, increased matrix metalloproteinase-9 (MMP-9) activity and vascular endothelial growth factor (VEGF) production [Jin et al., 2014]. In addition, $P2Y_2$ receptor knockdown abolished ATP effects, confirming an involvement of $P2Y_2$ receptors. These results suggested that $P2Y_2$ receptors may play an important role in cancer metastasis via modulation of the crosstalk between cancer cells and endothelial cells [Jin et al., 2014]. Conversely, it is reported that in some cancers such as esophageal cancer and colorectal cancer, an activation of $P2Y_2$ receptors resulted in a decrease of cell proliferation [Hopfner et al., 2001 and Maaser et al., 2002].

Considering the diversity of P2 receptor signaling and role of ATP in cancers, this thesis evaluated the role of ATP and its effects on the sensitivity of ovarian cancer cells towards cisplatin. PCR and western blotting were used to characterize the expression of P2 receptors in A2780 cells and its cisplatin-resistant subline A2780CisR. $P2Y_1$, $P2Y_2$, $P2Y_{11}$, $P2Y_{13}$ and $P2X_4$ receptors were found to be expressed in both cells. $P2Y_6$ receptors were expressed only in A2780 cells while $P2X_7$ receptors were detected only in the A2780CisR cells (Figure 6.1 and 6.2). ATP increased the concentration of intracellular calcium in a concentration-dependent manner, assuming functionally active P2 receptors (Figure 6.5B). The inhibitory effect of the non-selective P2 receptor antagonist suramin on ATP-induced increase in

intracellular calcium confirmed that ATP signaling was mediated via P2 receptors (Figure 6.6B). More specifically, the selective $P2Y_2$ receptor antagonist AR-C118925 inhibited ATP-induced increase in intracellular calcium whereas other selective receptor antagonists for $P2Y_1$, $P2Y_{11}$, $P2X_4$ and $P2X_7$ receptors did not show any inhibitory effects (Figures 6.7, 6.8 and 6.9B). These findings indicated that $P2Y_2$ receptors are functionally active and responsible for ATP-induced P2 receptor activation in ovarian cancer cell lines. In accordance to a recent study reporting that $P2Y_2$ receptors are expressed and functionally active in the ovarian cancer cells SKOV-3 [Robels-Martinez et al., 2017], the data from this thesis support a favorite role of $P2Y_2$ receptors in ovarian cancer cells over other subtypes of P2 receptors. Noteworthy, the functional activity of P2 receptors in the cisplatin-resistant cell line A2780CisR was lower than in the parental A2780 cell line (Figure 6.10) and not significantly different from untreated cells, possibly due to lower expression or lower functional activity of P2 receptors in the cisplatin-resistant cell line.

Next, the cytotoxicity of ATP in A2780 and A2780CisR cells was evaluated using MTT cell viability assay. After 72 h of ATP incubation, cell viability was decreased by 30% to 50% in comparison to untreated control (Figure 6.14), indicating that ATP has low cytotoxicity in A2780 and A2780CisR cell lines. However, these results are in contrast to previous studies describing that ATP signaling via $P2Y_2$ receptors induced cell proliferation in ovarian cancer cells [Popper et al., 1993 and Schultze-Mosgau et al., 2000]. In this thesis, 500 µM of ATP for 48 h induced cell cycle arrest in S-phase (Figure 6.24) and slightly induced apoptosis (Figure 6.25A). These results are in agreement with other studies in human umbilical vein endothelial cells (HUVECs) and human aortic endothelial cells (HAECs), reporting that treatment with ATP did not induce apoptosis but instead induced cell cycle arrest in S-phase [Xiao et al., 2011].

The most important finding in this part of the thesis is the enhancing effect of ATP on cisplatin cytotoxicity. The combination treatment of ATP and cisplatin (500 µM of ATP for 48 h prior to 72 h co-incubation with cisplatin) significantly decreased the $IC_{50}$ values of cisplatin compared to cisplatin treatment alone, resulting in a mean shift factor of around 3 in parental A2780 cells and a lower shift factor of 2 in A2780CisR cells (Figure 6.15C and Table 6.3). Even though these shift factors are rather low, they are in the range of resistance factors of ovarian cancer cells against cisplatin and clinically meaningful [Eckstein et al., 2009 and Engelke et al., 2016]. Interestingly, simultaneous incubation of ATP and cisplatin in A2780 or A2780CisR cells did not decrease the $IC_{50}$ values of cisplatin (Figure 6.15C).

Presence of the selective $P2Y_2$ receptor antagonist AR-C118925 prior to combination treatment of ATP and cisplatin did however not inhibit ATP-enhanced cisplatin cytotoxicity (Figure 6.16 and Table 6.4), indicating that $P2Y_2$ receptors are not involved in the ATP-enhanced cisplatin cytotoxicity in ovarian cancer cells. On the other hand, presence of the nucleoside transporter inhibitor dipyridamole completely abrogated ATP-enhanced cisplatin cytotoxicity in A2780 and A2780CisR cells (see Figure 6.17 and Table 6.5). This result suggests that ATP-enhanced cisplatin cytotoxicity occurred after degradation of ATP to adenosine by ectonucleotidases CD39 and CD73 [Montalban et al., 2016] and subsequent intracellular adenosine uptake but not via functionally active P2 receptors. These data are in accordance with a study in cervical cancer cells reporting that an uptake of adenosine played an essential role for ATP cytotoxicity [Mello et al., 2014]. The importance of adenosine uptake after degradation of ATP throws light on the role of adenosine and the activity of ectonucleotidases highly expressed in ovarian cancer cells [Montalban et al., 2016] and excludes a major role of P2 receptor signaling.

## 7.2 Effects of adenosine in ovarian cancer cells

Based on the appealing role of adenosine in the combination treatment of ATP and cisplatin discussed in topic 7.1 and literature studies addressing the effects of adenosine on growth, proliferation and death of different cancer cells including ovarian cancer, the second part of this thesis studied how adenosine alone and in combination with cisplatin exerts cytotoxic effects in ovarian cancer cells with different cisplatin sensitivity. Cisplatin-sensitive A2780 cells, moderate cisplatin-sensitive HEY cells and cisplatin-resistant A2780CisR cells served as models for ovarian cancer cells. The term cisplatin-sensitive, moderate-sensitive and resistant were defined by their $IC_{50}$ values of cispatin shown in Table 6.6. A1, A2A and A2B adenosine receptors were found to be expressed by PCR and western blotting whereas A3 receptors could not be detected. A cAMP reporter gene assay confirmed functionally active A1 and A2B receptors by using the selective A1 and A2B receptor antagonists SLV320 and PSB603, respectively (Figure 6.12A and 6.12B) whereas the selective A2A antagonist SCH442416 had no effect (Figure 6.12C), suggesting lack of functional signaling of A2A receptors in the examined cell lines. In accordance to this thesis, expression and functional activity of A2B receptors was also found in OVCAR-3, Caov-4 and SKOV-3 ovarian cancer cells [Hajiahmadi et al., 2015(a)].

In A2780, A2780CisR, and HEY cells, adenosine displayed concentration-dependent cytotoxicity (Figure 6.18) and induction of caspase-mediated apoptosis shown by an increase in apoptotic nuclei (sub G1), PARP-cleavage and by using the caspase inhibitor QVD-OPh (Figure 6.25B, 6.27 and 6.28). These results are in agreement with a study by Shirali et al. demonstrating that adenosine significantly inhibited ovarian cancer OVCAR-3 cell proliferation in a concentration–dependent manner by inducing cell cycle arrest in G0/G1 phase, induction of apoptosis including down-regulation of Bcl-2, up-regulation of Bax and activation of caspase-3 [Shirali et al., 2013]. In another study, NECA, a non-selective adenosine analog, inhibited cell growth and induced apoptosis in ovarian cancer cells by activation of caspase-3 and loss of mitochondrial membrane potential. In addition, down-regulation of Bcl-2 and up-regulation of Bax were also observed [Hajiahmadi et al., 2015(b)]. Conversely, it is reported that activation of adenosine receptors, mainly A2B receptors induced cell growth and proliferation in several prostate cancer cell lines (PC-3, DU145 and LNCaP). Treatment with NECA and the selective A2B receptor agonist BAY60-6583 increased cell proliferation in a concentration-dependent manner. The involvement of A2B receptors was confirmed by siRNA knockdown of A2B receptors and the selective A2B receptor antagonist PSB603 diminishing NECA-induced cell proliferation [Wei et al., 2013]. A1 receptors were found to be overexpressed in primary breast cancer tissues and their activation enhanced breast cancer cell proliferation [Mirza et al., 2005]. Further, activation of A2A receptors on endothelial cells significantly enhanced tumor angiogenesis [Ahmad et al., 2009]. A2A receptor activation can further protect cancer cells from cytotoxic T cells [Ohta et al., 2006] and results in tumor immune escape [Leone et al., 2015].

Above mentioned adenosine-cancer studies emphasize adenosine signaling via adenosine GPCRs. In contrast, in this thesis it was demonstrated that adenosine-induced cytotoxicity and apoptosis were significantly inhibited by the nucleoside transporter inhibitor dipyridamole whereas the selective A1 and A2B receptor antagonists SLV320 and PSB603 had no effects (Figure 6.20 and 6.26). These results are supported by studies describing adenosine effects through adenosine receptor-independent pathways. Virtanen et al. found that treatment with low micromolar concentrations of adenosine inhibited cell invasion and migration in breast and prostate cancer cells. These inhibitory effects occurred via intrinsic receptor-independent mechanisms despite the abundant expression of A2B adenosine receptors [Virtanen et al., 2014]. Another study in cervical cancer cells reported that dipyridamole almost totally prevented the cytotoxic effect of adenosine. Moreover, induction of apoptosis, PARP cleavage and induction of autophagy by adenosine were also inhibited by

dipyridamole [Mello et al., 2014]. Further, a study in the hepatoma cell lines HuH-7 and HepG2 demonstrated that dipyridamole could prevent adenosine-induced apoptosis and cytotoxicity [Yang et al., 2011 and Wu et al., 2006]. Similarly, adenosine-induced apoptosis in gastric cancer cell lines GT3-TKB, MKN28 and MKN45 was inhibited by dipyridamole while it was not affected by inhibitors of adenosine receptors [Soitoh et al., 2004 and Tsuchiya et al., 2015].

According to the literature, intracellular adenosine is converted to AMP by adenosine kinase, leading to an increase in the AMP/ATP ratio. AMP or ADP bind to the γ subunits of AMPK and induce conformational changes of catalytic α subunits allowing phosphorylation at Thr172 in α1 and α2 by the LKB1 upstream kinase [Dasgupta et al., 2016]. In this thesis, a significant increase in phosphorylated AMPK (pAMPK) at Thr172 was observed after adenosine treatment, indicating an activation of AMPK (Figure 6.31). Further, high concentrations of adenosine (1000 μM) significantly decreased phosphorylated S6K (pS6K) at Thr389, suggesting an inhibition of mTOR which could be partially reversed by dipyridamole (Figure 6.32).

These findings may obtain significance since adenosine acts as a dual-edged sword: whereas adenosine can inhibit cancer cell growth and induces apoptosis, adenosine may also suppress anti-cancer immune response via A2A receptor stimulation in immune cells [Ohta et al., 2006]. If thus adenosine mediates cell growth inhibition and apoptosis induction after intracellular uptake and not via G protein-coupled adenosine receptors, this may open a dual strategy using A2A antagonists for immune cell-mediated cancer cell removal [Ohta et al., 2006 and Montalban Del Barrio et al., 2016] and short-term adenosine treatment to inhibit cancer cell growth and to induce apoptosis after adenosine uptake into cancer cells.

The most important finding of this study is however that adenosine treatment of ovarian cancer cells acts in a synergistic manner with cisplatin which is pharmacodynamically equivalent to the clinically used carboplatin (Figure 6.19 and Table 6.6). Presence of adenosine significantly enhanced cisplatin-induced cytotoxicity by decreasing the $IC_{50}$ of cisplatin by a factor of up to 4 (Figure 6.19D). This was confirmed in MTT assay, PARP cleavage, apoptosis induction, and combination index (CI) analysis according to Chou-Talalay [Chou, 2006] (Table 6.7). In addition, mTOR inhibition as observed by a decrease in pS6K did not occur upon cisplatin treatment alone but upon the combination of adenosine and cisplatin (Figure 6.32).

Interestingly, the synergistic effect between adenosine and cisplatin was more pronounced in A2780 cells, showing the highest sensitivity against cisplatin, than in HEY or A2780CisR

cells (Figure 6.19D). This finding could indicate that a co-treatment of cisplatin with adenosine should start early to maintain a high sensitivity of cisplatin and possibly prevent the development of cisplatin resistance in ovarian cancer cells. Noteworthy, the synergistic effects of adenosine and cisplatin did not occur in the non-cancer cell line HEK293, indicating some selectivity of adenosine effects on cisplatin sensitization for cancer over non-cancer cells (Figure 6.33 and 6.34).

In conclusion, the second part of this thesis reveals that adenosine acts synergistically with cisplatin in ovarian cancer cell lines and improves the chemosensitivity of cisplatin in an adenosine receptor-independent pathway by adenosine uptake with subsequent AMPK activation and mTOR inhibition. This may open a novel strategy to prevent / delay the development of platinum resistance and overall improve the treatment of ovarian cancer.

# 8. Conclusions

The present study emphasized the role of the purinergic ligands ATP and adenosine in order to reinforce the sensitivity of cisplatin, a pharmacodynamically equivalent chemotherapeutic agent to carboplatin currently used as first-line chemotherapy for ovarian cancer treatment [Coward et al., 2015]. Adenosine has been identified as the metabolite responsible for ATP effects. Adenosine enhances cisplatin cytotoxicity in ovarian cancer cells via a purinergic receptor-independent pathway. After intracellular uptake, adenosine activates AMPK and inhibits mTOR, leading to inhibition of cell growth and induction of apoptosis. These findings suggest a beneficial role of adenosine for cisplatin or carboplatin treatment of ovarian cancer. Due to the rather short exposure times with cisplatin in clinical treatment cycles, there is no need for long-term co-treatment with adenosine, thus avoiding detrimental immunological effects [Ohta et al., 2006]. The summarized findings from this current study are shown in Figure 8.1.

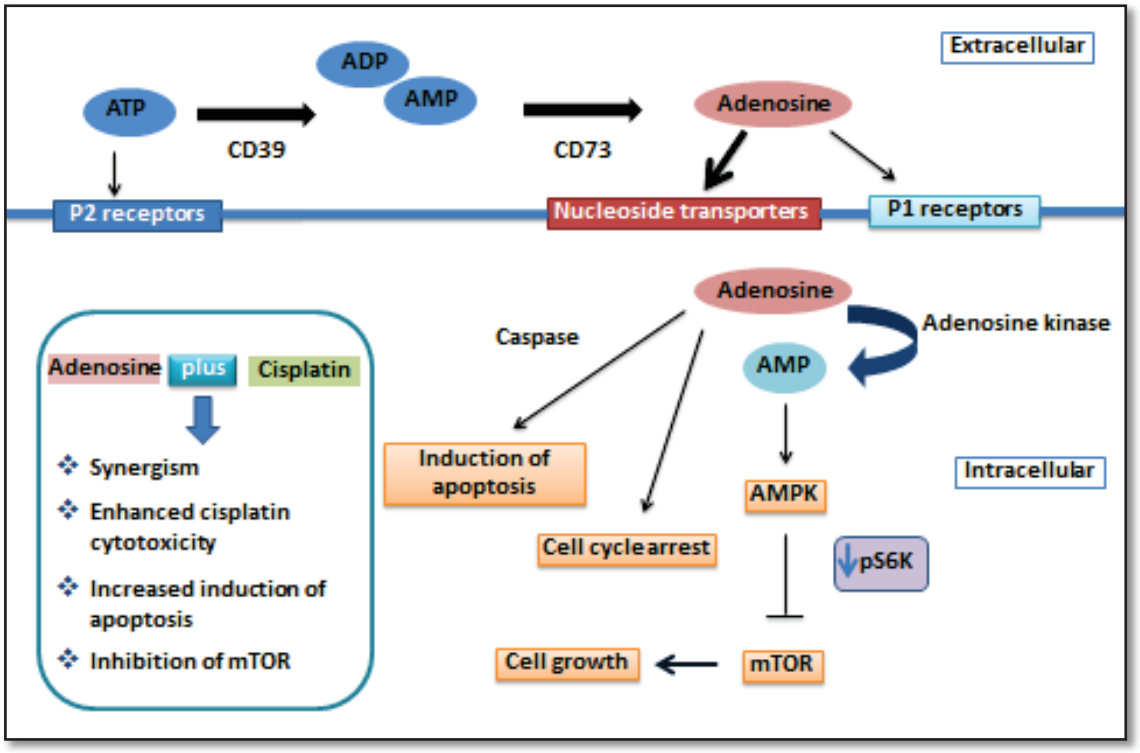


**Figure 8.1 Summary results of the study**

# References


1. Abbracchio M, Jacobson KA, Burnstock G, et al. P2Y receptors, introduction. Last modified on 07/02/2017. Accessed on 06/09/2017. IUPHAR/BPS Guide to PHARMACOLOGY,http://www.guidetopharmacology.org/GRAC/FamilyIntroductionForward?familyId=52.

2. Abu-Jawdeh GM, Faix JD, Niloff J, et al. Strong expression of vascular permeability factor (vascular endothelial growth factor) and its receptors in ovarian borderline and malignant neoplasms. Lab Invest. 1996; 74(6): 1105-1115.

3. Adenolfi E, Melchiorri L, Falzoni S, et al. P2X7 receptor expression in evolutive and indolent forms of chronic B lymphocytic leukemia. Blood. 2002; 99: 706-708.

4. Aebi S, Kurdi-Haidar B, Gordon R, et al. Loss of DNA mismatch repair in acquired resistance to cisplatin. Cancer Res. 1996; 56: 3087–3090.

5. Agarwal R, Kaye SB. Ovarian cancer: strategies for overcoming resistance to chemotherapy. Nature reviews Cancer. 2003;3(7):502-16.

6. Alvero AB, O'Malley D, Brown D, et al. Molecular mechanism of phenoxodiol-induced apoptosis in ovarian cancinoma cells. Cancer. 2006; 106(3): 599-608.

7. Appleyard MV, Murray KE, Coates PJ, Wullschleger S, Bray SE, Kernohan NM, et al. Phenformin as prophylaxis and therapy in breast cancer xenografts. British journal of cancer. 2012;106(6):1117-1122.

8. Asoh K, Saburi Y, Sato S, et al. Potentiation of some anticancer agents by dipyridamole against drug-sensitive and drug-resistant cancer cell lines. Jpn J Cancer Res. 1989; 80(5): 475-481.

9. Baldwin SA, Beal PR, Yao SY, et al.The equilibrative nucleoside transporter family, SLC29. Pflugers Arch.2004; 735-743.

10. Baur JA, Pearson KJ, Price NL, Jamieson HA, Lerin C, Kalra A, Prabhu VV et al. Resveratrol improves health and survival of mice on a high-calorie diet. Nature 2006, 444: 337–342.

11. Bhoola S, Hoskins WJ. Diagnosis and management of epithelial ovarian cancer. Obstetrics and gynecology. 2006;107(6):1399-1410.

12. Blay J, White TD, Hoskin DW. The extracellular fluid of solid carcinomas contains immunosuppressive concentrations of adenosine.Cancer Res. 1997; 57(13): 2602-2605.

13. Bookman MA, Greer BE, Ozols RF. Optimal therapy of advanced ovarian cancer: Carboplatin and paclitaxel vs. cisplatin and paclitaxel (GOG 158) and an update on GOG0 182-ICON5. Int Gynecol Cancer 2003;136:735-740.

14. Bristow RE, Tomacruz RS, Armstrong DK, Trimble EL, Montz FJ. Survival effect of maximal cytoreductive surgery for advanced ovarian carcinoma during the platinum era: a meta-analysis. Journal of clinical oncology. 2002; 20(5):1248-1259.

15. Brozovic A, Fritz G, Christmann M, et al. Long-term activation of SAPK/JNK, p38 kinase and fas-L expression by cisplatin is attenuated in human carcinoma cells that acquired drug resistance. Int J Cancer. 2004; 112:974–985.

16. Burger RA, Sill MW, Monk BJ, Greer BE, Sorosky JI. Phase II trial of bevacizumab in persistent or recurrent epithelial ovarian cancer or primary peritoneal cancer: a Gynecologic Oncology Group Study. J Clin Oncol. 2007; 25(33):5165–5171.

17. Burnstock G. Pathophysiology and therapeutic potential of purinergic signaling. Pharmacological reviews. 2006;58(1):58-86.

18. Cannistra SA. Cancer of the ovary. The New England journal of medicine. 2004;351(24):2519-2529.

19. Characterization of [3H] LUF5834: A novel non-ribose high-affinity agonist radioligand for the adenosine A1 receptor.

20. Cherry C, Vacchiano SA. Ovarian cancer screening and prevention. Seminars in oncology nursing. 2002;18(3):167-173.

21. Colombo N, Van Gorp T, Parma G, Amant F, Gatta G, Sessa C, et al. Ovarian cancer. Critical reviews in oncology/hematology. 2006;60(2):159-179.

22. Cooper BC, Ritchie JM, Broghammer CL, et al. Preoperative serum vascular endothelial growth factor levels: significance in ovarian cancer. Clin Cancer Res. 2002; 8(10): 3193-3197.

23. Coutinho-Silva R, Stahl L, Cheung KK, et al. P2X and P2Y purinergic receptors on human intestinal epithelial carcinoma cells: effects of extracellular nucleotides on apoptosis and cell proliferation. Am J Physiol Gastrointest Liver Physiol. 2005; 288(5):G1024-1035.

24. Coward JI, Middleton K, Murphy F. New perspectives on targeted therapy in ovarian cancer. Int J Womens Health. 2016; 7: 189-203.

25. Crute BE, Seefeld K, Gamble J, Kemp BE, Witters LA. Functional domains of the alpha1 catalytic subunit of the AMP-activated protein kinase. The Journal of biological chemistry. 1998; 273(52):35347-35354.

26. da Silva GC, Jarzyna R, Specht A and Kaczmarek E. Extracellular nucleotides and adenosine independently active AMP-activated protein kinase in endothelial cells; involvement of P2 receptor and adenosine transporters. Cir Res.2006; 98:e39-e47.

27. Dasgupta B, Chhipa RR. Evolving lessons on the complex role of AMPK in normal physiology and cancer. Trends in pharmacological sciences. 2016; 37(3):192-206.

28. Dasgupta B, Ju JS, Sasaki Y, Liu X, Jung SR, Higashida K, et al. The AMPK beta2 subunit is required for energy homeostasis during metabolic stress. Molecular and cellular biology. 2012;32(14):2837-2848.

29. Dasgupta B, Milbrandt J. Resveratrol stimulates AMP kinase activity in neurons. Proceedings of the National Academy of Sciences of the United States of America. 2007;104(17):7217-7222.

30. Davies SP, Hawley SA, Woods A, Carling D, Haystead TA, Hardie DG. Purification of the AMP-activated protein kinase on ATP-gamma-sepharose and analysis of its subunit structure. European journal of biochemistry. 1994; 223(2):351-357.

31. De Geest K, Blessing JA, Morris RT, et al. Phase II clinical trial of ixabepilone in patients with recurrent or persistent platinum- and taxane-resistant ovarian or primary peritoneal cancer: a gynecologic oncology group study. J Clin Oncol. 2010; 28(1): 149-153.

32. Di Virgilio F, Adinolfi E. Extracellular purines, purinergic receptors and tumor growth. Oncogene. 2017; 36(3):293-303.

33. Doubeni CA, Doubeni AR, Myers AE. Diagnosis and Management of Ovarian Cancer. American family physician. 2016;93(11):937-944.

34. du Bois A, Luck HJ, Meier W, et al. A randomized clinical trial of cisplatin/paclitaxel versus carboplatin/paclitaxel as first-line treatment of ovarian cancer.J Natl Cancer Inst 2003;3(95):1320-1329.

35. Eckstein N, Servan K, Hildebrandt B, et al. Hyperactivation of the insulin-like growth factor receptor I signaling pathway is an essential event for cisplatin resistance of ovarian cancer cells. Cancer Res. 2009; 69(7): 2996-3003.

36. Edmondson RJ, Monaghan JM. The epidemiology of ovarian cancer. International journal of gynecological cancer. 2001;11(6):423-429.

37. Engelke LH, Hamacher A, Proksch P, Kassack MU. Ellagic Acid and Resveratrol Prevent the Development of Cisplatin Resistance in the Epithelial Ovarian Cancer Cell Line A2780. J Cancer. 2016; 7(4):353-363.

38. Etique N, Grillier-Vuissoz I, Lecomte J, et al. Crosstalk between adenosine receptor (A2A isoform) and ERalpha mediates ethanol action in MCF-7 breast cancer cells. Oncol Rep. 2009; 21(4): 977-981.

39. Falzoni S, Donvito G, Di Virgilio F. Detecting adenosine triphosphate in pericellular space. Interface Focus. 2013; 3:20120101.

40. Farmer H, McCabe N, Lord CJ, et al. Targeting the DNA repair defect in BRCA mutantcells as a therapeutic strategy. Nature. 2005; 434: 917–921.

41. Fink D, Aebi S, Howell SB. The role of DNA mismatch repair in drug resistance. Clin Cancer Res. 1998; 4: 1–6.

42. Fogarty S, Hawley SA, Green KA, Saner N, Mustard KJ, Hardie DG. Calmodulin-dependent protein kinase kinase-beta activates AMPK without forming a stable complex: synergistic effects of $Ca2^{+}$ and AMP. The Biochemical journal. 2010; 426(1):109-118.

43. Galluzzi L, Senovilla L, Vitale I, Michels J, Martins I, Kepp O, et al. Molecular mechanisms of cisplatin resistance. Oncogene. 2012;31(15):1869-1883.

44. Galluzzi L, Vitale I, Michels J, et al. Systems biology of cisplatin resistance: past, present and future. Cell Death Dis. 2014; 5:e1257.

45. Ge SM, Zhan DL, Zhang SH, et al. Reverse screening approach to identify potential anti-cancer targets of dipyridamole. Am J Tranl Res. 2016; 8(12): 5187-5198.

46. Gessi S, Merighi S, Sacchetto V, Simioni C, Borea PA. Adenosine receptors and cancer. Biochimica et biophysica acta. 2011;1808(5):1400-1412.

47. Goda AE, Yoshida T, Horinaka M, Yasuda T, Shiraishi T, Wakada M, Sakai T. Mechanisms of enhancement of TRAIL tumoricidal activity against human cancer cells of different origin bydipyridamole. Oncogene. 2008; 27:3435–3445.

48. Godwin AK, Meister A, O'Dwyer PJ, et al. High resistance to cisplatin in human ovarian cancer cell lines is associated with marked increase of glutathione synthesis. Proc Natl Acad Sci USA. 1992; 89(7): 3070-3074.

49. Gomez G, Nardone V, Lotfi-Emran S, Zhao W, Schwartz LB. Intracellular adenosine inhibits IgE-dependent degranulation of human skin mast cells. J Clin Immunol. 2013;33:1349–1359.

50. Gonzalez VM, Fuertes MA, Alonso C and Perez JM. Is cisplatininduced cell death always produced by apoptosis? Mol Pharmacol. 2001;59: 657–663.

51. Gordon AN, Schultes BC, Gallion H, et al. CA125 and tumor specific T-cell responses correlate with prolonged survival in oregovomab-treated recurrent ovarian cancer patients. Gynecol Oncol. 2004; 94(2): 340-351.

52. Gowans GJ, Hawley SA, Ross FA, Hardie DG. AMP is a true physiological regulator of AMP-activated protein kinase by both allosteric activation and enhancing net phosphorylation. Cell metabolism. 2013; 18(4):556-566.

53. Greenhalf W, Ghaneh P, Neoptolemos JP, et al. Pancreatic cancer hENT1 expression and survival from gemcitabine in patients from the ESPAC-3 trial. J Natl Cancer Inst2014; 106(1).

54. Gwinn DM, Shackelford DB, Egan DF, Mihaylova MM, Mery A, Vasquez DS, et al. AMPK phosphorylation of raptor mediates a metabolic checkpoint. Molecular cell. 2008; 30(2):214-226.

55. Hajiahmadi S, Panjehpour M, Aghaei M, Mousavi S. Molecular expression of adenosine receptors in OVCAR-3, Caov-4 and SKOV-3 human ovarian cancer cell lines. Res Pharm Sci. 2015; 10(1): 43-51**.(a)**

56. Hajiahmadi S, Panjehpour M, Aghaei M, Shabani M. Activation of A2b adenosine receptor regulates ovarian cancer cell growth: involvement of Bax/Bcl-2 and caspase-3. Biochem Cell Biol. 2015; 93(4): 321-329**.(b)**

57. Hawley SA, Gadalla AE, Olsen GS, Hardie DG. The antidiabetic drug metformin activates the AMP-activated protein kinase cascade via an adenine nucleotide-independent mechanism. Diabetes. 2002; 51(8):2420-2425.

58. Hanahan D, and Weinberg RA. Hallmarks of Cancer: The Next Generation. Cell. 2011; 144: 646-674.

59. Hengstler JG, Lange J, Kett A, et al. Contribution of c-erbB-2 and topoisomerase II alpha to chemoresistance in ovarian cancer. Cancer Res. 1999; 59: 3206–3214.

60. Hird V, Maraveyes A, Snook D, et al. Adjuvant therapy of ovarian cancer with radioactive monoclonal antibody. Br J Cancer. 1993; 68(2): 403-406.

61. Hoffman MS, Griffin D, Tebes S, Cardosi RJ, Martino MA, Fiorica JV, et al. Sites of bowel resected to achieve optimal ovarian cancer cytoreduction: implications regarding surgical management. American journal of obstetrics and gynecology. 2005;193(2):582-6; discussion 6-8.

62. Holschneider CH, Berek JS. Ovarian cancer: epidemiology, biology, and prognostic factors. Seminars in surgical oncology. 2000;19(1):3-10.

63. Hopfner M, Lemmer K, Jansen A, et al. Expression of functional P2-purinergic receptors in primary cultures of human colorectal carcinoma cells. Biochemical and biophysical research communications. 1998; 251(3): 811-817.

64. Humphreys BD, Rice J, Kertesy SB, et al. Stress-activated protein kinase/JNK activation and apoptotic induction by the macrophage P2X7 nucleotide receptor. J Biol Chem. 2000;275(35): 26792-26798.

65. Jemal A, Siegel R, Ward E, Murray T, Xu J, Thun MJ. Cancer statistics, 2007. CA: a cancer journal for clinicians. 2007;57(1):43-66.

66. Jin H, Eun SY, Lee JS, Park SW, Lee JH, Chang KC, et al. P2Y2 receptor activation by nucleotides released from highly metastatic breast cancer cells increases tumor growth and invasion via crosstalk with endothelial cells. Breast cancer research. 2014;16(5):R77.

67. Jordan P, Carmo-Fonseca M. Molecular mechanisms involved in cisplatin cytotoxicity. Cell Mol Life Sci. 2000; 57(8-9): 1229-1235.

68. Kalk P, Eggert B, Relle K, Godes M, Heiden S, Sharkovska Y, et al. The adenosine A1 receptor antagonist SLV320 reduces myocardial fibrosis in rats with 5/6 nephrectomy without affecting blood pressure. British journal of pharmacology. 2007; 151(7):1025-1032.

69. Kamsteeg M, Rutherford T, Sapi E, et al. Phenoxodiol-an isoflavone analog induces apoptosis in chemoresistant ovarian cancer cells. Oncogene. 2003; 22(17): 2611-2620.

70. Kazak L, Reyes A and Holt TJ. Minimizing the damage: repair pathways keep mitochondrial DNA intact. Nat Rev Mol Cell Biol. 2012; 13(10): 659-671.

71. Kelland LR. Preclinical perspectives on platinum resistance. Drugs. 2000. 59 (Suppl 4): 1–8; discussion 37-38.

72. Kelly MG, Mor G, Husband A, et al. Phase II evaluation of phenoxodiol in combination with cisplatin or paclitaxel in women with platinum/taxane-refractory/resistant epithelial ovarian, fallopian tube, or primary peritoneal cancers. Int J Gynecol Cancer. 2011; 21(4): 633-639.

73. Khalid M, Brisson L,Tariq M, et al. Carcinoma-specific expression of $P2Y_{11}$ receptor and its contribution in ATP-induced purinergic signalling and cell migration in human hepatocellular carcinoma cells. Oncotarget. 2017; 8:37278-37290.

74. Kim I, He YY. Targeting the AMP-Activated Protein Kinase for Cancer Prevention and Therapy. Frontiers in oncology. 2013;3:175.

75. Koberle B, Tomicic MT, Usanova S, Kaina B. Cisplatin resistance: preclinical findings and clinical implications. Biochim Biophys Acta. 2010; 1806: 172–182.

76. Kotsopoulos IC, Papanikolaou A, Lambropoulos AF, Papazisis KT, Tsolakidis D, Touplikioti P, et al. Serous ovarian cancer signaling pathways. International journal of gynecological cancer. 2014;24(3):410-417.

77. Koumenis C, Hammond E, Giaccia A. Tumor microenvironment and cellular stress: signaling, metabolism, imaging, and therapeutic targets. Preface. Advances in experimental medicine and biology. 2014; 772:v-viii.

78. Krasner CN, McMeekin DS, Chan S, et al. A Phase II study of trabectedin single agent in patients with recurrent ovarian cancer previously treated with platinum-based regimens. Br J Cancer. 2007; 97(12): 1618-1624.

79. Kumar V. Adenosine as an endogenous immunoregulator in cancer pathogenesis: where to go? Purinergic signal. 2013; 9(2):145–165.

80. Kuznetsov JN, Leclerc GJ, Leclerc GM, Barredo JC. AMPK and Akt determine apoptotic cell death following perturbations of one-carbon metabolism by regulating ER stress in acute lymphoblastic leukemia. Molecular cancer therapeutics. 2011;10(3):437-47.

81. Lane J, Martin TA, McGuigan C, et al. The differential expression of hCNT1 and hENT1 in breast cancer and the possible impact on breast cancer therapy. J Exp Ther Oncol. 2010; 8:203-210.

82. Leclerc GM, Leclerc GJ, Fu G, Barredo JC. AMPK-induced activation of Akt by AICAR is mediated by IGF-1R dependent and independent mechanisms in acute lymphoblastic leukemia. Journal of molecular signaling. 2010; 5:15.

83. Ledermann JA, Raja FA, Fotopoulou C, Gonzalez-Martin A, Colombo N, Sessa C. Newly diagnosed and relapsed epithelial ovarian carcinoma: ESMO Clinical Practice Guidelines for diagnosis, treatment and follow-up. Annals of oncology: official journal of the European Society for Medical Oncology. 2013;24 Suppl 6:vi24-32.

84. Legrand O, Simonin G, Perrot JY, Zittoun R, Marie JP. Pgp and MRP activities using calcein-AM are prognostic factors in adult acute myeloid leukemia patients. Blood. 1998; 91(12):4480-4488.

85. Lerner JP, Timor-Tritsch IE, Federman A, Abramovich G. Transvaginal ultrasonographic characterization of ovarian masses with an improved, weighted scoring system. American journal of obstetrics and gynecology. 1994;170(1 Pt 1):81-85.

86. Liang J, Mills GB. AMPK: a contextual oncogene or tumor suppressor? Cancer research. 2013;73(10):2929-2935.

87. Liu H, Scholz C, Zang C, Schefe JH, Habbel P, Regierer AC, et al. Metformin and the mTOR inhibitor everolimus (RAD001) sensitize breast cancer cells to the cytotoxic effect of chemotherapeutic drugs in vitro. Anticancer research. 2012; 32(5):1627-1637.

88. Liu S, Fang Y, Shen H, Xu W, Li H. Berberine sensitizes ovarian cancer cells to cisplatin through miR-21/PDCD4 axis. Acta Biochim Biophys Sin 2013, 45: 756–762.

89. Lux MP, Fasching PA, Beckmann MW. Hereditary breast and ovarian cancer: review and future perspectives. Journal of molecular medicine. 2006;84(1):16-28.

90. Ma XM, Blenis J. Molecular mechanisms of mTOR-mediated translational control. Nature reviews Molecular cell biology. 2009; 10(5):307-318.

91. Maaser K, Höpfner M, Kap H, et al. Extracellular nucleotides inhibit growth of human oesophageal cancer cells via $P2Y_2$ receptors. Br J Cancer. 2002; 86(4):636-644.

92. Mandic A, Hansson J, Linder S and Shoshan MC. Cisplatin induces endoplasmic reticulum stress and nucleus-independent apoptotic signaling. J Biol Chem. 2003; 278: 9100–9106.

93. Mansouri A, Ridgway LD, Korapati AL, et al. Sustained activation of JNK/p38 MAPK pathways in response to cisplatin leads to Fas ligand induction and cell death in ovarian carcinoma cells. J Biol Chem. 2003; 278: 19245–19256.

94. Mantia-Smaldone GM, Edwards RP and Vlad AM. Targeted treatment of recurrent platinum-resistant ovarian cancer: current and emerging therapies. Cancer Management and Research. 2011;3:25-38.

95. Martin C, Leone M, Viviand X, Ayem ML, Guieu R. High adenosine plasma concentration as a prognostic index for outcome in patients with septic shock. Crit Care Med. 2000; 28:3198–3202.

96. Martin VR. Ovarian cancer. Seminars in oncology nursing. 2002;18(3):174-183.

97. Mayer AR, Chambers SK, Graves E, Holm C, Tseng PC, Nelson BE, et al. Ovarian cancer staging: does it require a gynecologic oncologist? Gynecologic oncology. 1992;47(2):223-227.

98. McGuire WP. Hoskins WJ, Brady MF, et al. Cyclophosphamide and cisplatin compared with paclitaxel and cisplatin in patients with stage III and stage IV ovarian cancer. N Eng J Med. 1996; 334:1-6.

99. Mello Pde A, Filippi-Chiela EC, Nascimento J, Beckenkamp A, Santana DB, Kipper F, et al. Adenosine uptake is the major effector of extracellular ATP toxicity in human cervical cancer cells. Mol Biol Cell. 2014; 25(19): 2905-2918.

100. Merighi S, Mirandola P, Milani D, et al. Adenosine receptors as mediators of both cell proliferation and cell death of cultured human melanoma cells. J Invest Dermatol. 2002; 119(4): 923-933.

101. Miller DS, Blessing JA, Krasner CN, et al. Phase III evaluation of premetrexed in the treatment of recurrent or persistent platinum-resistant ovarian or primary peritoneal carcinoma: a study of the Gynecologic Oncology Group. J Clin Oncol. 2009; 27(16): 2686-2691.

102. Mirza A, Basso A, Black S, et al. RNA interference targeting of A1 receptor-overexpressing breast carcinoma cells leads to diminished rates of cell proliferation and induction of apoptosis. Cancer biology & therapy. 2005;4(12):1355-1360.

103. Mitchelhill KI, Stapleton D, Gao G, House C, Michell B, Katsis F, et al. Mammalian AMP-activated protein kinase shares structural and functional homology with the catalytic domain of yeast Snf1 protein kinase. The Journal of biological chemistry. 1994; 269(4):2361-2364.

104. More SS, Akil O, Ianculescu AG, Geier EG, et al. Role of the copper transporter, CTR1, in platinum-induced ototoxicity. J Neurosci. 2010; 30: 9500–9509.

105. Muggia FM, Hainsworth JD, Jeffers S, Miller P, Groshen S, Tan M, et al. Phase II study of liposomal doxorubicin in refractory ovarian cancer: antitumor activity and toxicity modification by liposomal encapsulation. Journal of clinical oncology. 1997;15(3):987-993.

106. Muñoz-Espín D, Cañamero M, Maraver A, et al. Programmed cell senescence during mammalian embryonic development. Cell. 2013; 155(5): 1104-1108.

107. Myers TJ, Brenaman LH, Stevenson M, et al. Mitochondrial reactive oxygen species mediate GPCR-induced TACE/ADAM17-dependent transforming growth factor-alpha shedding. Mol Biol Cell. 2009; 20: 5236-5249.

108. Neijt JP, Engelholm SA, Tuxen MK, et al. Exploratory Phase III study of paclitaxel and cisplatin versus placlitaxel and carboplatin in advanced ovarian cancer. J Clin Oncol 2000;18:3084-3092.

109. Nguyen HN, Averette HE, Hoskins W, Penalver M, Sevin BU, Steren A. National survey of ovarian carcinoma. Part V. The impact of physician's specialty on patients' survival. Cancer. 1993;72(12):3663-3670.

110. Nicholson S, Bomphray CC, Thomas H, et al. A phase I trial of idiotypic vaccination with HMFG1 in ovarian cancer. Cancer Immunol Immunother. 2004; 53(9): 809-819.

111. Noji T, Karasawa A, Kusaka H. Adenosine uptake inhibitors. European journal of pharmacology. 2004; 495(1):1-16.

112. Opipari AW Jr, Tan L, Boitano AE, Sorenson DR, Aurora A, Liu JR. Resveratrol-induced autophagocytosis in ovarian cancer cells. Cancer Res 2004, 64: 696–703.

113. Ozols R. Systemetic therapy for ovarian cancer: Current status and new treatments. Semin Oncol. 2006; 33(Suppl 6):S3-S11.

114. Ozols RF, Bundy BN, Green BE, et al. Phase III trial of carboplatin and paclitaxel compared with cisplatin and paclitaxel in patients with optimally resected stage III ovarian cancer: A Gynecologic Oncology Group Study. J Clin Oncol 2003;21:3194-3200.

115. Ozols RF. The current role of gemcitabine in ovarian cancer. Seminars in oncology. 2001;28(2 Suppl 7):18-24.

116. Patterson DM, Rustin GJ. Controversies in the management of germ cell tumors of the ovary. Current opinion in oncology. 2006;18(5):500-506.

117. Pecorelli S, Fallo L. Hormone replacement therapy in gynecological cancer survivors. Critical reviews in oncology/hematology. 1998;27(1):1-10.

118. Piccart MJ, Bertelsen K, Stuart G, et al. Long-term follow-up confirms a survival advantage of the paclitaxel-cisplatin regimen over the cyclophosphamide-cisplatin combination in advanced ovarian cancer. Int J Gynecol Cancer. 2003:13(Suppl 2):144-148.

119. Pignata S, Scambia G, Ferrandina G, et al. Carboplatin plus paclitaxel vesus carboplatin plus pegylated liposomal doxorubicin as first-line treatment for patients with ovarian cancer: the MITO2 randomized phase III trial. J Clin Oncol 2011;29:3628-3635.

120. Popper LD and Batra S. Calcium mobilization and cell proliferation activated by extracellular ATP in human ovarian tumour cells. Cell Cacium. 1993; 14(3): 209-218.

121. Poveda A. Gemcitabine in patients with ovarian cancer. Cancer Treat Rev.2005; 31(Suppl 4): S29-S37.

122. Prat J, Oncology FCoG. FIGO's staging classification for cancer of the ovary, fallopian tube, and peritoneum: abridged republication. J Gynecol Oncol. 2015;26(2):87-89.

123. Pressacco J, Wiley JS, Jamieson GP, et al. Modulation of the equilibrative nucleoside transporter by inhibitors of DNA synthesis. Br. J. Cancer. 1995; 72:939-942.

124. Pujade-Lauraine E, Hilpert F, Weber B, et al. Bevacizumab combined with chemotherapy for platinum-resistant recurrent ovarian cancer: The AURELIA open-label randomized phase III trial. J Clin Oncol. 2014;32(13):1302–1308.

125. Quentin T, Kitz J, Steinmetz M, Poppe A, Bar K, Kratzner R. Different expression of the catalytic alpha subunits of the AMP activated protein kinase--an immunohistochemical study in human tissue. Histology and histopathology. 2011;26(5):589-596.

126. Rafehi M, Burbiel JC, Attah IY, Abdelrahman A, Muller CE. Synthesis, characterization, and in vitro evaluation of the selective $P2Y_2$ receptor antagonist AR-C118925. Purinergic signalling. 2017;13(1):89-103.

127. Rehan S, Ashok Y, Nanekar R, et al. Thermodynamics and kinetics of inhibitor binding to human equilibrative nucleoside transporter subtype-1. Biochemical Pharmacology.2015; 98(4): 681-689.

128. Rotte A, Garmann D, Buss I and Jaehde U. Effect of extracellular ATP on cisplatin-induced cytotoxicity in human ovarian carcinoma cells. Chemotherapy.2010; 56:1-568.

129. Runnebaum I.B. and Stickeler E. Epidermiological and molecular aspects of ovarian cancer risk. J Cancer Res Clin Oncol.2001; 127:73-79.

130. Saitoh M, Nagai K, Nakagawa K, Yamamura T, Yamamoto S, Nishizaki T. Adenosine induces apoptosis in the human gastric cancer cells via an intrinsic pathway relevant to activation of AMP-activated protein kinase. Biochem Pharmacol.2004; 67(10): 2005-2011.

131. Sakai W, Swisher EM, Karlan BY, et al. Secondary mutations as a mechanism of cisplatin resistance in BRCA2-mutated cancers. Nature. 2008; 451: 1116–1120.

132. Sakamoto M, Kondo A, Kawasaki K, et al. (2001). Analysis of gene expression profiles associated with cisplatin resistance in human ovarian cancer cell lines and tissues using cDNA microarray. Hum Cell. 2001; 14: 305–315.

133. Sauer H, Klimm B, Hescheler J, et al. Activation of p90RSK and growth stimulation of multicellular tumor spheroids and dependent on reactive oxygen species generated after purinergic receptor stimulation by ATP. FASEB J. 2001; 15: 2539-2541.

134. Schafer R, Sedehizade F, Welte T, et al. ATP- and UTP-activated P2Y receptors differently regulate proliferation of human lung epithelial tumor cells. Am J Physiol Lung Cell Mol Physiol. 2003; 285(2):L376-385.

135. Schultze-Mosgau A, Katzur AC, Arora KK, et al. Characterisation of calcium mobilising, purinergic P2Y2 receptors in human ovarian cancer cells. Mol Hum Reprod. 2000; 6: 435-442.

136. Seidman JD, Kurman RJ. Pathology of ovarian carcinoma. Hematology/oncology clinics of North America. 2003;17(4):909-925, vii.

137. Shan Q, Storm DR. Optimization of a cAMP response element signal pathway reporter system. Journal of neuroscience methods. 2010;191(1):21-25.

138. Shepherd JE. Current strategies for prevention, detection and treatment of ovarian cancer. J Am Pharm Assoc.2000; 40: 392-401.

139. Shin C, Chen VJ, Gossett LS, et al. LY231514, a pyrrolo[2,3-d]pyrimidine-based antifolate that inhibits multiple folate-requiring enzymes. Cancer Res. 1997; 57(6): 1116-11123.

140. Shirali S, Aghaei M, Shabani M, Fathi M, Sohrabi M, Moeinifard M. Adenosine induces cell cycle arrest and apoptosis via cyclinD1/Cdk4 and Bcl-2/Bax pathways in human ovarian cancer cell line OVCAR-3.Tumour Biol.2013; 34(2): 1085-1095.

141. Siddik Z. Cisplatin mode of cytotoxic action and molecular basis of resistance. Oncogene. 2003; 22: 7265-7279.

142. Smith JA and Wolf JK. “Ovarian cancer” in Pharmacotherapy, A Pathophysiology Approach 7th edition. McGraw-Hill; 2008: 2245-2258.

143. Spano D, Marshall JC, Marino N, De Martino D, Romano A, Scoppettuolo MN, Bello AM, Di Dato V, Navas L, De Vita G, Medaglia C, Steeg PS, Zollo M. Dipyridamole prevents triple-negative breast-cancer progression. Clin Exp Metastasis. 2013;30:47–68.

144. Sperlagh B, Doda M, Baranyi M, Hasko G. Ischemia-like condition releases norepinephrine and purines from different sources in superfused rat spleen strips. J Neuroimmunol. 2000; 111:45–54.

145. Stagg J and Smyth. Extracellular adenosine triphosphate and adenosine in cancer. Oncogene.2010; 29: 5364-5358.

146. Stratton JF, Tidy JA and Peterson ML. The surgical management of ovarian cancer. Cancer Treat Rev.2001; 27: 111-118.

147. Swisher EM, Mutch DG, Rader JS, et al. Topotecan in platinum-and paclitaxel-resistant ovarian cancer. Gynecol Oncol.1997; 66: 480-486.

148. Tait SW and Green DR. Mitochondria and cell death: outer membrane permeabilization and beyond. Nat Rev Mol Cell Biol. 2010;11(9):621-632.

149. Thorn JA, Jarvis SM. Adenosine transporters. General pharmacology. 1996;27(4):613-20.

150. Timerbaev AR, Hartinger CG, Aleksenko SS, Keppler BK. Interactions of antitumor metallodrugs with serum proteins:advances in characterization using modern analytical methodology. Chem Rev. 2006; 106: 2224–2248.

151. Tomida A and Tsuro T. Drug resistance mediated by cellular stress response to the microenvironment of solid tumors. Anticancer Drug Des. 1999; 14(2): 169-177.

152. Tsuchiya A. and Nishizaki T. Anticancer effect of adenosine on gastric cancer via diverse signaling pathways. World J Gastroenterol.2015; 21(39):10931-10935.

153. Turner N, Li JY, Gosby A, To SW, Cheng Z, Miyoshi H, Taketo MM et al. Berberine and its more biologically available derivative, dihydroberberine, inhibit mitochondrial respiratory complex I: a mechanism for the action of berberine to activate AMP-activated protein kinase and improve insulin action. Diabetes 2008, 57: 1414–1418.

154. US Food & Drug Administration (USFDA). Adenosine. https://www.accessdata.fda.gov. Accessed 27 July 2017.

155. Vaisman A, Varchenko M, Umar A, , et al. The role of hMLH1, hMSH3, and hMSH6 defects in cisplatin and oxaliplatin resistance: correlation with replicative bypass of platinum-DNA adducts. Cancer Res. 1998; 58: 3579–3585.

156. Vasey PA, Jayson GC, Gordon A, et al. Phase III randomized trial of docetaxel-carboplatin versus paclitaxel-carboplatin as first-line chemotherapy for ovarian carcinoma. J Natl Cancer Inst 2004;96:1682-1691.

157. Vasu S, Bandettini WP, Hsu LY, Kellman P, Leung S, Mancini C, Shanbhag SM, Wilson J, Booker OJ, Arai AE. Regadenoson and adenosine are equivalent vasodilators and are superior than dipyridamole- a study of first pass quantitative perfusion cardiovascular magnetic resonance. J Cardiovasc Magn Reson. 2013;15: 85–91.

158. Venkitaraman AR. Cancer susceptibility and the functions of BRCA1 and BRCA2. Cell. 2002; 108: 171–182.

159. Virtanen SS, Kukkonen-Macchi A, Vainio M, Elima K, Harkonen PL, Jalkanen S, et al. Adenosine inhibits tumor cell invasion via receptor-independent mechanisms. Mol Cancer Res.2014; 12(12): 1863-1874.

160. Vlad AM, Budiu RA, Lenzner DE, et al. A phase II trial of intraperitoneal interleukin-2 in patients with platinum-resistant of platinum-refractory ovarian cancer. Cancer Immunol Immunother. 2009. [Epub ahead of print].

161. Wang C, Schwab LP, Fan M, Seagroves TN, Buolamwini JK. Chemoprevention activity of dipyridamole in the MMTV-PyMT transgenic mouse model of breast cancer. Cancer Prev Res. 2013;6:437–447.

162. Wang YW, He SJ, Feng X, et al. Metformin: a review of its potential indications. Drug Des Devel Ther. 2017; 11:2421-2429.

163. Watanabe R, Wei L, Huang J. mTOR signaling, function, novel inhibitors, and therapeutic targets. Journal of nuclear medicine: official publication, Society of Nuclear Medicine. 2011; 52(4):497-500.

164. Wei Q, Costanzi S, Balasubramanian R, Gao ZG, Jacobson KA. A2B adenosine receptor blockade inhibits growth of prostate cancer cells. Purinergic signalling. 2013; 9(2):271-80.

165. White N and Burnstock G. P2 receptors and cancer. TRENDS in Pharmacological Science.2006; 27(4): 211-217.

166. William WN, Kim JS, Liu DD, Solis L, Behrens C, Lee JJ, et al. The impact of phosphorylated AMP-activated protein kinase expression on lung cancer survival. Annals of oncology. 2012; 23(1):78-85.

167. Wilson FH, Johannessen CM, Piccioni F, et al. A functional landscape of resistance to ALK inhibition in lung cancer. Cancer Cell. 2015; 27(3): 397-408.

168. Woods A, Johnstone SR, Dickerson K, Leiper FC, Fryer LG, Neumann D, et al. LKB1 is the upstream kinase in the AMP-activated protein kinase cascade. Current biology. 2003;13(22):2004-2008.

169. Wu LF, Li GP, Feng JL, Pu ZJ. Molecular mechanisms of adenosine-induced apoptosis in human HepG2 cells. Acta Pharmacol Sin.2006; 27(4): 477-484.

170. Wu N, Gu C, Gu H, Hu H, Han Y, Li Q. Metformin induces apoptosis of lung cancer cells through activating JNK/p38 MAPK pathway and GADD153. Neoplasma. 2011;58(6):482-490.

171. Wullschleger S, Loewith R, Hall MN. TOR signaling in growth and metabolism. Cell. 2006;124(3):471-84.

172. Xiao B, Sanders MJ, Underwood E, Heath R, Mayer FV, Carmena D, et al. Structure of mammalian AMPK and its regulation by ADP. Nature. 2011; 472(7342):230-233.

173. Yang D, Yaguchi T, Nakano T, Nishizaki T. Adenosine activates AMPK to phosphorylate Bcl-XL responsible for mitochondrial damage and DIABLO release in HuH-7 cells. Cell Physiol Biochem.2011; 27(1): 71-78.

174. Yang D, Yaguchi T, Nakano T, Nishizaki T. Adenosine activates AMPK to phosphorylate Bcl-XL responsible for mitochondrial damage and DIABLO release in HuH-7 cells. Cell Physiol Biochem.2011; 27(1): 71-78.

175. Ye J, Coulouris G, Zaretskaya I, Cutcutache I, Rozen S, Madden TL. Primer-BLAST: a tool to design target-specific primers for polymerase chain reaction. BMC bioinformatics. 2012;13:134.

176. Yegutkin GG. Enzymes involved in metabolism of extracellular nucleotides and nucleosides: functional implications and measurement of activities. Crit Rev Biochem Mol Biol. 2014; 49(6): 473-497.

177. Yeung PK, Mosher SJ, Macrae DA, Klassen GA. Effect of diltiazem and its metabolites on the uptake of adenosine in blood: an in-vitro investigation. The Journal of pharmacy and pharmacology. 1991;43(10):685-9.

178. Yoshida S, Hong S, Suzuki T, et al. Redox regulates mammalian target of rapamycin complex 1 (mTORC1) activity by modulating the TSC1/TSC2-Rheb GTPase pathway. J Biol Chem. 2011;286(37):32651–32660.

179. Yu SY, Chan DW, Liu VW, Ngan HY. Inhibition of cervical cancer cell growth through activation of upstream kinases of AMP-activated protein kinase. Tumour Biol 2009, 30: 80–85.

180. Yung MM, Ngan HY and Chan DW. Targeting AMPK in combating ovarian cancers: opportunities and challenges. Acta Biochim Biophys Sin. 2016; 48(4):301-317.

181. Yung MM, Ross FA, Hardie DG, Leung TH, Zhan J, Ngan HY, Chan DW. Bitter melon (Momordica charantia) extract inhibits tumorigenicity and overcomes cisplatin-resistance in ovarian cancer cells through targeting AMPK signaling cascade. Integr Cancer Ther 2015.

182. Zadra G, Batista JL, Loda M. Dissecting the Dual Role of AMPK in Cancer: From Experimental to Human Studies. Molecular cancer research : MCR. 2015;13(7):1059-1072.

183. Zakikhani M, Dowling R, Fantus IG, Sonenberg N, Pollak M. Metformin is an AMP kinase-dependent growth inhibitor for breast cancer cells. Cancer Res 2006, 66: 10269–10273.